Left document: Old manuscript.pdf

Right document: Revised manuscript.pdf

What is this document?

This is a comparison of two documents. The two documents are interleaved such that the left document is displayed on even pages and the right document is displayed on odd pages.

Is there a specific way I should view this file?

This document is intended to be viewed in Two Page Continuous mode (or sometimes called 'Two Page Scrolling'). It should open in this mode by default when using Adobe Acrobat and most popular PDF readers.

If the document opens in a different view, you can often change this in the settings. In Adobe Acrobat, go to **View > Page Display > Two Page Scrolling**.

Why are there blank pages?

Blank pages are inserted to keep both documents as aligned as much as possible.

How do I read the changes?

Text deleted from the left document and, hence, not in right document is highlighted red. Text added to the right document and, hence, not in left document is highlighted green.

Tip for printing

When printing this document, we recommend printing double-sided and include this first page. This will result in the matching text being displayed on different pages and easily readable, much like a book.

Collisional Transport Coefficients
In Kappa-Distributed Plasmas

Mahmood Jwailes[1][*], Imad Barghouthi[2], Qusay Atawnah[3]

[1][2][3] Department of physics, Al-Quds university, Jerusalem, Palestine.

[*]mahmood.jwailes@students.alquds.edu

Abstract

In this paper, we present a set of transport equations (continuity, momentum, and energy) using the Kappa velocity distribution as our zeroth-order function within the framework of the five-moment approximation. Then, we derive the corresponding transport momentum and energy coefficients using the Boltzmann collision integral. The results are expressed in terms of hypergeometric functions. These calculations have been done for three types of collisions: Coulomb collisions, hard-sphere interactions, and Maxwell molecules collisions. Furthermore, we explore the transport coefficients in two special cases: (1) the limiting case when kappa index approaches infinity, where the results converge to those of the Maxwellian distribution, and (2) the case of a non-drifting Kappa distribution. Finally, we discuss the behaviour of the transport coefficients in the case of Coulomb collisions for the Kappa distribution and compare it with the result of Maxwellian distribution.

keywords Transport equations, Five-moment approximation, Transport coefficients, Kappa distribution, Coulomb collisions.

1   Introduction

The transport equations based on the Maxwellian velocity distribution function were first derived by Tanenbaum [1967] and Burgers [1969], with a subsequent review by Schunk [1977]. These studies also obtained the transport coefficients (i.e. the collision integrals) using the Boltzmann collision integral approach and expressed them in terms of Chapman-Cowling collision integrals Chapman and Cowling [1970]. These coefficients are valid for arbitrary temperature differences between the interacting gases but are restricted to small drift velocities. In Jubeh and Barghouthi [2018], the transport coefficients were calculated, for the five-moment approximation, without restriction on the drift velocity and presented in closed form using hypergeometric functions. The transport equations and the transport coefficients for a bi-Maxwellian velocity distribution function have also been derived in several studies Chew et al. [1956], Demars and Schunk [1979], Hellinger and Trávníček [2009], and Jubeh and Barghouthi [2017] in order to develop a more accurate model. Since, in space plasmas, the particle velocity distribution functions often deviate from the standard Maxwellian distribution, exhibiting non thermal suprathermal tails that decreases following a power law in terms of velocity. Such distributions are well-fitted by the so-called Kappa velocity distribution function, or generalized Lorentzian velocity distribution functions. The Kappa distribution, is a power-law distribution with long tails describing highly energetic particles, appears in a wide variety of settings, from low-density to high-density plasmas. It is commonly found at high altitudes in the solar wind and in various locations, including the terrestrial magnetosphere, radiation belts, and the magnetospheres of planets like Jupiter, Saturn, Uranus, and Neptune, as well as in other space plasma environments like Titan and the Io plasma torus. The prevalence of Kappa distributions in these regions has been extensively corroborated by Observations and satellite data from WIND Collier et al. [1996], Ulysses Meyer-Vernet et al. [1995], Cassini Steffl et al. [2004], and the Hubble Space Telescope Retherford et al.

Transport coefficients in modified Kappa distributed plasmas

Mahmood J. Jwailes [1], **Imad A. Barghouthi** [2], **and Qusay S. Atawnah** [3]

[1,2,3]Department of physics, Al-Quds university, Jerusalem, Palestine.

Correspondence: Mahmood J. Jwailes (mahmood.jwailes@students.alquds.edu)

Abstract. This work derives transport coefficients, i.e., electrical conductivity, thermoelectric, diffusion, and mobility coefficients, for a Lorentz plasma with a modified Kappa distribution. The derivation begins by formulating transport equations (continuity, momentum, and energy) within the five-moment approximation, using the modified Kappa distribution as the zeroth-order function. Subsequently, the corresponding momentum and energy collision terms are evaluated via the Boltzmann collision integral for different types of collisions, including Coulomb collisions, hard-sphere interactions, and Maxwell molecule collisions. Next, we use the momentum equation from the five-moment approximation to obtain the generalized Ohm's law and extended Fick's law, leading to the transport coefficients. Furthermore, the influence of the kappa parameter on the collision terms and transport coefficients is analyzed. The traditional results based on the Maxwellian distribution are recovered in the limit as kappa parameter approaches infinity.

1 Introduction

In space plasmas, the particles' velocity distribution often deviates from the Maxwellian form. These deviations arise from processes such as wave-particle interactions, turbulence, and particle acceleration at shocks, which generate non-Maxwellian distributions. Some of these distributions exhibit non-thermal suprathermal tails that follow a power-law dependence on velocity. Such distributions are well fitted by the Kappa velocity distribution (Marsch, 2006). The Kappa distribution provides a more accurate representation of the particles' velocity distribution in non-equilibrium systems compared to the Maxwellian distribution that predicts a Gaussian function behavior of the particle velocities and fails to account for the suprathermal particles. In contrast, the Kappa distribution introduces a power-law tail that decays more slowly than the exponential tail of the Maxwellian, enabling it to accurately describe systems with significant populations of high-energy particles (Vasyliunas, 1968). This flexibility is controlled by the kappa parameter, κ, which controls the sharpness of the tail. As κ increases, the distribution approaches the Maxwellian, while lower values of κ emphasize the suprathermal component (Pierrard and Lazar, 2010). With κ values usually between 2 and 6, Kappa distributions have been observed across a wide range of plasma environments, with direct measurements from several satellite missions. In the solar wind, the electron velocity distribution functions typically exhibit a thermal core, a suprathermal halo population present in all directions, and a component aligned with the interplanetary magnetic field (Pierrard et al., 2001). Kappa-distributed electrons and ions have been observed by missions such as Ulysses and Cluster. For instance, Maksimovic et al. (1997) showed that Ulysses data, fitted with Kappa functions, revealed an inverse relationship between solar wind speed and the kappa parameter κ, suggesting that suprathermal electrons influence solar wind acceleration. Similarly, Qureshi et al. (2003) also used Cluster observations to fit generalized Kappa functions to the ions' velocity distribution functions. In the Earth's magnetosheath, proton energy spectra data collected using the Heos I spacecraft confirmed that they are well fitted by Kappa distribution functions, with a kappa value around 2, particularly during crossings where no upstream waves were detected (Formisano et al., 1973). Beyond Earth, Kappa distributions have been observed in different space environments, such as Jupiter, where data from the Voyager 2 spacecraft showed that particle velocities in the planet's middle and outer magnetosphere are fitted by a Kappa distribution, with moderate kappa values indicating a transition between Maxwellian and power-law tails (Collier and Hamilton, 1995).

Given the wide range of the Kappa velocity distribution function observed in situ across planetary magnetospheres and the heliosphere and its ability to account for non-equilibrium conditions and suprathermal particles (see Pierrard and Lazar (2010), Livadiotis (2018), Davis et al. (2023), and Shizgal (2007) for more details), recent studies have investigated transport coefficients in nonequilibrium plasmas with the Kappa distribution function. In particular, Wang and Du (2017) and Ebne Abbasi et al. (2017) derived the diffusion coefficient—defined as the flux of particles due to a density gradient in the plasma—using Kappa statistics to account for suprathermal tails. Similarly, Wang and Du (2017) evaluated the mobility coefficient, which describes the particle flux under an applied electric field, within the Kappa framework. Furthermore, Du (2013) and Ebne Abbasi et al. (2017) analyzed the connection between mobility, electrical conductivity, and current density to provide a consistent description of charged-particle transport in nonequilibrium systems. In addition, Du (2013); Guo and Du (2019) calculated the thermoelectric coefficient, which links electric fields to temperature gradients and leads to the generation of electric voltages and currents, based on Kappa distributions. Finally, Du (2013); Guo and Du (2019) and Ebne Abbasi and Esfandyari-Kalejahi (2019) derived the thermal conductivity, which determines heat flux under a temperature gradient, using Kappa statistics to capture deviations from equilibrium behaviour. It is important to note that these studies primarily employed the modified Kappa distribution, which assumes a κ-independent temperature, that is, both the modified Kappa and Maxwellian distributions share the same thermal energy. This formulation makes the modified Kappa produces a stronger low-energy core and suprthermal tails compared to the Maxwellian distribution. In contrast, the standard Kappa distribution, originally introduced by Olbert (1968) and Vasyliunas (1968), is defined by κ-independent thermal speeds but κ-dependent temperatures, leading to higher-energy tails than the modified Kappa and reduced core populations lower than the Maxwellian. Distinguishing between these two forms is crucial, as the choice of distribution affects the derived transport coefficients and the physical interpretation of nonequilibrium plasma behavior, as shown by Husidic et al. (2021) which derived the electrical conductivity, thermoelectric coefficient, thermal conductivity, and diffusion and mobility coefficients for electron populations described by the standard Kappa distribution and then compared these results with those obtained for the modified Kappa distribution.

All the reviewed studies used simplified collision models rather than the full Boltzmann collision integral. The simplest models appear in Wang and Du (2017) and Ebne Abbasi and Esfandyari-Kalejahi (2019), which used Krook-type or BGK operators, offering computational simplicity but limited accuracy. More physically based models—such as those proposed by Du (2013) and Guo and Du (2019)—used macroscopic transport equations derived from idealized re-laxation assumptions. The most advanced work, presented by Ebne Abbasi et al. (2017), used the Fokker-Planck equation to model Coulomb collisions. While this captures cumulative small-angle scattering and better represents long-range Coulomb forces, it remains an approximation of the Boltzmann collision integral. Thus, all reviewed works share the same limitation: reliance on simplified collision models. Motivated by this issue, in this paper we propose a comprehensive re-evaluation of the transport coefficients based on the modified Kappa distribution, employing the Boltzmann collision integral as our collision model and adopting a more general and consistent approach through the five-moment approximation of the transport equations.

The transport equations describe the spatial and temporal evolution of the physically significant velocity moments (density, drift velocity, temperature, pressure tensor, stress tensor, and heat flow vector) derived as a practical reduction of the Boltzmann equation from a seven-dimensional partial differential equation (time plus phase space) to a set of four-dimensional equations (time and space). However, this process leads to an infinite chain of equations. To make the system solvable, a closure condition is applied by approximating the distribution function with a zeroth-order function and assuming that deviations from it are small. Different choices of the zeroth-order function have been used for closure, with the Maxwellian velocity distribution being the most common. The transport equations based on this assumption were first derived by Tanenbaum (1967) and Burgers (1969), followed by a subsequent review by Schunk (1977). These studies also obtained the collision terms—also known as transfer integrals—using the Boltzmann collision integral approach and expressed them in terms of the Chapman–Cowling collision integrals, as given in Chapman and Cowling (1990). To better capture anisotropies and departures from equilibrium, several studies have adopted more general zeroth-order forms. In particular, the bi-Maxwellian velocity distribution function—characterized by different temperatures parallel and perpendicular to the magnetic field—has been employed in several works (Demars and Schunk, 1979; Barakat and Schunk, 1981, 1982; Hellinger and Trávníček, 2009; Jubeh and Barghouthi, 2017). Beyond the pure bi-Maxwellian form, more advanced models incorporate anisotropy alongside nonthermal tails, skewness, or partial isotropization. For example, LeBlanc and Hubert (1997); Leblanc and Hubert (1998); Leblanc et al. (2000) introduced a hybrid distribution function that blends the bi-Maxwellian structure with additional functional forms to better match measured particle velocity spectra in space plasmas.

The approach used in this study involves developing a new transport theory that takes the modified Kappa distribution as the zeroth-order function, in which we derive the five-moment approximation of the transport equations and the collision terms via the Boltzmann collision integral for different types of collisions. We then relate the five-moment momentum equation to the generalized Ohm's law and the

[2003]. For a detailed discussion of the Kappa distribution, see Pierrard and Lazar [2010], Livadiotis [2018] and Davis et al. [2023]. Due to the frequent occurrence of the Kappa distribution in many space plasma environments, it's significantly important to see how the transport equations and the transport coefficients will be affected when we expand the velocity distribution function around the Kappa distribution. To address this, the study starts in Section 2 with a discussion of the theoretical formulation of Boltzmann's equation and the relevant collision terms, i.e., the Boltzmann collision integral. Section 3 presents the five-moment approximation of the transport equations. In Section 4, we derive the five-moment approximation for the Kappa velocity distribution function. Then, in Section 5, we calculate the transport coefficients for drifting Kappa plasmas, applicable for arbitrary drift velocity differences as well as temperature differences between the interacting plasma species. Next, we express the resulting coefficients in a hypergeometric representation. Section 6 investigates two special cases; the first, where the kappa index approaches infinity; the second, for the non-drifting Kappa distribution. These calculations cover three types of interactions: Coulomb collisions, hard-sphere interactions, and Maxwell molecules collisions. Finally, in Section 7, we study the behaviour of the transport coefficients in the case of Coulomb collisions and see how collisions affect both the momentum and the energy of the colliding particles, as well as how the effect differs for both Maxwellian and Kappa distributions.

2 Boltzmann Equation

In dealing with plasma, we describe each species in the plasma by a separate velocity distribution function $f_s(\mathbf{r}, \mathbf{v}_s, t)$, defined such that $f_s(\mathbf{r}, \mathbf{v}_s, t) \, d\mathbf{v}_s d\mathbf{r}$ represents the number of particles of specie s, which at time t have velocity between $\mathbf{v}_s$ and $\mathbf{v}_s + d\mathbf{v}_s$ and positions between $\mathbf{r}$ and $\mathbf{r} + d\mathbf{r}$. The evolution in time of the species velocity distribution function is determined by the net effect of collisions and the flow in phase space of species under the effect of external forces. The mathematical description of this evolution is given by Boltzmann equation, Schunk [1977],

$$\frac{\partial f_s}{\partial t} + \mathbf{v}_s \cdot \nabla f_s + \mathbf{a}_s \cdot \nabla_{v_s} f_s = \frac{\delta f_s}{\delta t}. \tag{1}$$

Here, ∇ represents the gradient in coordinate space, ∇_{v_s} is the gradient in velocity space, and $\mathbf{a}_s$ denotes the particle acceleration due to external forces. In most plasma applications, the main external forces acting on the charged particles are gravitational and Lorentz forces . With allowance for these forces, the acceleration becomes

$$\mathbf{a}_s = \mathbf{G} + \frac{e_s}{m_s} \left(\mathbf{E} + \frac{\mathbf{v}_s \times \mathbf{B}}{c} \right), \tag{2}$$

where $\mathbf{G}$ is the acceleration due to gravity, e_s and m_s are the charge and mass of species s respectively, $\mathbf{E}$ is the electric field, $\mathbf{B}$ is the magnetic field, and c is the speed of light. The quantity in the right side of the Boltzmann equation, $(\delta f_s/\delta t)$, represents the rate of change of f_s in a given region of phase space as a result of collisions, and its form depends on the type of collision process.

Boltzmann Collision Integral

The appropriate expression for $(\delta f_s/\delta t)$ in case of binary elastic collisions between particles (collisions governed by inverse power potentials, and resonant charge exchange collisions) is the Boltzmann collision integral, given by, Schunk [1977], Schunk and Nagy [2009]

$$\frac{\delta f_s}{\delta t} = \sum_t \int_{\mathbb{R}^3 \times \Omega} [f_s' f_t' - f_s f_t] \, \mathrm{g}_{st} \, \sigma_{st}(\mathrm{g}_{st}, \theta) \, d\Omega \, d\mathbf{v}_t, \tag{3}$$

where $d\mathbf{v}_t$ is the velocity space volume element for the target species t, $\mathbf{g}_{st}$ is the relative velocity of the colliding particles s and t, written as

$$\mathbf{g}_{st} = \mathbf{v}_s - \mathbf{v}_t, \qquad \text{and} \qquad \mathrm{g}_{st} = |\mathbf{v}_s - \mathbf{v}_t|, \tag{4}$$

extended Fick's law, from which the transport coefficients are obtained. The proposed methodology is implemented as follows: In Section 2, we begin with the theoretical formulation of the transport equations. Starting from Boltzmann's equation and the Boltzmann collision integral, we derive the five-moment approximation and the corresponding collision terms for the modified Kappa velocity distribution function, considering arbitrary drift velocity differences as well as temperature differences between the interacting plasma species. Next, we express the resulting collision terms in a hypergeometric representation and investigate the limiting cases where the kappa parameter approaches infinity. All these calculations cover three types of collisions: Coulomb collisions, hard-sphere interactions, and Maxwell molecules collisions. We then explore how the modified Kappa distribution influences the effective collision frequency and the thermalisation rate, providing a physical interpretation of these effects. Subsequently, we analyse the behaviour of the collision terms in the case of Coulomb collisions, focusing on how collisions affect both the momentum and the energy of the colliding particles, and how these effects differ for Maxwellian and the modified Kappa distributions. Finally, in Section 3, we derive the transport coefficients using the five-moment approximation and the obtained collision terms, followed by a discussion of how these coefficients are affected by the kappa parameter. We also provide a comparison between the derived formulas and other studies, focusing on the dependence on the kappa parameter.

2 Transport equations

In dealing with plasma, we describe each species in the plasma by a separate velocity distribution function $f_s(\mathbf{r}, \mathbf{v}_s, t)$, defined such that $f_s(\mathbf{r}, \mathbf{v}_s, t)\, d\mathbf{v}_s d\mathbf{r}$ represents the number of particles of species s, which at time t have velocity between $\mathbf{v}_s$ and $\mathbf{v}_s + d\mathbf{v}_s$ and positions between $\mathbf{r}$ and $\mathbf{r} + d\mathbf{r}$. The evolution in time of the species' velocity distribution function is determined by the net effect of collisions and the flow in phase space of species under the effect of external forces. The mathematical description of this evolution is given by the Boltzmann equation (Schunk, 1977),

$$\frac{\partial f_s}{\partial t} + \mathbf{v}_s \cdot \nabla f_s + \mathbf{a}_s \cdot \nabla_{\mathbf{v}_s} f_s = \frac{\delta f_s}{\delta t}. \tag{1}$$

Here, ∇ represents the gradient in coordinate space, $\nabla_{\mathbf{v}_s}$ is the gradient in velocity space, and $\mathbf{a}_s$ denotes the particle acceleration due to external forces. In most plasma applications, the main external forces acting on the charged particles are gravitational and Lorentz forces. With allowance for these forces, the acceleration becomes

$$\mathbf{a}_s = \mathbf{G} + \frac{e_s}{m_s}\left(\mathbf{E} + \frac{\mathbf{v}_s \times \mathbf{B}}{c}\right), \tag{2}$$

where $\mathbf{G}$ is the acceleration due to gravity, e_s and m_s are the charge and mass of species s, respectively, $\mathbf{E}$ is the elec-

tric field, $\mathbf{B}$ is the magnetic field, and c is the speed of light. The term on the right-hand side of the Boltzmann equation, $(\delta f_s / \delta t)$, represents the rate of change of the velocity distribution function f_s in a given region of phase space as a result of collisions, and its form depends on the type of collision process considered. The appropriate expression in the case of binary elastic collisions between particles (collisions governed by inverse power laws, and resonant charge exchange collisions) is the Boltzmann collision integral (Schunk, 1977; Schunk and Nagy, 2009), given by

$$\frac{\delta f_s}{\delta t} = \sum_t \int_{\mathbb{R}^3 \times \Omega} [f_s' f_t' - f_s f_t]\, g_{st}\, \sigma_{st}(g_{st}, \theta)\, d\Omega\, d\mathbf{v}_t, \tag{3}$$

where $d\mathbf{v}_t$ is the velocity space volume element for the target species t, g_{st} is the magnitude of the relative velocity of the colliding particles s and t, with $\mathbf{g}_{st}$ defined as

$$\mathbf{g}_{st} = \mathbf{v}_s - \mathbf{v}_t, \tag{4}$$

$d\Omega$ is the element of solid angle in the s particle reference frame, θ is the scattering angle, $\sigma_{st}(g_{st}, \theta)$ is the differential scattering cross-section, defined as the number of particles scattered per solid angle $d\Omega$, per unit time, divided by the incident intensity, and the primes denote quantities evaluated after the collision. The microscopic properties of a given species s can be defined and fully described by its velocity distribution function, from which, for example, the number density of particles, the zeroth-order moment, can be obtained by integrating the distribution function over the velocity space, as

$$n_s(\mathbf{r}, t) = \int_{\mathbb{R}^3} f_s(\mathbf{r}, \mathbf{v}_s, t)\, d\mathbf{v}_s, \tag{5}$$

and the drift velocity of species s, the first-order moment, is given by the following relation

$$\mathbf{u}_s(\mathbf{r}, t) = \langle \mathbf{v}_s \rangle, \tag{6}$$

where $\langle \mathbf{v}_s \rangle$ is the average value of $\mathbf{v}_s$, with the average value of $\xi_s(\mathbf{v}_s)$ at any position $\mathbf{r}$ and time t, defined as

$$\langle \xi_s \rangle = \frac{1}{n_s} \int_{\mathbb{R}^3} \xi_s(\mathbf{v}_s)\, f_s(\mathbf{r}, \mathbf{v}_s, t)\, d\mathbf{v}_s. \tag{7}$$

For higher-order moments, it is more convenient to evaluate them with respect to the drift velocity $\mathbf{u}_s$. Accordingly, Grad (1949) introduced the random velocity, defined as

$$\mathbf{c}_s(\mathbf{r}, \mathbf{v}_s, t) = \mathbf{v}_s - \mathbf{u}_s, \tag{8}$$

$d\Omega$ is the element of solid angle in the s particle reference frame, θ is the scattering angle, $\sigma_{st}(\mathrm{g}_{st}, \theta)$ is the differential scattering cross-section, defined as the number of particles scattered per solid angle $d\Omega$, per unit time, divided by the incident intensity, and the primes denote quantities evaluated after the collision.

$$f_s' f_t' = f_s'(\mathbf{r}, \mathbf{v}_s', t)\, f_t'(\mathbf{r}, \mathbf{v}_t', t)$$

Moments Of The Velocity Distribution Function

If $N_s(\mathbf{r}, \mathbf{v}_s, t)$ represents the number of species s at a given point in phase space $(\mathbf{r}, \mathbf{v}_s, t)$, then, by the definition of the velocity distribution function, we can write, Bittencourt [2004],

$$dN_s = f_s\, d\mathbf{v}_s\, d\mathbf{r}. \tag{5}$$

Dividing both sides of the equation (5) by the volume element $d\mathbf{r}$, and then integrate over the velocity space, gives the zeroth-order moment,

$$n_s(\mathbf{r}, t) = \int_{\mathbb{R}^3} f_s\, d\mathbf{v}_s, \tag{6}$$

which represents the *number density* of particles. Hence, the number density n_s is the number of particles per unit volume. From relation in equation (6), it is clear that the term f_s/n_s represents a normalized probability density function. As a result, the average value of $\xi_s(\mathbf{v}_s)$ at any position $\mathbf{r}$ and time t is given by

$$\langle \xi_s \rangle = \frac{1}{n_s} \int_{\mathbb{R}^3} \xi_s\, f_s\, d\mathbf{v}_s. \tag{7}$$

The first-order moment is the average value of $\mathbf{v}_s$, and it represents the *drift velocity* of a species s,

$$\mathbf{u}_s(\mathbf{r}, t) = \langle \mathbf{v}_s \rangle.$$

For higher moments, it is more convenient to evaluate them with respect to the drift velocity $\mathbf{u}_s$, so we introduce the *random velocity*, Grad [1949], as follows

$$\mathbf{c}_s(\mathbf{r}, \mathbf{v}_s, t) = \mathbf{v}_s - \mathbf{u}_s, \tag{8}$$

clearly,

$$\langle \mathbf{c}_s \rangle = 0. \tag{9}$$

Then, the physically significant velocity moments of the species distribution function are

$$\text{Temperature:} \qquad T_s(\mathbf{r}, t) = \frac{m_s}{3 k_B} \left\langle c_s^2 \right\rangle, \tag{10}$$

$$\text{Pressure tensor:} \qquad \mathbf{P}_s(\mathbf{r}, t) = n_s m_s \left\langle \mathbf{c}_s \mathbf{c}_s \right\rangle, \tag{11}$$

$$\text{Stress tensor:} \qquad \boldsymbol{\tau}_s(\mathbf{r}, t) = \mathbf{P}_s - p_s\, \mathbf{I}, \tag{12}$$

$$\text{Heat flow vector:} \qquad \mathbf{q}_s(\mathbf{r}, t) = \frac{n_s m_s}{2} \left\langle c_s^2\, \mathbf{c}_s \right\rangle, \tag{13}$$

$$\text{Heat flow tensor:} \qquad \mathbf{Q}_s(\mathbf{r}, t) = n_s m_s \left\langle \mathbf{c}_s \mathbf{c}_s \mathbf{c}_s \right\rangle. \tag{14}$$

$$\text{Higher-order pressure tensor:} \qquad \boldsymbol{\mu}_s(\mathbf{r}, t) = \frac{n_s m_s}{2} \left\langle c_s^2\, \mathbf{c}_s \mathbf{c}_s \right\rangle, \tag{15}$$

where k_B is the Boltzmann constant, $\mathbf{I}$ is a unit dyadic, p_s is the partial pressure and defined as

$$p_s = n_s k_B\, T_s. \tag{16}$$

The average value, defined in equation (7), can be written using the definition of the random velocity,

so that the physically significant velocity moments of the species distribution function can be written as

$$\text{Temperature}: \quad T_s(\mathbf{r},t) = \frac{m_s}{3k_B}\left\langle c_s^2\right\rangle, \quad (9)$$

$$\text{Pressure tensor}: \quad \mathbf{P}_s(\mathbf{r},t) = n_s m_s\left\langle \mathbf{c}_s \mathbf{c}_s\right\rangle, \quad (10)$$

$$\text{Stress tensor}: \quad \boldsymbol{\tau}_s(\mathbf{r},t) = \mathbf{P}_s - p_s\,\mathbf{I}, \quad (11)$$

$$\text{Heat flow vector}: \quad \mathbf{q}_s(\mathbf{r},t) = \frac{n_s m_s}{2}\left\langle c_s^2\,\mathbf{c}_s\right\rangle, \quad (12)$$

where k_B is the Boltzmann constant, $\mathbf{I}$ is a unit dyadic, p_s is the partial pressure and defined as

$$p_s = n_s k_B T_s. \quad (13)$$

The starting point for deriving the transport equations is the Boltzmann equation. These equations can be obtained by multiplying the Boltzmann equation by an appropriate function of velocity and then integrating over the velocity space. In particular, multiplying equation (1) by the factors 1, $m_s \mathbf{c}_s$, $\frac{1}{2}m_s c_s^2$, $m_s \mathbf{c}_s \mathbf{c}_s$, and $\frac{1}{2}m_s c_s^2 \mathbf{c}_s$, followed by integration over the velocity space, gives the continuity, momentum, energy, pressure tensor, and heat flow equations, respectively. Together, these form the general transport equations for species s, as presented in Schunk (1977), Schunk and Nagy (2009), and Bittencourt (2004). The general transport equations do not constitute a closed system because the equation governing the moment of order l contains the moment of order $l+1$. That is, the continuity equation describes the evolution of the density, but it also contains the drift velocity, and similar dependencies occur in the higher order moment equations. To close the system, it is necessary to adopt an approximate expression for the velocity distribution function f_s. A common mathematical technique can be used to do that, is expanding f_s in a complete orthogonal series of the form (Grad, 1949; Mintzer, 1965),

$$f_s(\mathbf{r},\mathbf{c}_s,t) = f_s^{(0)}(\mathbf{r},\mathbf{c}_s,t)\sum_i a_i(\mathbf{r},t)M_i(\mathbf{r},\mathbf{c}_s,t), \quad (14)$$

where $f_s^{(0)}$ is an appropriate zeroth-order velocity distribution function, M_i represents a complete set of orthogonal polynomials, and a_i are the unknown expansion coefficients. The zeroth-order distribution function and the orthogonal set of polynomials are generally chosen so that the series converges rapidly, meaning that only a few terms in the series expansion are needed to describe the distribution function. Different levels of approximation are possible, depending on the number of terms retained in the series expansion.

2.1 The five - moment approximation

The first term in the series expansion of equation (14) is 1, regardless of which zeroth-order distribution function $f_s^{(0)}$

is chosen (Mintzer, 1965). Therefore, assuming the species distribution function f_s is represented by the first term of the expansion, we have

$$f_s(\mathbf{r},\mathbf{c}_s,t) = f_s^{(0)}(\mathbf{r},\mathbf{c}_s,t). \quad (15)$$

The approximation in equation (15) reduces the general system of transport equations to just the continuity, momentum, and energy equations for each species s,

$$\frac{\delta n_s}{\delta t} = \frac{\partial n_s}{\partial t} + \nabla\cdot(n_s\mathbf{u}_s), \quad (16)$$

$$\frac{\delta \mathbf{M}_s}{\delta t} = n_s m_s\frac{\mathrm{D}_s\mathbf{u}_s}{\mathrm{D}t} + \nabla\cdot\mathbf{P}_s$$
$$\qquad - n_s m_s\mathbf{G} - n_s e_s\left(\mathbf{E} + \frac{\mathbf{u}_s\times\mathbf{B}}{c}\right), \quad (17)$$

$$\frac{\delta E_s}{\delta t} = \frac{3}{2}\frac{\mathrm{D}_s p_s}{\mathrm{D}t} + \frac{3}{2}p_s(\nabla\cdot\mathbf{u}_s) + \nabla\cdot\mathbf{q}_s + \mathbf{P}_s:\nabla\mathbf{u}_s, \quad (18)$$

where the operation $\mathbf{P}_s:\nabla\mathbf{u}_s$ corresponds to the double product of the two tensors $\mathbf{P}_s$ and $\nabla\mathbf{u}_s$, and the operator $\mathrm{D}_s/\mathrm{D}t$ is defined as

$$\frac{\mathrm{D}_s}{\mathrm{D}t} = \frac{\partial}{\partial t} + \mathbf{u}_s\cdot\nabla. \quad (19)$$

The set of equations (16−18) was initially derived with no assumption about the zeroth-order function $f_s^{(0)}$ (Tanenbaum, 1967). In the present study, we adopt the drifting modified Kappa distribution (MK) as the zeroth-order function. The drifting modified Kappa distribution is commonly written in the following form (Livadiotis, 2018; Davis et al., 2023),

$$f_s^{(0)} = f_s^{\text{MK}}(\mathbf{r},\mathbf{c}_s,t) = \frac{n_s\eta(\kappa_s)}{\pi^{3/2}\,w_s^3}\left(1 + \frac{c_s^2}{\kappa_{0_s}\,w_s^2}\right)^{-\kappa_s-1}, \quad (20)$$

where the thermal velocity of species s, denoted by w_s, is given by

$$w_s = \sqrt{\frac{2k_B T_s}{m_s}}, \quad (21)$$

with m_s and T_s denoting the mass and the absolute temperature of species s respectively, and k_B is the Boltzmann constant. The function $\eta(\kappa_s)$, which depends on the kappa parameter κ_s, is defined as

$$\eta(\kappa_s) = \kappa_{0s}^{-3/2}\frac{\Gamma(\kappa_s+1)}{\Gamma(\kappa_s-1/2)}, \quad \kappa_{0_s} = \kappa_s - \frac{3}{2}. \quad (22)$$

Here, κ_{0_s} is the invariant kappa index, and κ_s is a shape parameter that controls the power-law tails, sometimes referred to as the spectral index, with the condition $\kappa_s > 3/2$. This condition prevents the modified Kappa distribution function in equation (20) from collapsing (Pierrard and Lazar, 2010). If the chosen zeroth-order distribution function $f_s^{(0)}$ satisfies

$$\mathbf{q}_s = \boldsymbol{\tau}_s = 0, \quad (23)$$

from which the relation $d\mathbf{c}_s = d\mathbf{v}_s$ follows, as

$$\langle \xi_s(\mathbf{c}_s) \rangle = \frac{1}{n_s} \int \xi_s(\mathbf{c}_s) \, f_s(\mathbf{r}, \mathbf{c}_s, t) \, d\mathbf{c}_s. \tag{17}$$

3   The Five-Moment Approximation

The transport equations describe the spatial and temporal evolution of the physically significant velocity moments, mentioned in the previous section. These equations can be obtained by multiplying the Boltzmann equation by an appropriate function of velocity and then integrating over the velocity space. If we multiply equation (1) by the factors 1, $m_s\mathbf{c}_s$, $\frac{1}{2}m_s c_s^2$, $m_s\mathbf{c}_s\mathbf{c}_s$, and $\frac{1}{2}m_s c_s^2 \mathbf{c}_s$, and then integrate over the velocity space, we obtain the continuity, momentum, energy, pressure tensor, and heat flow equations, respectively. These are the general transport equations for species s, as given in Schunk [1977], Schunk and Nagy [2009], and Bittencourt [2004]. The general transport equations do not constitute a closed system because the equation governing the moment of order l contains the moment of order $l+1$. That is, the continuity equation describes the evolution of the density, but it also contains the drift velocity, and similar dependencies occur in the higher moment equations. In order to close the system, it is necessary to adopt an approximate expression for f_s. A common mathematical technique can be used to do that, is expanding f_s in a complete orthogonal series of the form, Grad [1949] and Mintzer [1965],

$$f_s(\mathbf{r}, \mathbf{c}_s, t) = f_s^{(0)}(\mathbf{r}, \mathbf{c}_s, t) \sum_p a_p(\mathbf{r}, t) M_p(\mathbf{r}, \mathbf{c}_s, t), \tag{18}$$

where $f_s^{(0)}$ is an appropriate zeroth-order velocity distribution function, M_p represents a complete set of orthogonal polynomials, a_p represents the unknown expansion coefficients, and the subscript p is used to indicate that the summation is generally over more than one coordinate index. The zeroth-order distribution function and the orthogonal set of polynomials are generally chosen so that the series converges rapidly, meaning that only a few terms in the series expansion are needed to describe the distribution function. Different levels of approximation are possible depending on the number of terms retained in the series expansion. The first term in the series expansion in equation (18) is 1, regardless of the choice of the zeroth-order distribution function $f_s^{(0)}$ Mintzer [1965]. Therefore, assuming the species distribution function f_s is represented by the first term of the expansion, we have

$$f_s = f_s^{(0)}. \tag{19}$$

This approximation reduces the general system of transport equations to just the continuity, momentum, and energy equations for each species,

$$\frac{\delta n_s}{\delta t} = \frac{\partial n_s}{\partial t} + \nabla \cdot (n_s \mathbf{u}_s), \tag{20}$$

$$\frac{\delta \mathbf{M}_s}{\delta t} = n_s m_s \frac{\mathrm{D}_s \mathbf{u}_s}{\mathrm{D} t} + \nabla \cdot \mathbf{P}_s - n_s m_s \mathbf{G} - n_s e_s \left(\mathbf{E} + \frac{\mathbf{u}_s \times \mathbf{B}}{c} \right), \tag{21}$$

$$\frac{\delta E_s}{\delta t} = \frac{\mathrm{D}_s}{\mathrm{D} t} \left(\frac{3}{2} p_s \right) + \frac{3}{2} p_s (\nabla \cdot \mathbf{u}_s) + \nabla \cdot \mathbf{q}_s + \mathbf{P}_s : \nabla \mathbf{u}_s, \tag{22}$$

where the operation $\mathbf{P}_s : \nabla \mathbf{u}_s$ corresponds to the double product of the two tensors $\mathbf{P}_s$ and $\nabla \mathbf{u}_s$, and

$$\frac{\mathrm{D}_s}{\mathrm{D} t} = \frac{\partial}{\partial t} + \mathbf{u}_s \cdot \nabla. \tag{23}$$

The set of equations (20−22) were initially derived with no assumption about the $f_s^{(0)}$, Tanenbaum [1967]. If the choice of zeroth-order distribution function $f_s^{(0)}$ satisfies

$$\mathbf{q}_s = \boldsymbol{\tau}_s = 0, \tag{24}$$

as in the drifting Maxwellian distribution, we can write equations (20−22) as, Schunk [1977],

$$\frac{\delta n_s}{\delta t} = \frac{\partial n_s}{\partial t} + \nabla \cdot (n_s \mathbf{u}_s) \tag{25}$$

$$\frac{\delta \mathbf{M}_s}{\delta t} = n_s m_s \frac{\mathrm{D}_s \mathbf{u}_s}{\mathrm{D}\,t} + \nabla p_s - n_s m_s \mathbf{G} - n_s e_s \left(\mathbf{E} + \frac{\mathbf{u}_s \times \mathbf{B}}{c} \right) \tag{26}$$

$$\frac{\delta E_s}{\delta t} = \frac{\mathrm{D}_s}{\mathrm{D}\,t} \left(\frac{3}{2} p_s \right) + \frac{5}{2} p_s \left(\nabla \cdot \mathbf{u}_s \right) \tag{27}$$

These equations are known as the five-moment approximation of the transport equations because each species is characterized by five parameters: density, three components of drift velocity, and temperature. At this level of approximation, stress, heat flow, and all higher-order velocity moments are neglected, and the properties of the species are expressed in terms of just the species density, drift velocity, and temperature. The terms on the left-hand side of equations (25−27) are called the collision integrals, or, as we will refer to, the transport coefficients. These coefficients are the moments of the Boltzmann collision integral and describe the rate of change of density, momentum, and energy due to collisions. They are defined as follows:

$$\frac{\delta n_s}{\delta t} = \int_{\mathbb{R}^3} \frac{\delta f_s}{\delta t} \, d\mathbf{c}_s, \tag{28}$$

$$\frac{\delta \mathbf{M}_s}{\delta t} = m_s \int_{\mathbb{R}^3} \mathbf{c}_s \frac{\delta f_s}{\delta t} \, d\mathbf{c}_s, \tag{29}$$

$$\frac{\delta E_s}{\delta t} = \frac{m_s}{2} \int_{\mathbb{R}^3} c_s^2 \frac{\delta f_s}{\delta t} \, d\mathbf{c}_s, \tag{30}$$

where the Boltzmann's collision integral, expressed in terms of the random velocities $\mathbf{c}_s$ and $\mathbf{c}_t$, and takes the form:

$$\frac{\delta f_s}{\delta t} = \sum_t \int_{\mathbb{R}^3 \times \Omega} [f_s' f_t' - f_s f_t] \, \mathrm{g}_{st} \, \sigma_{st}(\mathrm{g}_{st}, \theta) \, d\Omega \, d\mathbf{c}_t, \tag{31}$$

with the functions f_s', f_t', f_s, and f_t depends on $(\mathbf{r}, \mathbf{c}_s \text{ or } \mathbf{c}_t, t)$.

4   The Five-Moment Approximation For Drifting Kappa Distribution

In 3-dimensions, the drifting Kappa distribution function of particle velocities is commonly written in the form, Livadiotis [2018], Davis et al. [2023],

$$f_\alpha^{\kappa_\alpha}(\mathbf{r}, \mathbf{c}_\alpha, t) = \frac{n_\alpha \eta(\kappa_\alpha)}{\pi^{3/2} \, w_\alpha^3} \left(1 + \frac{c_\alpha^2}{\kappa_{0_\alpha} \, w_\alpha^2} \right)^{-\kappa_\alpha - 1}, \tag{32}$$

where α denotes the particle type, $\mathbf{c}_\alpha$ is the random velocity of species α, and it is defined in terms of the particle drift velocity $\mathbf{u}_\alpha$, as

$$\mathbf{c}_\alpha = \mathbf{v}_\alpha - \mathbf{u}_\alpha, \tag{33}$$

the thermal velocity of particle α, w_α, is given by

$$w_\alpha = \sqrt{\frac{2 k_B T_\alpha}{m_\alpha}}, \tag{34}$$

as in the drifting Maxwellian distribution and the drifting modified Kappa distribution (Scherer et al., 2019), we can write equations (16−18) as (Schunk, 1977),

$$\frac{\delta n_s}{\delta t} = \frac{\partial n_s}{\partial t} + \nabla \cdot (n_s \mathbf{u}_s), \tag{24}$$

$$\frac{\delta \mathbf{M}_s}{\delta t} = n_s m_s \frac{\mathrm{D}_s \mathbf{u}_s}{\mathrm{D} t} + \nabla p_s$$
$$- n_s m_s \mathbf{G} - n_s e_s \left(\mathbf{E} + \frac{\mathbf{u}_s \times \mathbf{B}}{c} \right), \tag{25}$$

$$\frac{\delta E_s}{\delta t} = \frac{3}{2} \frac{\mathrm{D}_s p_s}{\mathrm{D} t} + \frac{5}{2} p_s (\nabla \cdot \mathbf{u}_s). \tag{26}$$

These equations are known as the five-moment approximation of the transport equations because each species is characterized by five parameters: density, three components of drift velocity, and temperature. At this level of approximation, stress, heat flow, and all higher-order velocity moments are neglected, and the species' properties are expressed in terms of density, drift velocity, and temperature.

2.2 Collision terms

The terms appearing on the left-hand side of the five-moment approximation, equations (24−26), are called the collision terms, also known as the transfer collision integral. These terms represent the moments of the Boltzmann collision integral and describe the rate of change of density, momentum, and energy due to collisions, and they are defined as follows

$$\frac{\delta n_s}{\delta t} = \int_{\mathbb{R}^3} \frac{\delta f_s}{\delta t} \, d\mathbf{c}_s, \tag{27}$$

$$\frac{\delta \mathbf{M}_s}{\delta t} = m_s \int_{\mathbb{R}^3} \mathbf{c}_s \frac{\delta f_s}{\delta t} \, d\mathbf{c}_s, \tag{28}$$

$$\frac{\delta E_s}{\delta t} = \frac{m_s}{2} \int_{\mathbb{R}^3} c_s^2 \frac{\delta f_s}{\delta t} \, d\mathbf{c}_s, \tag{29}$$

where the Boltzmann's collision integral, expressed in terms of the random velocities $\mathbf{c}_s$ and $\mathbf{c}_t$, takes the form:

$$\frac{\delta f_s}{\delta t} = \sum_t \int_{\mathbb{R}^3 \times \Omega} [f_s' f_t' - f_s f_t] \, g_{st} \, \sigma_{st}(g_{st}, \theta) \, d\Omega \, d\mathbf{c}_t, \tag{30}$$

with the functions f_s', f_t', f_s, and f_t depend on $(\mathbf{r}, t, \mathbf{c}_s$ or $\mathbf{c}_t)$. Calculating the collision terms involves solving the integrals appearing in equations (27-29). The process begins by substituting the Boltzmann collision integral from equation (30) and rewriting the resulting integrals in an equivalent form that does not require the distribution functions after the collision, $f_s' f_t'$. We then use the momentum transfer cross-section integral, defined as

$$Q_{st}^{(1)}(g_{st}) = \int_{\Omega} (1 - \cos\theta) \, \sigma_{st}(g_{st}, \theta) \, d\Omega, \tag{31}$$

to write the collision terms as (Schunk and Nagy, 2009),

$$\frac{\delta n_s}{\delta t} = 0, \tag{32}$$

$$\frac{\delta \mathbf{M}_s}{\delta t} = -\sum_t m_{st} \int_{\mathbb{R}^3 \times \mathbb{R}^3} f_s f_t \, g_{st} \, \mathbf{Q}_{st}^{(1)} \, \mathbf{g}_{st} \, d\mathbf{c}_t d\mathbf{c}_s, \tag{33}$$

$$\frac{\delta E_s}{\delta t} = -\sum_t m_{st} \int_{\mathbb{R}^3 \times \mathbb{R}^3} f_s f_t \, g_{st} \, \mathbf{Q}_{st}^{(1)} \left(\hat{\mathbf{V}}_c \cdot \mathbf{g}_{st} \right) d\mathbf{c}_t \, d\mathbf{c}_s, \tag{34}$$

where the dot product is written as

$$\hat{\mathbf{V}}_c \cdot \mathbf{g}_{st} = \frac{m_s \mathbf{c}_s \cdot \mathbf{g}_{st} + m_t \mathbf{c}_t \cdot \mathbf{g}_{st} + m_t \Delta \mathbf{u} \cdot \mathbf{g}_{st}}{m_s + m_t}, \tag{35}$$

and the reduced mass m_{st} is expressed as

$$m_{st} = \frac{m_s m_t}{m_s + m_t}. \tag{36}$$

Equations (33) and (34) are expressed in terms of the momentum transfer cross-section integral $Q_{st}^{(1)}$, which depends explicitly on the nature of the particles' interaction; different collision models yield different functional forms for the cross-section. In the present work, we examine three distinct cases: Coulomb collisions, hard-sphere interactions, and Maxwell molecule collisions. The momentum transfer cross-section for Coulomb collisions is given by

$$Q_{st}^{(1)}(g_{st}) = \frac{Q_{Co}}{g_{st}^4}, \quad Q_{Co} = 4\pi \left(\frac{e_s e_t}{4\pi \varepsilon_0 m_{st}} \right)^2 \ln \Lambda, \tag{37}$$

where e_s and e_t are the charges of species s and t, respectively, ε_0 is the permittivity of free space, and $\ln \Lambda$ is the Coulomb logarithm. For hard-sphere interactions, the momentum transfer cross-section,

$$Q_{st}^{(1)} = Q_{HS} = \pi \sigma^2, \tag{38}$$

is a constant (σ is the sum of the radii of the colliding particles). In the case of Maxwell molecule collisions, the momentum transfer cross-section is

$$Q_{st}^{(1)} = \frac{Q_{MC}}{g_{st}}, \quad Q_{MC} = 0.844\pi \left(\frac{K_{st}}{m_{st}} \right)^{1/2}, \tag{39}$$

where K_{st} denotes a proportionality constant that measures the force magnitude between particles. Now, we proceed to calculate the momentum and energy collision terms, given in equations (33) and (34), for the five-moment approximation, under the assumption that the velocity distribution function of both interacting species s and t is a drifting modified Kappa distribution. The general expressions for the collision terms are summarized below, while detailed derivations for

m_α and T_α are the mass and the absolute temperature of particle α, respectively, k_B is the Boltzmann constant, $\eta(\kappa_\alpha)$ is a function of kappa index κ_α, defined as

$$\eta(\kappa_\alpha) = \kappa_{0\alpha}^{-3/2} \frac{\Gamma(\kappa_\alpha + 1)}{\Gamma(\kappa_\alpha - 1/2)}, \quad \kappa_{0\alpha} = \kappa_\alpha - \frac{3}{2}, \tag{35}$$

$\kappa_{0\alpha}$ is the invariant kappa index and κ_α is a shape parameter that controls the power-law tails, sometimes referred to as the spectral index, with the condition $\kappa_\alpha > 3/2$. This condition prevents the Kappa distribution function in equation (32) from collapsing, as the equivalent temperature would not be defined Pierrard and Lazar [2010]. Setting the zeroth-order distribution function $f_s^{(0)}$ to be a drifting Kappa distribution, it is expressed as

$$f_s^{(0)} = f_s^{\kappa_\alpha} = \frac{n_s \eta(\kappa_\alpha)}{\pi^{3/2} \, w_s^3} \left(1 + \frac{c_s^2}{\kappa_{0\alpha} \, w_s^2}\right)^{-\kappa_\alpha - 1}, \tag{36}$$

leads to the five-moment approximation described in equations (25–27), provided the condition in equation (24) is satisfied. Since if we substitute the following average values of the Kappa distribution, see Appendix A for details,

$$\langle \mathbf{c}_s \mathbf{c}_s \rangle = \frac{k_B T_s}{m_s} \, \mathbf{I}, \qquad \langle c_s^2 \, \mathbf{c}_s \rangle = 0. \tag{37}$$

into equations (11), (12), and (13) yields to

$$\mathbf{P}_s = n_s m_s \langle \mathbf{c}_s \mathbf{c}_s \rangle = n_s k_B T_s \, \mathbf{I} \tag{38}$$

$$\boldsymbol{\tau}_s = \mathbf{P}_s - p_s \mathbf{I} = 0, \tag{39}$$

$$\mathbf{q}_s = \frac{n_s m_s}{2} \langle c_s^2 \, \mathbf{c}_s \rangle = 0. \tag{40}$$

5 Transport Coefficients

Calculating the transport coefficients involves solving integrals known as the transfer collision integral, which take the form

$$\frac{\delta \xi_s}{\delta t} = \int_{\mathbb{R}^3} \xi_s \frac{\delta f_s}{\delta t} \, d\mathbf{c}_s, \tag{41}$$

where ξ_s represents a general velocity moment. Specifically, for $\xi_s = 1$, $m_s \mathbf{c}_s$, and $\frac{1}{2} m_s c_s^2$, the integral corresponds to the expressions in equations (28−30). We are interested in collisions described by the Boltzmann collision integral mentioned in equation (31). Therefore, the transfer collision integral is

$$\frac{\delta \xi_s}{\delta t} = \sum_t \int_{\mathbb{R}^3} \int_{\mathbb{R}^3 \times \Omega} \xi_s \left[f_s' f_t' - f_s f_t\right] \mathrm{g}_{st} \, \sigma_{st}(\mathrm{g}_{st}, \theta) \, d\Omega \, d\mathbf{c}_t \, d\mathbf{c}_s. \tag{42}$$

Rewriting equation (42) in an equivalent form

$$\frac{\delta \xi_s}{\delta t} = \sum_t \int_{\mathbb{R}^3} \int_{\mathbb{R}^3 \times \Omega} f_s f_t \left[\xi_s' - \xi_s\right] \mathrm{g}_{st} \, \sigma_{st}(\mathrm{g}_{st}, \theta) \, d\Omega \, d\mathbf{c}_t \, d\mathbf{c}_s, \tag{43}$$

that does not require the distribution functions after the collision, $f_s' f_t'$, which can be reorganized to obtain

$$\frac{\delta \xi_s}{\delta t} = \sum_t \int_{\mathbb{R}^3 \times \mathbb{R}^3} f_s f_t \, \mathrm{g}_{st} \left(\int_\Omega \left[\xi_s' - \xi_s\right] \sigma_{st}(\mathrm{g}_{st}, \theta) \, d\Omega\right) d\mathbf{c}_t \, d\mathbf{c}_s. \tag{44}$$

Since we are interested in the transport coefficients for density, momentum, and energy, we obtain the following by substituting the corresponding value of ξ_s into equation (44), and using the momentum transfer cross-section integral,

$$Q_{st}^{(1)}(\mathrm{g}_{st}) = \int_\Omega (1 - \cos\theta) \, \sigma_{st}(\mathrm{g}_{st}, \theta) \, d\Omega, \tag{45}$$

the three types of collisions are provided in Appendix A.

$$\frac{\delta n_s}{\delta t} = 0, \tag{40}$$

$$\frac{\delta \mathbf{M}_s}{\delta t} = \sum_t n_s m_s \nu_{st}^{\mathrm{MK}}(\kappa_s, \kappa_t) \Phi(\varepsilon_{st}) \Delta \mathbf{u}_{st}, \tag{41}$$

$$\frac{\delta E_s}{\delta t} = \sum_t n_s \left[\frac{3}{2} k_B \nu_{st,T}^{\mathrm{MK}}(\kappa_s, \kappa_t) \Psi(\varepsilon_{st}) \Delta \mathrm{T}_{st}^{\mathrm{MK}} \right.$$
$$\left. + m_{st} \nu_{st}^{\mathrm{MK}}(\kappa_s, \kappa_t) \Phi(\varepsilon_{st}) |\Delta \mathbf{u}_{st}|^2 \right], \tag{42}$$

where the relative drift velocity $\Delta \mathbf{u}_{st}$ and relative temperature difference $\Delta \mathrm{T}_{st}^{\mathrm{MK}}$ are defined by

$$\Delta \mathbf{u}_{st} = \mathbf{u}_t - \mathbf{u}_s, \tag{43}$$

$$\Delta \mathrm{T}_{st}^{\mathrm{MK}} = \mathrm{H}(\kappa_t) T_t - \mathrm{H}(\kappa_s) T_s, \tag{44}$$

and the drift-to-thermal speed ratio ε_{st} is given by

$$\varepsilon_{st} = \frac{|\Delta \mathbf{u}_{st}|}{w_{st}}, \quad w_{st} = \sqrt{\frac{2 k_B T_{st}}{m_{st}}}, \tag{45}$$

with the reduced mass m_{st} given in equation (36) and the reduced temperature T_{st} defined by

$$T_{st} = \frac{m_s T_t + m_t T_s}{m_s + m_t}. \tag{46}$$

The kappa-dependent terms ν_{st}^{MK} and $\nu_{st,T}^{\mathrm{MK}}$ represent, respectively, the effective collision frequency and the thermal equilibration rate (or simply the thermalisation rate) for systems described by the modified Kappa distribution, and they are defined as

$$\nu_{st}^{\mathrm{MK}}(\kappa_s, \kappa_t) = \nu_{st} \, \mathrm{D}(\kappa_s, \kappa_t), \tag{47}$$

$$\nu_{st,T}^{\mathrm{MK}}(\kappa_s, \kappa_t) = 2 \frac{m_{st}}{m_t} \nu_{st}^{\mathrm{MK}}, \tag{48}$$

where ν_{st} denote the effective collision frequency rate for systems governed by the Maxwellian distribution. The factors $\nu_{st}, \Phi, \Psi, \mathrm{D}$, and H forms change depending on the type of collision, such as Coulomb, hard-sphere, or Maxwell molecule collisions, and can be summarized as follows:

Coulomb collisions:

The effective collision frequency for Coulomb collisions in the Maxwellian case is

$$\nu_{st} = \nu_{st}^{\mathrm{Co}} = \frac{4}{3} \frac{n_t}{\pi^{1/2}} \frac{m_t}{m_s + m_t} \left(\frac{1}{2 k_B} \frac{m_{st}}{T_{st}} \right)^{3/2} \mathrm{Q}_{\mathrm{Co}}, \tag{49}$$

where Q_{Co} is defined in equation (37). The functions Φ and Ψ are given by

$$\Phi = \Phi_{\mathrm{Co}}(\varepsilon_{st}) = \frac{3\sqrt{\pi}}{4} \frac{\mathrm{erf}(\varepsilon_{st})}{\varepsilon_{st}^3} - \frac{3 e^{-\varepsilon_{st}^2}}{2 \varepsilon_{st}^2}, \tag{50}$$

$$\Psi = \Psi_{\mathrm{Co}}(\varepsilon_{st}) = e^{-\varepsilon_{st}^2}. \tag{51}$$

The kappa-dependent factors D and H are defined as

$$\mathrm{D}(\kappa_s, \kappa_t) = \frac{(\kappa_s - 1/2)}{(\kappa_s - 3/2)} \frac{(\kappa_t - 1/2)}{(\kappa_t - 3/2)}, \tag{52}$$

$$\mathrm{H}(\kappa_\alpha) = \frac{\Gamma(\kappa_\alpha)}{\Gamma(\kappa_\alpha + 1/2)} (\kappa_\alpha - 3/2)^{1/2}, \quad \alpha = s, t. \tag{53}$$

Hard-sphere interactions:

The effective collision frequency for Hard-sphere in the Maxwellian case is

$$\nu_{st} = \nu_{st}^{\mathrm{HS}} = \frac{8}{3} \frac{n_t}{\pi^{1/2}} \frac{m_t}{m_s + m_t} \left(2 k_B \frac{T_{st}}{m_{st}} \right)^{1/2} \mathrm{Q}_{\mathrm{HS}}, \tag{54}$$

where Q_{HS} is defined in equation (38). The functions Φ and Ψ are given by

$$\Phi = \Phi_{\mathrm{HS}}(\varepsilon_{st}) = \frac{3}{8} \left(1 + \frac{1}{2 \varepsilon_{st}^2} \right) e^{-\varepsilon_{st}^2}$$
$$+ \frac{3 \sqrt{\pi}}{8} \left(\varepsilon_{st} + \frac{1}{\varepsilon_{st}} - \frac{1}{4 \varepsilon_{st}^3} \right) \mathrm{erf}(\varepsilon_{st}), \tag{55}$$

$$\Psi = \Psi_{\mathrm{HS}}(\varepsilon_{st}) = \frac{\sqrt{\pi}}{2} \left(\varepsilon_{st} + \frac{1}{2 \varepsilon_{st}} \right) \mathrm{erf}(\varepsilon_{st}) + \frac{e^{-\varepsilon_{st}^2}}{2}. \tag{56}$$

The kappa-dependent factors D and H are defined the same as in equation (52) and (53).

Maxwell molecule collisions

The effective collision frequency for Maxwell molecule collisions in the Maxwellian case is

$$\nu_{st} = \nu_{st}^{\mathrm{MC}} = \frac{n_t m_t}{m_s + m_t} \mathrm{Q}_{\mathrm{MC}}, \tag{57}$$

where Q_{MC} is defined in (39). The functions Φ and Ψ are given by

$$\Phi = \Phi_{\mathrm{MC}}(\varepsilon_{st}) = 1, \quad \Psi = \Psi_{\mathrm{MC}}(\varepsilon_{st}) = 1, \tag{58}$$

The factors D and H are defined as

$$\mathrm{D}(\kappa_s, \kappa_t) = 1, \quad \mathrm{H}(\kappa_\alpha) = 1, \quad \alpha = s, t. \tag{59}$$

The collision terms can be derived for non-drifting modified Kappa distributions by setting the drift velocities of both interacting particles s and t to zero, $\mathbf{u}_s = \mathbf{u}_t = 0$, which gives $\Delta \mathbf{u}_{st} = 0$ and $\Phi(0) = \Psi(0) = 1$, in equations (40-42). The same expressions are obtained when the drift velocities of species s and t are equal, i.e., $\mathbf{u}_s = \mathbf{u}_t$.

2.2.1 Hypergeometric representation

The resulting collision terms in case of Coulomb collision and hard sphere interaction can be written in terms of the hypergeometric functions. This is done by expressing the Φ's

we can write the transport coefficients as, Schunk and Nagy [2009],

$$\frac{\delta n_s}{\delta t} = 0, \tag{46}$$

$$\frac{\delta \mathbf{M}_s}{\delta t} = -\sum_t m_{st} \int_{\mathbb{R}^3 \times \mathbb{R}^3} f_s f_t \, \mathrm{g}_{st} \, Q_{st}^{(1)} \, \mathbf{g}_{st} \, d\mathbf{c}_t \, d\mathbf{c}_s, \tag{47}$$

$$\frac{\delta E_s}{\delta t} = -\sum_t m_{st} \int_{\mathbb{R}^3 \times \mathbb{R}^3} f_s f_t \, \mathrm{g}_{st} \, Q_{st}^{(1)} \, \left(\hat{\mathbf{V}}_c \cdot \mathbf{g}_{st} \right) d\mathbf{c}_t \, d\mathbf{c}_s, \tag{48}$$

where the dot product is written as

$$\hat{\mathbf{V}}_c \cdot \mathbf{g}_{st} = \frac{m_s \mathbf{c}_s \cdot \mathbf{g}_{st} + m_t \mathbf{c}_t \cdot \mathbf{g}_{st} + m_t \, \Delta \mathbf{u} \cdot \mathbf{g}_{st}}{m_s + m_t}, \tag{49}$$

and the reduced mass m_{st} defined as

$$m_{st} = \frac{m_s m_t}{m_s + m_t}. \tag{50}$$

Equations (47) and (48) are expressed in terms of the momentum transfer cross-section integral $Q_{st}^{(1)}$, which is considered in three cases: Coulomb collisions, hard-sphere interactions, and Maxwell molecule collisions.

Coulomb Collision

The momentum transfer cross-section for Coulomb collisions is given by

$$Q_{st}^{(1)} \left(\mathrm{g}_{st} \right) = \frac{Q_{\mathrm{Co}}}{\mathrm{g}_{st}^4}, \tag{51}$$

where

$$Q_{\mathrm{Co}} = 4\pi \left(\frac{e_s e_t}{4\pi \varepsilon_0 m_{st}} \right)^2 \ln \Lambda, \tag{52}$$

Here, e_s and e_t are the charges of species s and t, respectively, ε_0 is the permittivity of free space, and $\ln \Lambda$ is the Coulomb logarithm.

Hard-Sphere Interactions

For hard-sphere interactions, the momentum transfer cross-section,

$$Q_{st}^{(1)} = Q_{\mathrm{HS}} = \pi \, \sigma^2, \tag{53}$$

is a constant (σ is the sum of the radii of the colliding particles).

Maxwell Molecule Collisions

In the case of Maxwell molecule collisions, the product of the relative velocity and the momentum transfer cross-section,

$$\mathrm{g}_{st} Q_{st}^{(1)} = Q_{\mathrm{MC}}, \tag{54}$$

is constant and can be removed from the integrals in equations (46−48).

Transport Coefficients For Drifting Kappa Distribution

Up to this point, the evaluation of the transport coefficients was generalized. Now, we will calculate the transport coefficients for the five-moment approximation, under the assumption that the velocity distribution function is a drifting Kappa distribution for both interacting particles. Evaluating the transport coefficients for each type of collision for the drifting Kappa distribution requires rewriting the distribution in an integral representation. So, rather than writing the distributions in the form

of equation (32), they can be written as

$$f_s^{\kappa_s} = \frac{n_s \eta(\kappa_s)}{\pi^{3/2} \, w_s^3} \frac{1}{\Gamma(\kappa_s + 1)} \int_0^\infty \xi_1^{\kappa_s} \, e^{-\xi_1} \exp\left[-\frac{\xi_1 \, c_s^2}{\kappa_{0_s} \, w_s^2}\right] d\xi_1, \tag{55}$$

$$f_t^{\kappa_t} = \frac{n_t \eta(\kappa_t)}{\pi^{3/2} \, w_t^3} \frac{1}{\Gamma(\kappa_t + 1)} \int_0^\infty \xi_2^{\kappa_t} \, e^{-\xi_2} \exp\left[-\frac{\xi_2 \, c_t^2}{\kappa_{0_t} \, w_t^2}\right] d\xi_2, \tag{56}$$

Coulomb Collision

Using equation (51), The transport coefficients for Coulomb collisions, are

$$\frac{\delta n_s}{\delta t} = 0, \tag{57}$$

$$\frac{\delta \mathbf{M}_s}{\delta t} = -\sum_t m_{st} \, \mathrm{Q_{Co}} \int_{\mathbb{R}^3 \times \mathbb{R}^3} f_s^{\kappa_s} f_t^{\kappa_t} \frac{\mathbf{g}_{st}}{\mathrm{g}_{st}^3} \, d\mathbf{c}_t \, d\mathbf{c}_s, \tag{58}$$

$$\frac{\delta E_s}{\delta t} = -\sum_t m_{st} \, \mathrm{Q_{Co}} \int_{\mathbb{R}^3 \times \mathbb{R}^3} f_s^{\kappa_s} f_t^{\kappa_t} \frac{(\hat{\mathbf{V}}_c \cdot \mathbf{g}_{st})}{\mathrm{g}_{st}^3} \, d\mathbf{c}_t \, d\mathbf{c}_s. \tag{59}$$

The Momentum Coefficient

The momentum coefficient for Coulomb collision is given in equation (58). Substituting the distributions given in equations (55) and (56) into the integral

$$I_M = \int_{\mathbb{R}^3 \times \mathbb{R}^3} f_s^{\kappa_s} f_t^{\kappa_t} \frac{\mathbf{g}_{st}}{\mathrm{g}_{st}^3} \, d\mathbf{c}_t \, d\mathbf{c}_s, \tag{60}$$

gives

$$I_M = \frac{n_s n_t}{\pi^3 \, w_s^3 \, w_t^3} \frac{\eta(\kappa_s)\eta(\kappa_t)}{\Gamma(\kappa_s + 1)\Gamma(\kappa_t + 1)} \int_0^\infty \int_0^\infty \xi_1^{\kappa_s} \, \xi_2^{\kappa_t} \, e^{-\xi_1 - \xi_2}$$

$$\left(\int_{\mathbb{R}^3} \int_{\mathbb{R}^3} \exp\left[-\frac{\xi_1 \, c_s^2}{\kappa_{0_s} \, w_s^2} - \frac{\xi_2 \, c_t^2}{\kappa_{0_t} \, w_t^2}\right] \frac{\mathbf{g}_{st}}{\mathrm{g}_{st}^3} \, d\mathbf{c}_s d\mathbf{c}_t\right) d\xi_1 \, d\xi_2. \tag{61}$$

To solve the integral in equation (61) we will introduce the following transformation, let

$$\mathbf{c}_s = \left(\frac{\kappa_{0_s}}{\xi_1}\right)^{1/2} (\mathbf{c}_* - \mathrm{A} \, \mathbf{g}_*), \qquad \mathbf{c}_t = \left(\frac{\kappa_{0_t}}{\xi_2}\right)^{1/2} (\mathbf{c}_* + \mathrm{B} \, \mathbf{g}_*). \tag{62}$$

The constant A and B are defined as:

$$\mathrm{A} = \frac{m_t T_s}{m_t T_s + m_s T_t}, \qquad \mathrm{B} = \frac{m_s T_t}{m_t T_s + m_s T_t}. \tag{63}$$

The variables $\mathbf{c}_*$ and $\mathbf{g}_*$ are expressed as:

$$\mathbf{c}_* = \mathbf{V}_c - \mathbf{u}_c + \xi \, \Delta \mathbf{u} + \xi \, \mathbf{g}_{st}, \tag{64}$$

$$\mathbf{g}_* = -\mathbf{g}_{st} - \Delta \mathbf{u}, \tag{65}$$

with

$$\mathbf{u}_c = \frac{m_s \mathbf{u}_s + m_t \mathbf{u}_t}{m_s + m_t}, \qquad \xi = \frac{m_{st}}{m_s + m_t} \frac{T_t - T_s}{T_{st}}. \tag{66}$$

The reduced temperature T_{st} are defined as:

$$T_{st} = \frac{m_s T_t + m_t T_s}{m_s + m_t}, \tag{67}$$

and the difference between the drift velocities of s and t particles is

$$\Delta\mathbf{u} = \mathbf{u}_t - \mathbf{u}_s. \tag{68}$$

By calculating the determinant of the Jacobian matrix $\mathbf{J}$ for the transformation described in equations (62) and (63), we have

$$d\mathbf{c}_s d\mathbf{c}_t = \det(\mathbf{J})\, d\mathbf{c}_* d\mathbf{g}_* = \left[\frac{\kappa_{0_s}\kappa_{0_t}}{\xi_1\xi_2}\right]^{1/2} d\mathbf{c}_* d\mathbf{g}_*. \tag{69}$$

Applying the transformation make the integrals in equation (61) independent of each other, so by evaluating the integrals on $\mathbf{c}_*$, ξ_1 and ξ_2 , and rewriting the $\mathbf{g}_*$ integral, gives

$$I_M = \frac{n_s n_t}{\pi^{3/2}\, b^3}\, \mathrm{D}(\kappa_s, \kappa_t) \int_{\mathbb{R}^3} e^{-|\mathbf{g}_{st}+\Delta\mathbf{u}|^2/b^2}\, \frac{\mathbf{g}_{st}}{\mathrm{g}_{st}^3}\, d\mathbf{g}_{st}. \tag{70}$$

where

$$\mathrm{D}(\kappa_s, \kappa_t) = \frac{(\kappa_s - 1/2)\,(\kappa_t - 1/2)}{(\kappa_s - 3/2)\,(\kappa_t - 3/2)} \tag{71}$$

and

$$b = \left(2k_B\,\frac{T_{st}}{m_{st}}\right)^{1/2}. \tag{72}$$

Using the result of the integral I_1^n for $n = -3$ (see Appendix B for details), we have

$$I_M = -\frac{4}{3}\frac{n_s n_t}{\pi^{1/2}\, b^3}\, \mathrm{D}(\kappa_s, \kappa_t)\, \Delta\mathbf{u}\, \Phi_{\mathrm{Co}}(\varepsilon_{st}). \tag{73}$$

Substituting equation (73) into equation (58), we can write the momentum coefficient for Coulomb collision as

$$\frac{\delta\mathbf{M}_s}{\delta t} = \sum_t n_s m_s \nu_{st}^{\mathrm{Co}}\, \mathrm{D}(\kappa_s, \kappa_t)\, \Delta\mathbf{u}\, \Phi_{\mathrm{Co}}(\varepsilon_{st}), \tag{74}$$

where Φ_{Co} is defined as in equation (153), Appendix B, and

$$\nu_{st}^{\mathrm{Co}} = \frac{4}{3}\frac{m_t}{m_s + m_t}\frac{n_t}{\pi^{1/2}\, b^3}\, \mathrm{Q}_{\mathrm{Co}}, \qquad \varepsilon_{st} = \frac{|\Delta\mathbf{u}|}{b}. \tag{75}$$

The Energy Coefficient

The energy coefficient for Coulomb collision is given in equation (59). Substitute the dot product from equation (49) into the integral

$$I_E = \int_{\mathbb{R}^3 \times \mathbb{R}^3} f_s^{\kappa_s} f_t^{\kappa_t}\, \frac{(\hat{\mathbf{V}}_c \cdot \mathbf{g}_{st})}{\mathrm{g}_{st}^3}\, d\mathbf{c}_t\, d\mathbf{c}_s, \tag{76}$$

leads to three integrals, which can be evaluated by following the same steps as the integral in equation (60), where we substitute the distributions given in equations (55) and (56) into the integrals, and apply the transformation mentioned in equations (62) and (63). This results in two integrals that depend on $\mathbf{g}_{st}$. Using the results of the integrals I_2^n and I_3^n at $n = -3$, as given in Appendix B, and combining all three integrals, we obtain:

$$I_E = -\frac{1}{m_s + m_t}\frac{4}{3}\frac{n_s n_t}{\pi^{1/2}\, b^3}\left[3k_B\,\Delta\mathrm{T}\, \mathrm{W}(\kappa_s, \kappa_t)\, \Psi_{\mathrm{Co}}(\varepsilon_{st}) + m_t\, \mathrm{D}(\kappa_s, \kappa_t)\, |\Delta\mathbf{u}|^2\, \Phi_{\mathrm{Co}}(\varepsilon_{st})\right], \tag{77}$$

where $\Delta\mathrm{T}$ is the difference between the drift velocities of s and t particles,

$$\Delta\mathrm{T} = T_t - T_s, \tag{78}$$

and $\mathrm{W}(\kappa_s, \kappa_t)$ defined as

$$\mathrm{W}(\kappa_s, \kappa_t) = \frac{1}{(\kappa_s - 3/2)^{1/2}}\frac{\Gamma(\kappa_s)}{\Gamma(\kappa_s - 1/2)}\frac{(\kappa_t - 1/2)}{(\kappa_t - 3/2)}. \tag{79}$$

Substituting equation (77) in equation (59), we can write the energy coefficient for Coulomb collision, as

$$\frac{\delta E_s}{\delta t} = \sum_t \frac{n_s m_s \nu_{st}^{\text{Co}}}{m_s + m_t} \left[3k_B \, \Delta \text{T} \, \text{W}(\kappa_s, \kappa_t) \, \Psi_{\text{Co}}(\varepsilon_{st}) + m_t \, \text{D}(\kappa_s, \kappa_t) \, |\Delta \mathbf{u}|^2 \, \Phi_{\text{Co}}(\varepsilon_{st}) \right], \tag{80}$$

where Φ_{Co} and Ψ_{Co} are defined as in equation (153) and (155), respectively, and

$$\nu_{st}^{\text{Co}} = \frac{4}{3} \frac{m_t}{m_s + m_t} \frac{n_t}{\pi^{1/2} \, b^3} \, \text{Q}_{\text{Co}}. \tag{81}$$

Hard-Sphere Interactions

Using equation (53), we can write the transport coefficients for hard-sphere interactions as

$$\frac{\delta n_s}{\delta t} = 0, \tag{82}$$

$$\frac{\delta \mathbf{M}_s}{\delta t} = -\sum_t m_{st} \, \text{Q}_{\text{HS}} \int_{\mathbb{R}^3 \times \mathbb{R}^3} f_s f_t \, \text{g}_{st} \, \mathbf{g}_{st} \, d\mathbf{c}_t \, d\mathbf{c}_s, \tag{83}$$

$$\frac{\delta E_s}{\delta t} = -\sum_t m_{st} \, \text{Q}_{\text{HS}} \int_{\mathbb{R}^3 \times \mathbb{R}^3} f_s f_t \, \text{g}_{st} \left(\hat{\mathbf{V}}_c \cdot \mathbf{g}_{st} \right) d\mathbf{c}_t \, d\mathbf{c}_s. \tag{84}$$

Calculating the transport coefficients for hard-sphere interactions follows the same steps that have been applied previously for the Coulomb collision, since the main difference between the integrals in equations (82−84) and those in equations (57−59) is that g_{st} has a power of 1 rather than −3. This results in a change only in the final integrals, where we use I_1^n, I_2^n, and I_3^n with $n = 1$, see Appendix B, to obtain the momentum coefficient for hard-sphere interactions,

$$\frac{\delta \mathbf{M}_s}{\delta t} = \sum_t n_s m_s \nu_{st}^{\text{HS}} \, \text{D}(\kappa) \, \Delta \mathbf{u} \, \Phi_{\text{HS}}(\varepsilon_{st}), \tag{85}$$

and the energy coefficient for hard-sphere interactions

$$\frac{\delta E_s}{\delta t} = \sum_t \frac{n_s m_s \nu_{st}^{\text{HS}}}{m_s + m_t} \left[3k_B \, \Delta \text{T} \, \text{W}(\kappa) \, \Psi_{\text{HS}}(\varepsilon_{st}) + m_t \, \text{D}(\kappa) \, |\Delta \mathbf{u}|^2 \, \Phi_{\text{HS}}(\varepsilon_{st}) \right], \tag{86}$$

where Φ_{HS} and Ψ_{HS} define as in equation (154) and (156), respectively, and

$$\nu_{st}^{\text{HS}} = \frac{8}{3} \frac{m_t}{m_s + m_t} \frac{n_t}{\pi^{1/2}} \, b \, \text{Q}_{\text{HS}}. \tag{87}$$

Maxwell Molecule Collisions

Using equation (54), the transport coefficients for Maxwell molecule collisions become,

$$\frac{\delta n_s}{\delta t} = 0, \tag{88}$$

$$\frac{\delta \mathbf{M}_s}{\delta t} = -\sum_t m_{st} \, \text{Q}_{\text{MC}} \int_{\mathbb{R}^3 \times \mathbb{R}^3} f_s^{\kappa_s} f_t^{\kappa_t} \, \mathbf{g}_{st} \, d\mathbf{c}_t \, d\mathbf{c}_s, \tag{89}$$

$$\frac{\delta E_s}{\delta t} = -\sum_t m_{st} \, \text{Q}_{\text{MC}} \int_{\mathbb{R}^3 \times \mathbb{R}^3} f_s^{\kappa_s} f_t^{\kappa_t} \left(\hat{\mathbf{V}}_c \cdot \mathbf{g}_{st} \right) d\mathbf{c}_t \, d\mathbf{c}_s. \tag{90}$$

There's no integration technique required to evaluate equations (88−90), since after rewriting the relative velocity in equation (4) and the dot product in equation (49) in terms of the random velocities c_s and c_t, as

$$\mathbf{g}_{st} = \mathbf{c}_s - \mathbf{c}_t - \Delta \mathbf{u}, \tag{91}$$

and

$$\hat{\mathbf{V}}_c \cdot \mathbf{g}_{st} = \frac{m_s c_s^2 - m_t c_t^2 + (m_t - m_s)\mathbf{c}_t \cdot \mathbf{c}_s + (m_t - m_s)\,\mathbf{c}_s \cdot \Delta\mathbf{u} - 2m_t \mathbf{c}_t \cdot \Delta\mathbf{u} - m_t|\Delta\mathbf{u}|^2}{m_s + m_t}. \tag{92}$$

We can use the following expectation values, see Appendix A,

$$\langle c_\alpha^2 \rangle = \frac{3k_B T_\alpha}{m_\alpha}, \qquad \langle \mathbf{c}_\alpha \rangle = 0, \qquad \langle A \rangle = A\,, A \text{ is constant} \tag{93}$$

to obtain the momentum coefficient for Maxwell molecule collisions

$$\frac{\delta \mathbf{M}_s}{\delta t} = \sum_t n_s m_s \nu_{st}^{\mathrm{MC}} \, \Delta\mathbf{u}, \tag{94}$$

and the energy coefficient for Maxwell molecule collisions

$$\frac{\delta E_s}{\delta t} = \sum_t \frac{n_s m_s \nu_{st}^{\mathrm{MC}}}{m_s + m_t} \left[3k_B\,\Delta\mathrm{T} + m_t\,|\Delta\mathbf{u}|^2 \right], \tag{95}$$

where

$$\nu_{st}^{\mathrm{MC}} = \frac{n_t\,m_t}{m_s + m_t}\, \mathrm{Q}_{\mathrm{MC}}. \tag{96}$$

Summary

The general expressions for the transport coefficients in the five-moment approximation, where the the distribution function is set to be drifting Kappa, are summarized as follows:

$$\frac{\delta n_s}{\delta t} = 0, \tag{97}$$

$$\frac{\delta \mathbf{M}_s}{\delta t} = \sum_t n_s m_s \nu_{st}\, \mathrm{D}(\kappa_s, \kappa_t)\, \Delta\mathbf{u}\, \Phi(\varepsilon_{st}), \tag{98}$$

$$\frac{\delta E_s}{\delta t} = \sum_t \frac{n_s m_s \nu_{st}}{m_s + m_t} \left[3k_B \Delta\mathrm{T}\, \mathrm{W}(\kappa_s, \kappa_t)\, \Psi(\varepsilon_{st}) + m_t\, \mathrm{D}(\kappa_s, \kappa_t)\, |\Delta\mathbf{u}|^2\, \Phi(\varepsilon_{st}) \right]. \tag{99}$$

where

$$\varepsilon_{st} = \left(\frac{1}{2k_B}\frac{m_{st}}{T_{st}} \right)^{1/2} |\Delta\mathbf{u}|, \qquad \Delta\mathbf{u} = \mathbf{u}_t - \mathbf{u}_s, \qquad \Delta\mathrm{T} = T_t - T_s, \tag{100}$$

and

$$\mathrm{D}(\kappa_s, \kappa_t) = \frac{(\kappa_s - 1/2)}{(\kappa_s - 3/2)}\frac{(\kappa_t - 1/2)}{(\kappa_t - 3/2)}, \qquad \mathrm{W}(\kappa_s, \kappa_t) = \frac{1}{(\kappa_s - 3/2)^{1/2}}\frac{\Gamma(\kappa_s)}{\Gamma(\kappa_s - 1/2)}\frac{(\kappa_t - 1/2)}{(\kappa_t - 3/2)}. \tag{101}$$

The factors ν_{st}, Φ, and Ψ change depending on the collision type, such as Coulomb, hard-sphere, and Maxwell molecule collisions. These are summarized as follows:

Coulomb collisions:

$$\nu_{st} = \nu_{st}^{\mathrm{Co}} = \frac{4}{3}\frac{n_t}{\pi^{1/2}}\frac{m_t}{m_s + m_t}\left(\frac{1}{2k_B}\frac{m_{st}}{T_{st}} \right)^{3/2} \mathrm{Q}_{\mathrm{Co}}, \qquad \mathrm{Q}_{\mathrm{Co}} = 4\pi\left(\frac{e_s e_t}{4\pi\varepsilon_0 m_{st}} \right)^2 \ln\Lambda, \tag{102}$$

and

$$\Phi(\varepsilon_{st}) = \Phi_{\mathrm{Co}}(\varepsilon_{st}) = \frac{3\sqrt{\pi}}{4}\frac{\mathrm{erf}(\varepsilon_{st})}{\varepsilon_{st}^3} - \frac{3}{2}\frac{e^{-\varepsilon_{st}^2}}{\varepsilon_{st}^2}, \tag{103}$$

$$\Psi(\varepsilon_{st}) = \Psi_{\mathrm{Co}}(\varepsilon_{st}) = e^{-\varepsilon_{st}^2}. \tag{104}$$

Hard-sphere interaction:

$$\nu_{st} = \nu_{st}^{\mathrm{HS}} = \frac{8}{3} \frac{n_t}{\pi^{1/2}} \frac{m_t}{m_s + m_t} \left(2k_B \frac{T_{st}}{m_{st}}\right)^{1/2} \mathrm{Q_{HS}}, \qquad \mathrm{Q_{HS}} = \pi \sigma^2, \tag{105}$$

and

$$\Phi(\varepsilon_{st}) = \Phi_{\mathrm{HS}}(\varepsilon_{st}) = \frac{3\sqrt{\pi}}{8} \left(\varepsilon_{st} + \frac{1}{\varepsilon_{st}} - \frac{1}{4\varepsilon_{st}^3}\right) \mathrm{erf}(\varepsilon_{st}) + \frac{3}{8} \left(1 + \frac{1}{2\varepsilon_{st}^2}\right) e^{-\varepsilon_{st}^2}, \tag{106}$$

$$\Psi(\varepsilon_{st}) = \Psi_{\mathrm{HS}}(\varepsilon_{st}) = \frac{\sqrt{\pi}}{2} \left(\varepsilon_{st} + \frac{1}{2\varepsilon_{st}}\right) \mathrm{erf}(\varepsilon_{st}) + \frac{1}{2} e^{-\varepsilon_{st}^2}. \tag{107}$$

Maxwell molecule collisions

$$\Phi(\varepsilon_{st}) = \Phi_{\mathrm{MC}}(\varepsilon_{st}) = 1/\mathrm{D}(\kappa_s, \kappa_t), \tag{108}$$

$$\Psi(\varepsilon_{st}) = \Psi_{\mathrm{MC}}(\varepsilon_{st}) = 1/\mathrm{W}(\kappa_s, \kappa_t), \tag{109}$$

and

$$\nu_{st} = \nu_{st}^{\mathrm{MC}} = \frac{n_t\, m_t}{m_s + m_t} \mathrm{Q_{MC}}, \qquad \mathrm{Q_{MC}} = \mathrm{g}_{st} Q_{st}^{(1)} = \text{constant.} \tag{110}$$

Hypergeometric Representation

Here, we rewrite the resulting transport coefficients in terms of the hypergeometric function, and this is done by expressing the Φ's and Ψ's in the hypergeometric representation, where they can be written as

Coulomb collisions:

$$\Phi_{\mathrm{Co}}(\varepsilon_{st}) = {}_1F_1\left(\frac{3}{2}; \frac{5}{2}; -\varepsilon_{st}^2\right), \tag{111}$$

$$\Psi_{\mathrm{Co}}(\varepsilon_{st}) = {}_1F_1\left(\frac{1}{2}; \frac{1}{2}; -\varepsilon_{st}^2\right). \tag{112}$$

Hard-sphere:

$$\Phi_{\mathrm{HS}}(\varepsilon_{st}) = {}_1F_1\left(-\frac{1}{2}; \frac{5}{2}; -\varepsilon_{st}^2\right), \tag{113}$$

$$\Psi_{\mathrm{HS}}(\varepsilon_{st}) = {}_1F_1\left(-\frac{1}{2}; \frac{3}{2}; -\varepsilon_{st}^2\right). \tag{114}$$

Maxwell molecule:

$$\Phi_{\mathrm{MC}}(\varepsilon_{st}) = 1/\mathrm{D}(\kappa_s, \kappa_t), \tag{115}$$

$$\Psi_{\mathrm{MC}}(\varepsilon_{st}) = 1/\mathrm{W}(\kappa_s, \kappa_t). \tag{116}$$

6 Special Cases

6.1 Limiting case

One of the special properties of the Kappa distribution is that as κ tends to infinity, the Kappa distribution turns to a Maxwellian distribution, where we have, Pierrard and Lazar [2010],

$$\lim_{\kappa \to \infty} \eta(\kappa) = 1 \qquad \text{and} \qquad \lim_{\kappa \to \infty} \left[1 + \frac{a}{(\kappa - 3/2)}\right]^{-\kappa - 1} = e^{-a}, \tag{117}$$
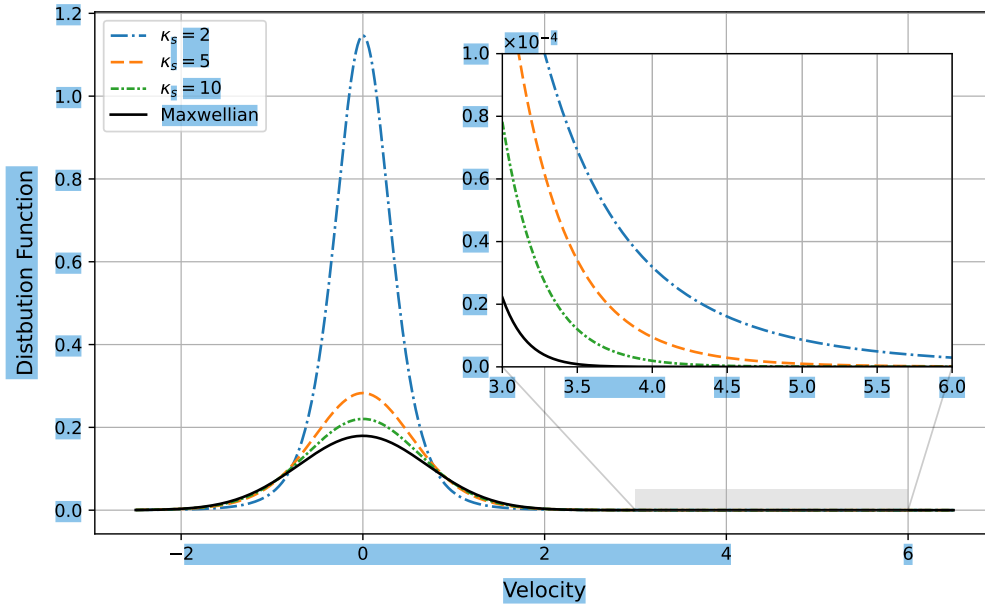
Figure 1. A schematic comparison between modified Kappa velocity distributions for κ_s values 2, 5, and 10, and the Maxwellian velocity distribution.

and Ψ's, equations (50, 51, 55, and 56), in the hypergeometric representation, such that

Coulomb collisions:

$$\Phi_{\mathrm{Co}}(\varepsilon_{st}) = {}_1F_1\left(\frac{3}{2};\frac{5}{2};-\varepsilon_{st}^2\right), \tag{60}$$

$$\Psi_{\mathrm{Co}}(\varepsilon_{st}) = {}_1F_1\left(\frac{1}{2};\frac{1}{2};-\varepsilon_{st}^2\right). \tag{61}$$

Hard-sphere interactions:

$$\Phi_{\mathrm{HS}}(\varepsilon_{st}) = {}_1F_1\left(-\frac{1}{2};\frac{5}{2};-\varepsilon_{st}^2\right), \tag{62}$$

$$\Psi_{\mathrm{HS}}(\varepsilon_{st}) = {}_1F_1\left(-\frac{1}{2};\frac{3}{2};-\varepsilon_{st}^2\right). \tag{63}$$

2.2.2 Limiting case: kappa parameter approaches infinity

One of the special properties of the modified Kappa distribution is that, as κ_s approaches infinity, the modified Kappa distribution reduces to a Maxwellian distribution (Pierrard and Lazar, 2010). Specifically, we have

$$\lim_{\kappa_s \to \infty} \eta(\kappa_s) = 1 \tag{64}$$

and

$$\lim_{\kappa_s \to \infty} \left[1 + \frac{a}{(\kappa_s - 3/2)}\right]^{-\kappa_s - 1} = e^{-a}, \tag{65}$$

Therefore, the modified Kappa distribution becomes identically Maxwellian distribution

$$\lim_{\kappa_s \to \infty} f_s^{\mathrm{MK}} = \frac{n_s}{\pi^{3/2} w_s^3} \exp\left(-\frac{c_s^2}{w_s^2}\right), \tag{66}$$

as shown in figure 1, where as κ_s gets larger, the distribution becomes closer and closer to the Maxwellian distribution. This provides further confirmation that the derived formulas are correct by taking the limit of the collision terms as $\kappa \to \infty$, $\kappa = \kappa_s = \kappa_t$, and comparing the resulting limits with existing formulas for the Maxwellian. The collision terms given in equations (40–42) depend on the kappa parameter through the effective collision frequency, the thermalisation rate, and the relative temperature difference, ν_{st}^{MK}, $\nu_{st,T}^{\mathrm{MK}}$, and $\Delta\mathrm{T}_{st}^{\mathrm{MK}}$, respectively. These quantities are expressed using the two functions $D(\kappa_s,\kappa_t)$ and $H(\kappa_\alpha)$, $\alpha = s, t$. Consequently, the limits of the collision terms reduce to the following limits

$$\lim_{\kappa \to \infty} \nu_{st}^{\mathrm{MK}}(\kappa,\kappa) = \nu_{st}, \tag{67}$$

$$\lim_{\kappa \to \infty} \nu_{st,T}^{\mathrm{MK}}(\kappa,\kappa) = \nu_{st,T}, \tag{68}$$

$$\lim_{\kappa \to \infty} \Delta\mathrm{T}_{st}^{\mathrm{MK}} = T_t - T_s = \Delta\mathrm{T}_{st}. \tag{69}$$

Hence,

$$\lim_{\kappa \to \infty} D(\kappa,\kappa) = \lim_{\kappa \to \infty} H(\kappa) = 1. \tag{70}$$

thus, the Kappa distribution becomes identically Maxwellian distribution

$$\lim_{\kappa \to \infty} f_\alpha^\kappa = \frac{n_\alpha}{\pi^{3/2} \, w_\alpha^3} \exp\left(-\frac{c_\alpha^2}{w_\alpha^2}\right) = f_\alpha^M, \tag{118}$$

which gives us one more step to be sure that the derived formulas are correct by taking the limit of transport coefficients as $\kappa \to \infty$ and comparing the resulting limit with existing formulas for the Maxwellian. The transport coefficients in the three cases Coulomb collisions, hard sphere, and Maxwell molecule are given in equation (97−99), and in the derived formulas the kappa index exist only in the two function $D(\kappa_s, \kappa_t)$ and $W(\kappa_s, \kappa_t)$ which mean that the limit of the transport coefficient is simplified to the two limits

$$\lim_{\kappa \to \infty} D(\kappa, \kappa) = \lim_{\kappa \to \infty} W(\kappa, \kappa) = 1, \qquad \kappa = \kappa_s = \kappa_t \tag{119}$$

so the limit of the transport equations (97−99), as κ goes to ∞ is

$$\lim_{\kappa \to \infty} \left[\frac{\delta n_s}{\delta t}\right] = 0, \tag{120}$$

$$\lim_{\kappa \to \infty} \left[\frac{\delta \mathbf{M}_s}{\delta t}\right] = \sum_t n_s m_s \nu_{st} \, \Delta\mathbf{u} \, \Phi(\varepsilon_{st}), \tag{121}$$

$$\lim_{\kappa \to \infty} \left[\frac{\delta E_s}{\delta t}\right] = \sum_t \frac{n_s m_s \nu_{st}}{m_s + m_t} \left[3k_B \, \Delta T \, \Psi(\varepsilon_{st}) + m_t |\Delta\mathbf{u}|^2 \, \Phi(\varepsilon_{st})\right]. \tag{122}$$

The resulting limit in the equations gives exactly the same result as the Maxwellian, as seen in Schunk and Nagy [2009], with the same definitions of Φ, Ψ, and ν_{st}.

6.2   Non‑Drifting Kappa Distribution

If we chose both species s and t to have non-drifting kappa distribution, then the drift velocities for both of the interacting particles is equal to zero, $\mathbf{u}_s = \mathbf{u}_t = 0$, and since we define, $\Delta\mathbf{u} = \mathbf{u}_t - \mathbf{u}_s$, we have

$$\Delta\mathbf{u} = 0, \qquad |\Delta\mathbf{u}| = 0 \tag{123}$$

then using the relation

$$\Psi_{Co}(0) = \Psi_{HS}(0) = 1, \qquad \Psi_{MC}(0) = 1/W(\kappa_s, \kappa_t), \tag{124}$$

the transport coefficient becomes

$$\frac{\delta n_s}{\delta t} = 0, \tag{125}$$

$$\frac{\delta \mathbf{M}_s}{\delta t} = 0, \tag{126}$$

$$\frac{\delta E_s}{\delta t} = \sum_t \frac{n_s m_s \nu_{st}}{m_s + m_t} \left[3k_B \, \Delta T \, W(\kappa_s, \kappa_t) \, F(\kappa_s, \kappa_t)\right]. \tag{127}$$

where F is a function of κ_s and κ_t defined for *Coulomb and Hard-sphere*, as

$$F(\kappa_s, \kappa_t) = F_{Co}(\kappa_s, \kappa_t) = F_{HS}(\kappa_s, \kappa_t) = 1, \tag{128}$$

and for *Maxwell molecule*, as

$$F(\kappa) = F_{MC}(\kappa) = 1/W(\kappa_s, \kappa_t). \tag{129}$$

When the drift velocities of the species s and t are equal, i.e. $\mathbf{u}_s = \mathbf{u}_t$, we obtain the same result as given in equations (125−127).

With $\nu_{st,T}$ denoting the thermalisation rate for systems governed by the Maxwellian distribution, defined as

$$\nu_{st,T} = 2 \frac{m_{st}}{m_t} \nu_{st}. \tag{71}$$

Therefore, in the limit κ approaches ∞, the collision terms (40–42) recover the form

$$\lim_{\kappa \to \infty} \left[\frac{\delta n_s}{\delta t} \right] = 0, \tag{72}$$

$$\lim_{\kappa \to \infty} \left[\frac{\delta \mathbf{M}_s}{\delta t} \right] = \sum_t n_s m_s \nu_{st} \, \Phi(\varepsilon_{st}) \, \Delta \mathbf{u}_{st}, \tag{73}$$

$$\lim_{\kappa \to \infty} \left[\frac{\delta E_s}{\delta t} \right] = \sum_t \frac{n_s m_s \nu_{st}}{m_s + m_t} \left[3 k_B \, \Psi(\varepsilon_{st}) \, \Delta \mathrm{T}_{st} \right.$$
$$\left. + m_t \, \Phi(\varepsilon_{st}) \, |\Delta \mathbf{u}_{st}|^2 \right]. \tag{74}$$

The resulting limits gives exactly the same results as the Maxwellian distribution (Schunk and Nagy, 2009), with the same definitions of Φ, Ψ, and ν_{st}.

2.3 Effective collision frequency and thermalisation rate in systems with modified Kappa distributions

Within the framework of the five-moment approximation of the transport equations, the effective collision frequency and the thermalisation rate can be obtained directly from the momentum and energy collision terms. As derived in the previous section for the modified Kappa distribution, equations (47) and (48) present the effective collision frequency and the thermalisation rate, which are essential for understanding the exchange of momentum and energy between particles due to collisions. The effective collision frequency reflects the average rate of how frequently collisions occur, determining the efficiency of momentum transfer within the system, while the thermalisation rate measures how rapidly the system approaches thermal equilibrium through collisions. Equations (47) and (48) show that the modified Kappa distribution affects the effective collision frequency and the thermalisation rate through the kappa dependent term $\mathrm{D}(\kappa_s, \kappa_t)$. This factor depends explicitly on the kappa parameters κ_s and κ_t of the interacting species s and t, and its form changes depending on the type of collisions under consideration. To compare the effective collision frequency and thermalisation rate of the modified Kappa and Maxwellian distributions, we must first understand how their particle velocity distributions differ. While the Maxwellian distribution has most particles concentrated around the distribution core, with low and intermediate velocity magnitudes, the modified Kappa distribution shifts this balance by increasing the number of particles both in the low-energy core and in the high-energy tails, (i.e., at low and high velocity magnitudes), as shown in Figure (1). This redistribution in the particle velocities is directly related to the effective collision frequency and the

thermalisation rate. In collision processes, such as Maxwell molecule collisions, where the collision frequency does not depend on particle velocity, the redistribution has no effect. The effective collision frequency and thermalisation rate remain the same even when modified Kappa distribution is used. This is confirmed by the result $\mathrm{D} = 1$, which shows that the kappa parameter does not change either the effective collision frequency or the thermalisation rate compared with the Maxwellian case,

$$\nu_{st}^{\mathrm{MK}} = \nu_{st}, \quad \text{and} \quad \nu_{st,T}^{\mathrm{MK}} = \nu_{st,T}. \tag{75}$$

In contrast, when collisions strongly depend on particle velocity, the modified Kappa distribution significantly affects both the effective collision frequency and the thermalisation rate. This effect becomes particularly evident in processes such as Coulomb collisions and hard-sphere interactions, where the velocity distribution strongly shapes the interaction dynamics. In these cases, the functions D vary according to the kappa parameters κ_s and κ_t, as given in equations (52). To compare the effective collision frequency and thermalisation rate with the Maxwellian case, and to better understand their behaviour, we consider the special case $\kappa = \kappa_s = \kappa_t$, so that the expressions, ν_{st}^{MK} and $\nu_{st,T}^{\mathrm{MK}}$, reduce to

$$\nu_{st}^{\mathrm{MK}} = \nu_{st} \left(\frac{\kappa - 1/2}{\kappa - 3/2} \right)^2, \tag{76}$$

$$\nu_{st,T}^{\mathrm{MK}} = 2 \frac{m_{st}}{m_t} \nu_{st}^{\mathrm{MK}}, \tag{77}$$

The effective collision frequency for the modified Kappa distribution in equation (76) agrees exactly with Livadiotis (2019) in the κ dependency, where both share the same functional form. Equations (76) and (77) show that for small values of κ, both the effective collision frequency and the thermalisation rate are large and decreasing as κ increases. As κ goes to infinity, the kappa term in equation (76) approaches 1, and the results converge to those of the Maxwellian distribution, as illustrated in Figure 2. In this figure, we have plotted the κ dependency for both the effective collision frequency and the thermalisation rate; in other words, the ratios $\nu_{st}^{\mathrm{MK}}/\nu_{st}$ and $\nu_{st,T}^{\mathrm{MK}}/\nu_{st,T}$ as functions of the kappa parameter. This behaviour arises from the redistribution of the particle velocities in the modified Kappa distribution, where at low values of κ, the number of particles near the core with a small velocity magnitudes is very high compared to the Maxwellian distribution. These particles increase the collision frequency in case of Coulomb collisions and Maxwell molecules interactions, since these interactions are inversely proportional to velocity, making the effective collision frequency and the thermalisation rate are enhanced at low kappa values.

7 Variations Of Transport Coefficients As A Result Of Coulomb Collisions

The transport coefficients for the five-moment approximation, presented in equations (97−99), describe how density, momentum, and energy, for particles s change under the effect of collisions. These coefficients depend on three variables, number density n_s, drift velocity $\mathbf{u}_s$, and temperature T_s for particles s, as well as on the parameters of particles t, number density n_t, drift velocity $\mathbf{u}_t$, and temperature T_t. Additionally, two functions of κ_s and κ_t, D(κ_s, κ_t) and W(κ_s, κ_t). The masses of both interacting particles, s and t, (m_s, m_t) are constant and remain unchanged throughout the collision process for all types of collisions, this makes the density coefficient to be zero according to equation (97). In this section, we will examine how these coefficients, in the case of Coulomb collisions, vary with respect to the variables $(n_s, \mathbf{u}_s, T_s)$, the parameters $(n_t, \mathbf{u}_t, T_t)$, and the functions D and W.

Maxwellian Distribution

In the Maxwellian case, both functions D(κ_s, κ_t) and W(κ_s, κ_t) are set to one, Section 6.1. For better clarity, we will discuss the behaviour of the transport coefficients in three cases. In each case, we will consider a specific set of variables or parameters.

First case, the *number density* of the interacting particles n_s and n_t. From equations (97−99), we see that n_s and n_t appear as a product. This indicates that an increase in the number density of either particle s or t will increase the influence of collisions on both momentum and energy of the s particles. Such a result is reasonable because the number density is defined as the number of particles per unit volume. Increasing the number density requires increasing the number of particles within the same volume. This results in more collisions between the interacting particles s and t, leading to a greater change in both momentum and energy due to the collisions.

Second case, the *drift velocities* of the interacting particles $\mathbf{u}_s$, $\mathbf{u}_t$, and the *temperature* of the s particles T_s. Equations (97−99) show that the transport coefficients depend on the difference in drift velocity, $\Delta\mathbf{u} = \mathbf{u}_t - \mathbf{u}_s$, and T_s. In Figures (1a) and (1c), we plot the isolines of the transport coefficients for momentum and energy as functions of $\Delta\mathbf{u}$ and T_s, with all other constants set to 1.0 for simplicity. Additionally, we assume identical parameters for all t particles, so the summation over t, in equations (97−99), reduces to multiplication by the number of t particles, N_t, which is set to 1000 for easier comparison with other cases. Figure (1a) shows the magnitude of the momentum transport coefficient, assuming that the direction of $\Delta\mathbf{u}$ is along the z-axis. From the figure, we can see that the momentum of the particles s does not change when the difference in drift velocities, $\Delta\mathbf{u}$, is zero, regardless of the temperature T_s. In other words, the drift velocities of the two particles are either equal or both zero, meaning that the particles are not moving relative to each other, or the system is in a state where there is no net current flow (e.g., no applied electric field). Under these conditions, Coulomb collisions can be treated as an elastic collisions, so that the total kinetic energy and momentum of the system are conserved, resulting in no change in momentum caused by the collisions. To see how momentum transport coefficient changes relative to $\Delta\mathbf{u}$, we plot the cross-section of the momentum transport coefficient at T_s equals to zero as shown in Figure (1b). We can observe that when one particle's drift velocity is slightly larger than the other's, the change in momentum of particle s due to collisions will increase until it reaches its maximum. Beyond this maximum point, as absolute value of the difference between the drift velocities becomes very large, i.e., $\mathbf{u}_s \gg \mathbf{u}_t$ or $\mathbf{u}_t \gg \mathbf{u}_s$, collisions have less and less effect on the momentum, and it approaches zero when $\Delta\mathbf{u}$ becomes very large, because when the interacting particles are moving at significantly different speeds (i.e., have large differences in drift velocities), they are more likely to move past each other without interacting, leading to decreasing in the number of collisions. Referring back to Figure (1a), as the temperature of the s particles increases, the impact of collisions on their momentum decreases until it eventually vanishes. This occurs because the mean collision frequency, ν, between the particles decreases with increasing temperature. Specifically, for Coulomb collisions,
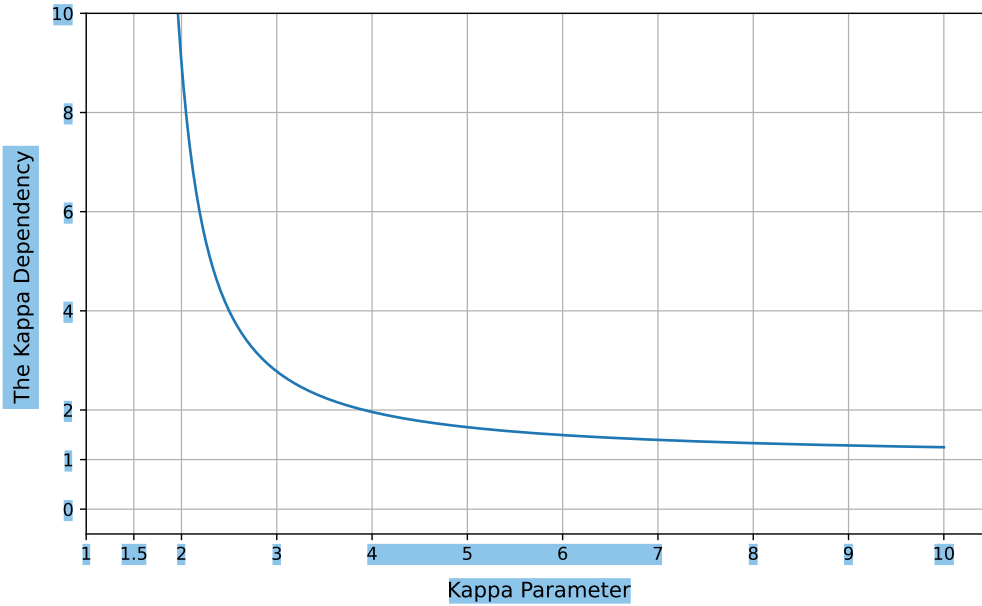
Figure 2. The kappa dependency for both the effective collision frequency and the thermalisation rate.

2.4 Variations of collision terms as a result of Coulomb collisions

The collision terms for the five-moment approximation, presented in equations (40−42), describe how density, momentum, and energy, for particles s change under the effect of collisions. These terms depend on three variables, number density n_s, drift velocity $\mathbf{u}_s$, and temperature T_s for particles s, as well as on the parameters of particles t, number density n_t, drift velocity $\mathbf{u}_t$, and temperature T_t. Additionally, two functions of κ_s and κ_t, $\mathrm{D}(\kappa_s,\kappa_t)$ and $\mathrm{H}(\kappa_\alpha), \alpha = s, t$, contribute to the effective collision frequency, the thermalisation rate and the relative temperature difference. The masses of both interacting particles s and t, (m_s, m_t), are constant and remain unchanged throughout the collision process for all types of collisions, this makes the density coefficient to be zero according to equation (40). In this section, we examine how the collision terms, in the case of Coulomb collisions, vary with respect to the variables $(n_s, \mathbf{u}_s, T_s)$, and the parameters $(n_t, \mathbf{u}_t, T_t)$, and we compare the results for the modified Kappa and Maxwellian distributions.

2.4.1 Maxwellian distribution

In the Maxwellian case, both functions $\mathrm{D}(\kappa_s,\kappa_t)$ and $\mathrm{H}(\kappa_\alpha), \alpha = s, t$ are set to one, see Sub-subsection 2.2.2. Consequently, the effective collision frequency, the thermalisation rate, and the relative temperature difference in the collision terms simplify to

$$\nu_{st}^{\mathrm{MK}} = \nu_{st}, \quad \nu_{st,T}^{\mathrm{MK}} = \nu_{st,T}, \quad \text{and} \quad \Delta\mathrm{T}_{st}^{\mathrm{MK}} = \Delta\mathrm{T}_{st}. \quad (78)$$

For clarity, we will discuss the behaviour of the collision terms in three cases, each involving a particular choice of variables or parameters.

First case, the *number density* of the interacting particles, n_s and n_t. From equations (40−42), n_s and n_t appears as a product, indicating that an increase in the number density of either particle s or t will increase the influence of collisions on both the momentum and energy of the s particles. Such a result is reasonable because the number density measures particles per unit volume—more particles in the same volume lead to more collisions between s and t, causing greater changes in momentum and energy due to collisions.

Second case, the *drift velocities* of the interacting particles $\mathbf{u}_s, \mathbf{u}_t$, and the *temperature* of the s particles T_s. Equations (40−42) show that the collision terms depend on the difference in drift velocity, $\Delta\mathbf{u}_{st} = \mathbf{u}_t - \mathbf{u}_s$, and on T_s. Figures (3a) and (3c) display the isolines of the momentum and energy collision terms as functions of $\Delta\mathbf{u}_{st}$ and T_s, with all other constants set to 1.0 for simplicity. Assuming identical parameters for all t particles, the summation over t, in equations (40−42), reduces to multiplication by their number, N_t, which is set to 1000 for easier comparison with other cases. Figure (3a) shows the magnitude of the momentum collision term, assuming that the direction of $\Delta\mathbf{u}_{st}$ is along the z-axis. The figure (3a) indicates that the momentum of the particles s remains unchanged when the difference in drift velocities, $\Delta\mathbf{u}_{st}$, is zero, regardless of the temperature T_s. This means that the drift velocities of the two particles are equal or both zero, so they are not moving relative to each other, or the system has no net current flow (e.g., no applied electric field).

the relationship given by Freidberg [2008],

$$\nu \propto \frac{1}{T^{3/2}}, \tag{130}$$

showing that collisions become less probable at higher temperatures, leading to a reduction in their influence on momentum. Figure (1c) represents the energy transport coefficient, the graph shows that the maximum energy exchange occurs when the difference in the drift velocities is zero. As we mentioned earlier, in this case, both momentum and kinetic energy are conserved, meaning there is no change in these quantities. The change in the energy comes from the potential energy, specifically the difference between the temperatures of the interacting particles. Figure (1d) presents the cross-section of the energy transport coefficient when $\Delta \mathbf{u}$ equals to zero. At T_s equals to zero, collisions have their highest effect, since particles s gains temperature from particles t, the energy change of particles s decreases as T_s approaches T_t, reducing the temperature transfer. Eventually, when
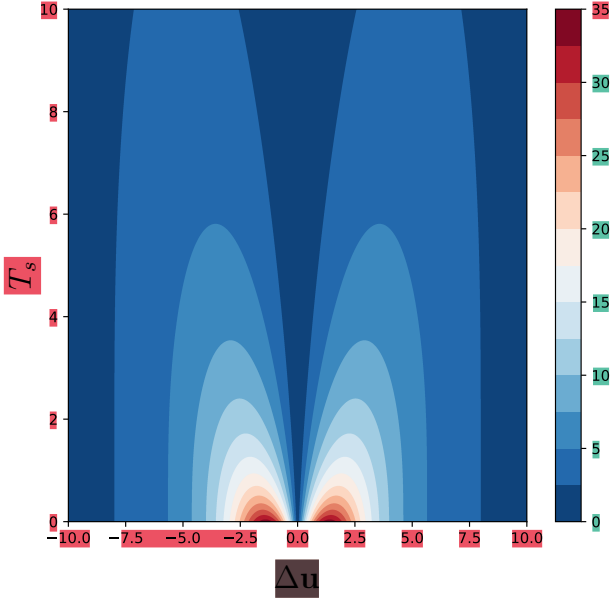
(a) $\delta \mathbf{M}_s/\delta t$
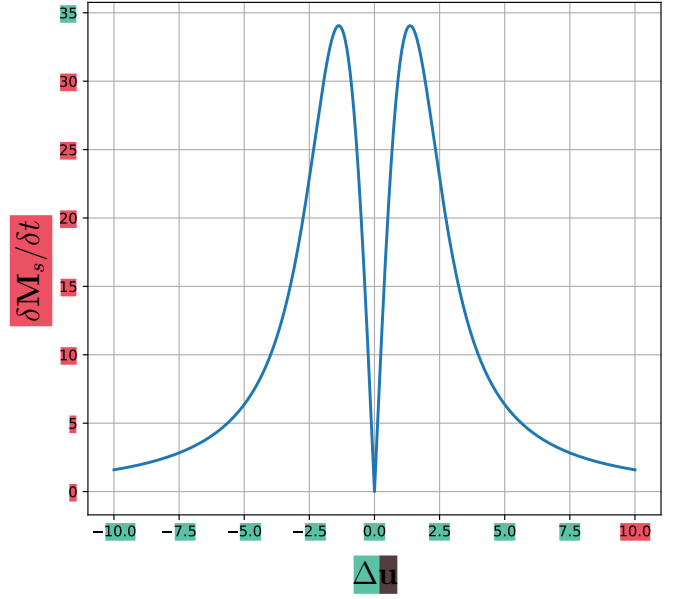
(b) $\delta \mathbf{M}_s/\delta t$ at $T_s = 0$
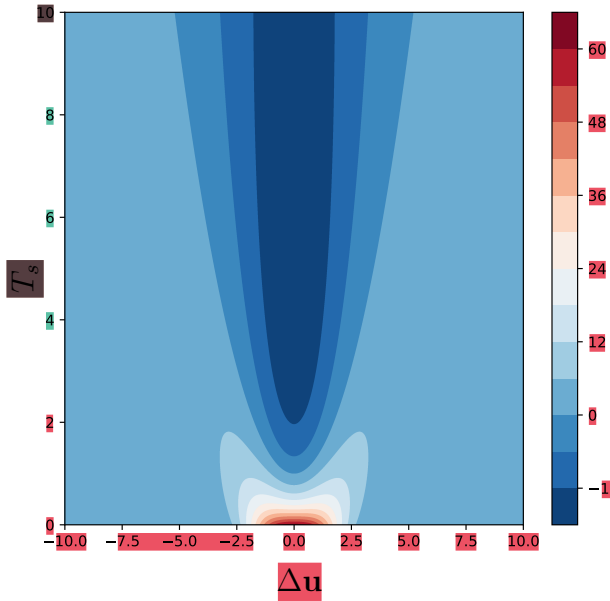
(c) $\delta \mathrm{E}_s/\delta t$
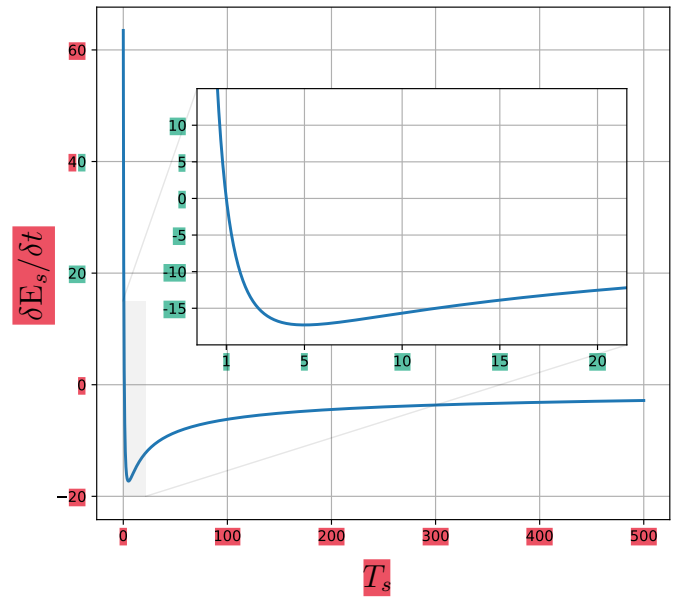
(d) $\delta \mathrm{E}_s/\delta t$ at $\Delta \mathbf{u} = 0$

Figure 1: The transport coefficients for momentum and energy for the Maxwellian velocity distribution function in the case of Coulomb collisions.

(a) $\delta\mathbf{M}_s/\delta t$

(b) $\delta\mathbf{M}_s/\delta t$ at $T_s = 0$

(c) $\delta\mathrm{E}_s/\delta t$

(d) $\delta\mathrm{E}_s/\delta t$ at $\Delta\mathbf{u}_{st} = 0$
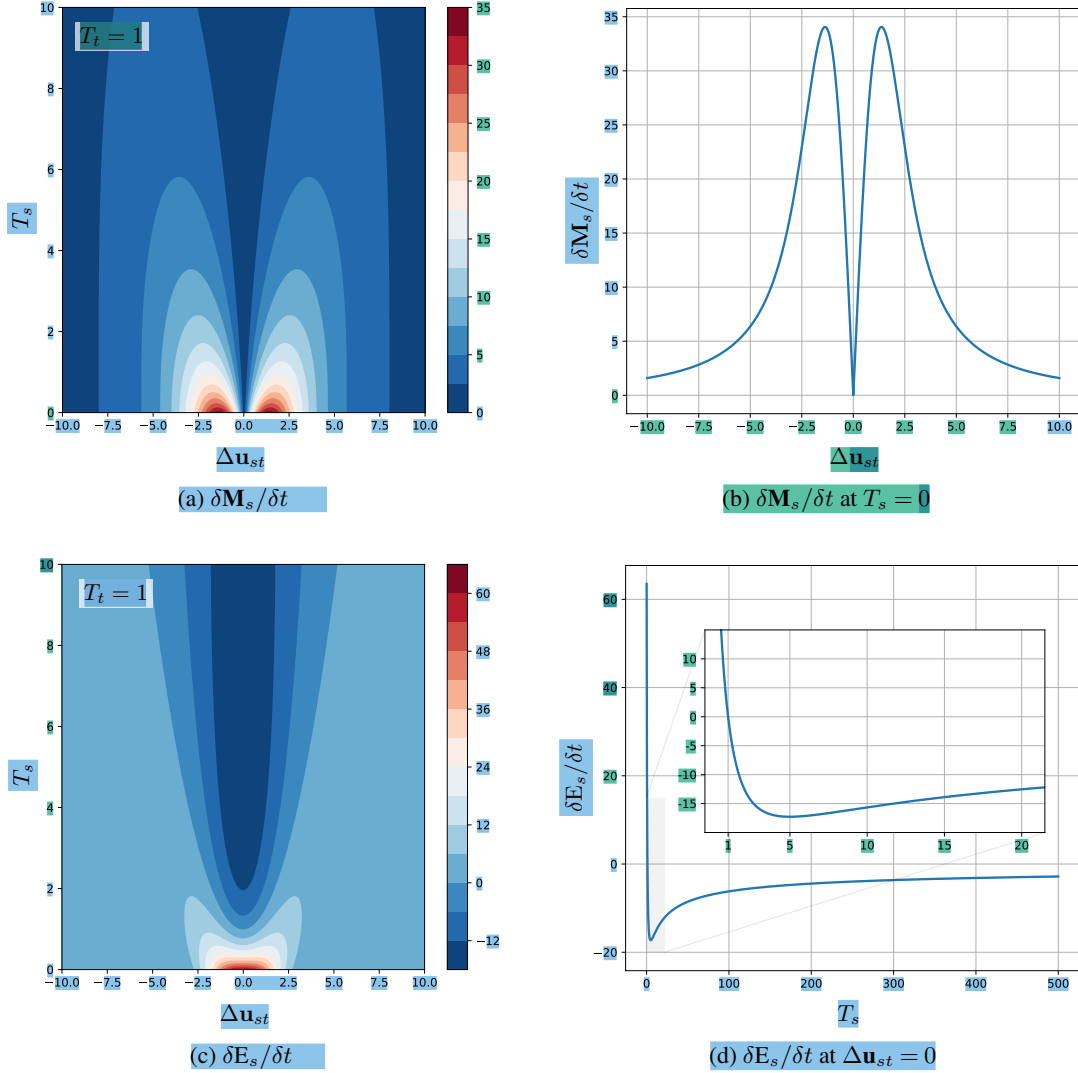
Figure 3. The momentum and energy collision terms for the Maxwellian velocity distribution function in the case of Coulomb collisions.

Under these conditions, Coulomb collisions can be treated as elastic collisions, so that the total kinetic energy and momentum of the system are conserved, resulting in no change in momentum caused by the collisions. To see how the momentum collision term changes relative to $\Delta\mathbf{u}_{st}$, we plot its cross-section at $T_s = 0$, as shown in Figure (3b). When one particle's drift velocity is slightly larger than the other's, the momentum change of particle s due to collisions increases until reaching its maximum. Beyond this maximum point, as the absolute value of the difference between the drift velocities becomes very large (i.e., $\mathbf{u}_s \gg \mathbf{u}_t$ or $\mathbf{u}_t \gg \mathbf{u}_s$), collisions have less effect on the momentum. In the limit of very large $\Delta\mathbf{u}_{st}$, the momentum collision term approaches zero because particles moving at significantly different speeds are more likely to pass each other without interacting, i.e. reducing the number of collisions. Referring back to Figure (3a),

as the temperature of the s particles increases, the impact of collisions on their momentum decreases until it eventually vanishes. This occurs because the effective collision frequency, ν_{st}, for Coulomb collisions in the Maxwellian case, defined in equation (49), between the particles decreases with increasing temperature as

$$\nu_{st} = \nu_{st}^{\mathrm{Co}} \propto 1/T_{st}^{3/2}, \tag{79}$$

showing that collisions become less probable at higher temperatures, leading to a reduction in their influence on momentum. Figure (3c) represents the energy collision term. The graph shows that maximum energy exchange occurs when the difference in the drift velocities is zero. As mentioned earlier, in this case, both momentum and kinetic energy are conserved, meaning there is no change in these quantities.

the temperatures of particles s and t are equal, $T_s = T_t$, the temperature difference becomes zero, $\Delta T = 0$, leading to no temperature transfer and the change in the energy of particle s is zero. This occurs in the Figure (1d) at $T_s = T_t = 1$. As the temperature of particles s increases above the temperature of particles t, $T_s > T_t$, particles s starts losing temperature to particles t, and this reduction increases as the temperature of particle s increases. Consequently, the energy transport coefficient becomes negative and continues decreasing until it reaches a minimum value, in our case, this happens at $T_s = 5$. After this point, the increase in the temperature of the particles s affects the collision frequency, meaning fewer collisions occur, as we see in equation (130). As a result, particles s keeps its temperature, without losing part of it to particles t. This explains the subsequent increase in the change of energy. Eventually, when the collision frequency reaches zero and the particles no longer collide, the change in the energy becomes zero, the limit of the transport coefficient as T_s approaches infinity is zero. Back to Figure (1c), as the absolute value of the difference in drift velocity becomes large, the distance between particles increase, which leads to a decrease in the energy change of particles s, because the particles become less likely to collide, the energy transport coefficient approaches zero as the drift velocity difference, $\Delta \mathbf{u}$, tends to $\pm\infty$, similar to the behaviour of the momentum transport coefficient when either $\mathbf{u}_s \gg \mathbf{u}_t$ or $\mathbf{u}_t \gg \mathbf{u}_s$.

Third case, the *temperature* of the t particles T_t. In Figure (2), we plot the isolines of the transport coefficients under the same conditions as in Figure (1), but for different values of T_t. As T_t increases the transport coefficients still exhibits the same behaviour, but the impact of collisions on the transport coefficients becomes smaller and smaller and the numerical values of the transport coefficients decreases. This can be seen by comparing the numbers on the color bars to those in Figure (1), (e.g. $\delta\mathbf{M}_s/\delta t$ equals 35 in Figure (1a) at $T_t = 1$, and 18 in Figure (2a) at $T_t = 2$; $\delta\mathrm{E}_s/\delta t$ equals 60 in Figure (1c) at $T_t = 1$, and 48 in Figure (2b) at $T_t = 2$), because as temperature increases, the number of collisions decreases as mentioned before. Another observation from Figure (2) is that the range of $\Delta\mathbf{u}$, which contributes to the transport coefficients (represented by the red area relative to the horizontal axis), expands as T_t increases. This occurs because a decrease in collision frequency results in fewer interruptions in particle motion. With fewer collisions, particles can accelerate more effectively under the influence of the external force, leading to an increase in their drift velocities.

Kappa Distribution

The Kappa distribution affects the transport coefficients through two functions $\mathrm{D}(\kappa_s, \kappa_t)$ and $\mathrm{W}(\kappa_s, \kappa_t)$, where we assume the kappa values for both species s and t to be equal, i.e., $\kappa_s = \kappa_t = \kappa$ so we can compare the results with the Maxwellian case. To understand how these two functions change the transport coefficients, we plot the isolines of the transport coefficients for momentum and energy as functions of $\Delta\mathbf{u}$ and T_s, as shown in Figures (3), with the same conditions as in Figure (1a), for various κ values. Additionally, in Figures (4), we show the cross-sections of these coefficients at $T_s = 0$. For the momentum coefficient, $\mathrm{D}(\kappa, \kappa)$ appears as a multiplication in equation (98), and this can be observed in Figures (3) and (4), as the behaviour of the momentum coefficient is similar to the Maxwellian case, with $\mathrm{D}(\kappa, \kappa)$ acting as a scaling parameter making the change of momentum increase at low kappa value. This occurs because at low κ, the suprathermal tails contain more particles with very high speeds. The extra particles increase the collision frequency, and the higher speeds lead to greater momentum transfer during collisions. For the energy coefficient, $\mathrm{W}(\kappa, \kappa)$ is multiplied in the first term of equation (99), which represents the change in the potential energy of the particles s, and $\mathrm{D}(\kappa, \kappa)$ is multiplied in the second term of the same equation, representing the change in the kinetic energy of the particles s. The general behaviour of the energy coefficient is approximately the same as in the Maxwellian case, particularly at high κ values. However, at low κ values, especially at $\kappa = 2$, the value of $\mathrm{D}(\kappa, \kappa)$ exceeds $\mathrm{w}(\kappa, \kappa)$, i.e., $\mathrm{D}(\kappa, \kappa) > \mathrm{W}(\kappa, \kappa)$, as outlined in Table (1). This causes the peaks near zero seen for $\kappa = 2$ in Figure (4b), due to the higher speeds of the extra particles, which cause greater kinetic energy exchange compared to the Maxwellian case. For both coefficients, as κ increases, the value of the transport coefficients decreases, and the result get closer to the result obtained by the Maxwellian distribution.

(a) $\delta\mathbf{M}_s/\delta t$ at $T_t = 2$

(b) $\delta\mathrm{E}_s/\delta t$ at $T_t = 2$

(c) $\delta\mathbf{M}_s/\delta t$ at $T_t = 5$

(d) $\delta\mathrm{E}_s/\delta t$ at $T_t = 5$

(e) $\delta\mathbf{M}_s/\delta t$ at $T_t = 10$
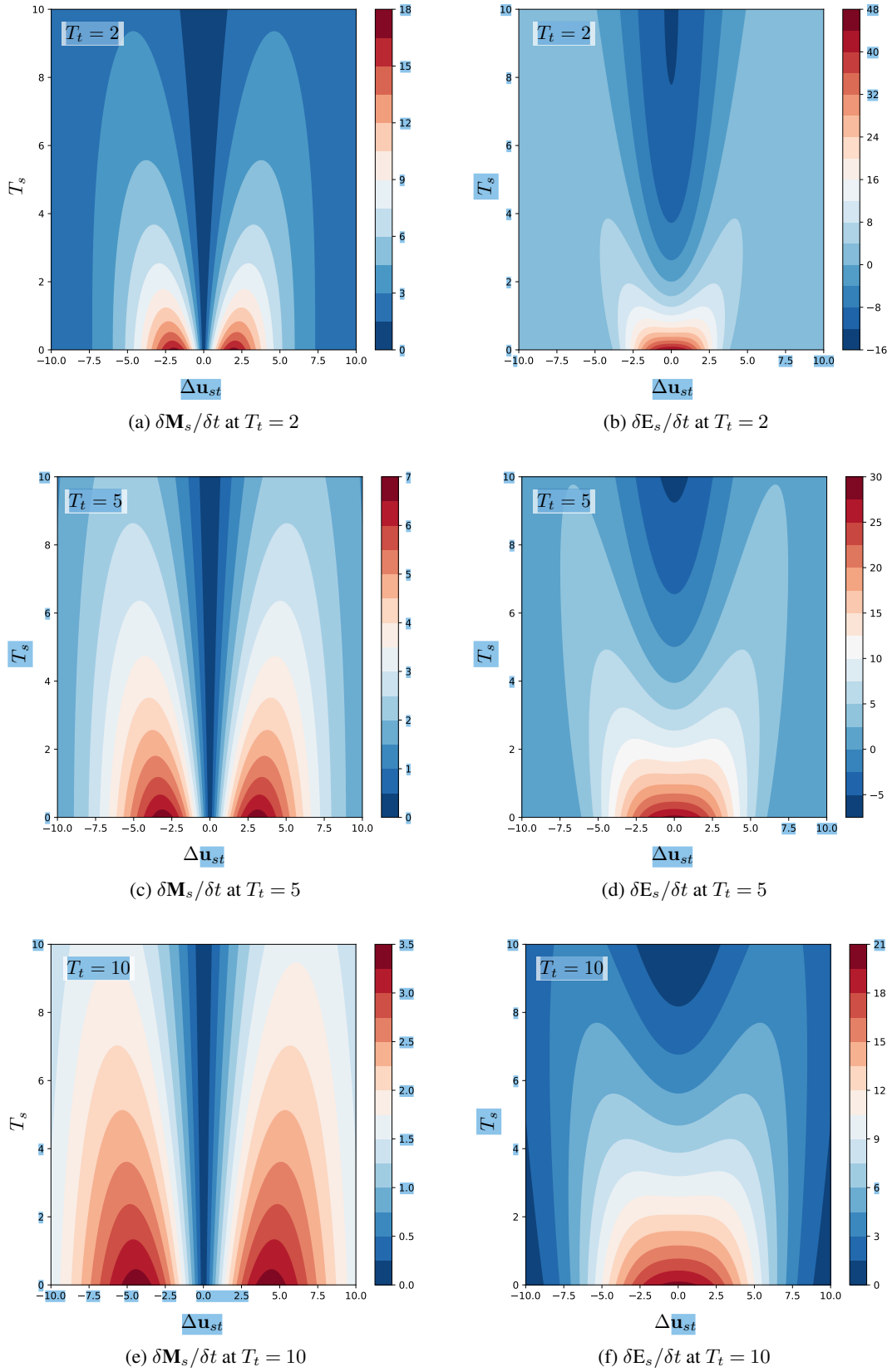
(f) $\delta\mathrm{E}_s/\delta t$ at $T_t = 10$

Figure 4. The momentum and energy collision terms for the Maxwellian velocity distribution function in the case of Coulomb collisions, at different values of T_t: 2, 5, and 10.
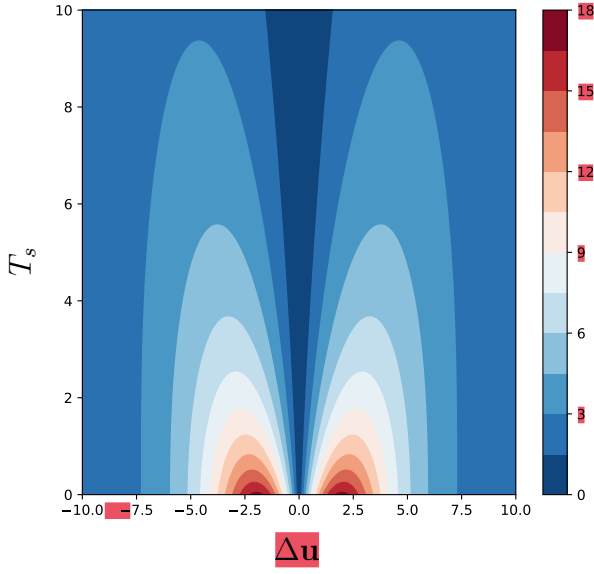
(a) $\delta\mathbf{M}_s/\delta t$ at $T_t = 2$
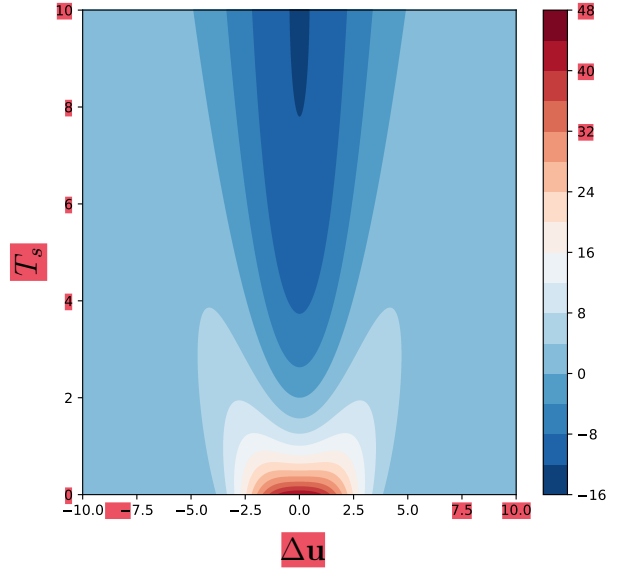
(b) $\delta\mathrm{E}_s/\delta t$ at $T_t = 2$
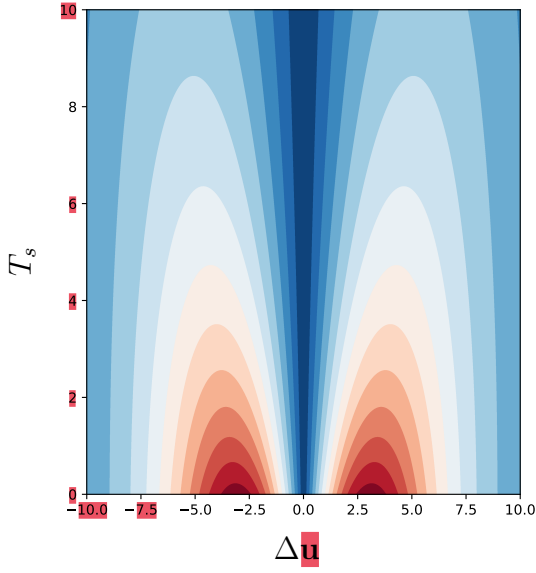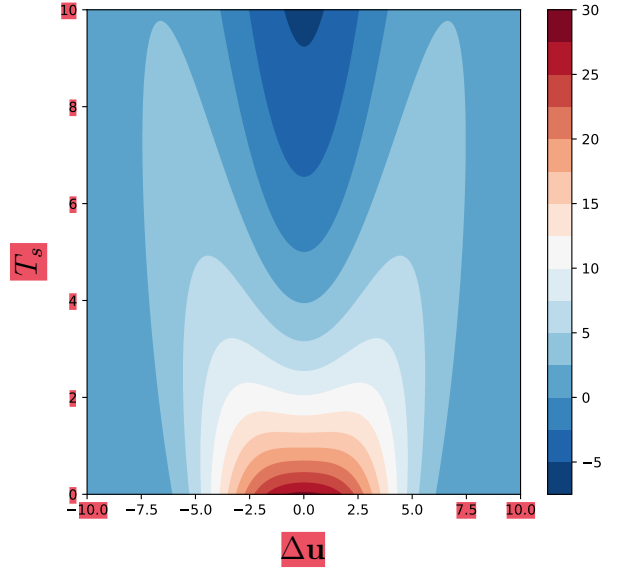
(c) $\delta\mathbf{M}_s/\delta t$ at $T_t = 5$
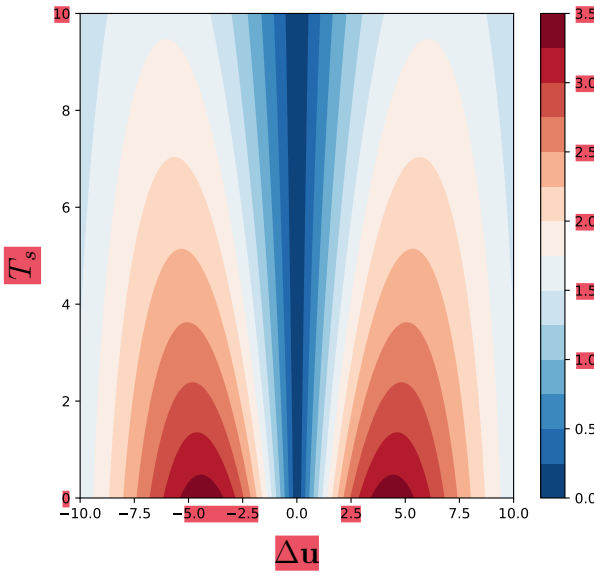
(d) $\delta\mathrm{E}_s/\delta t$ at $T_t = 5$
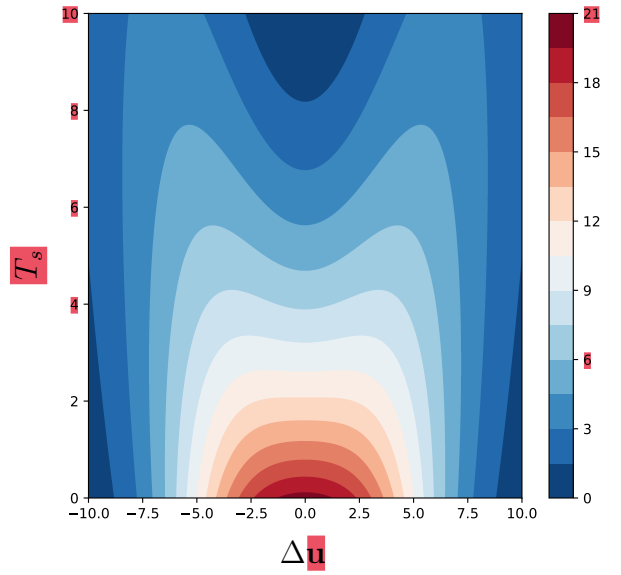
(e) $\delta\mathbf{M}_s/\delta t$ at $T_t = 10$

(f) $\delta\mathrm{E}_s/\delta t$ at $T_t = 10$

Figure 2: The transport coefficients for momentum and energy, for the Maxwellian velocity distribution function in the case of Coulomb collisions, at different values of T_t: 2, 5, and 10.
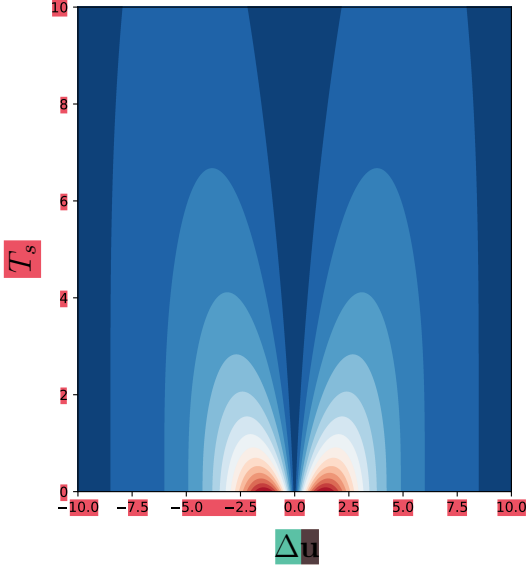
(a) $\delta \mathbf{M}_s/\delta t$ at $\kappa = 2$
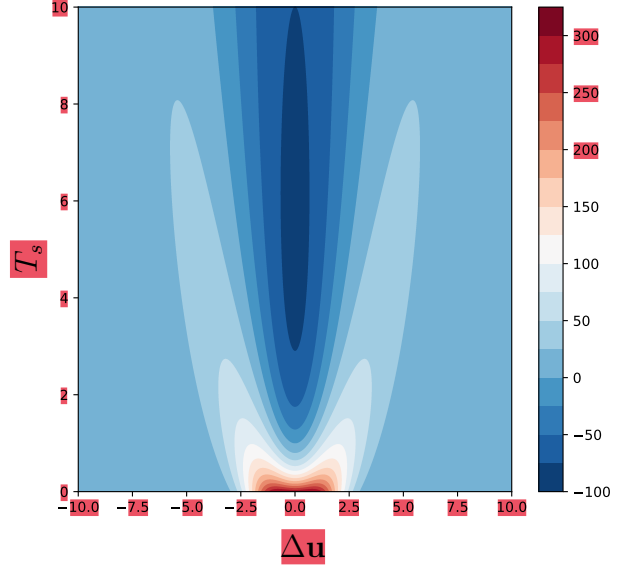
(b) $\delta \mathrm{E}_s/\delta t$ at $\kappa = 2$
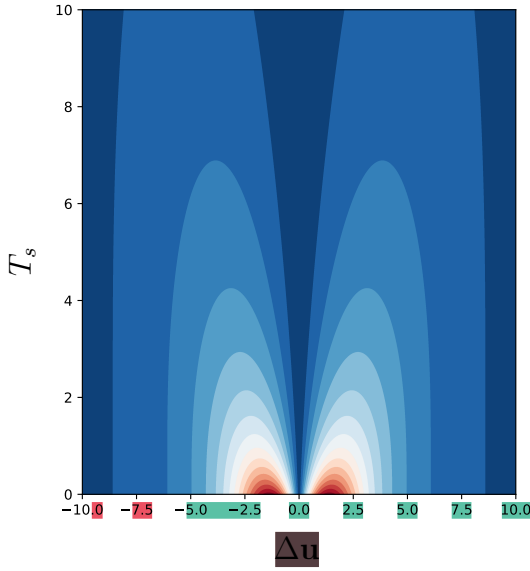
(c) $\delta \mathbf{M}_s/\delta t$ at $\kappa = 3$
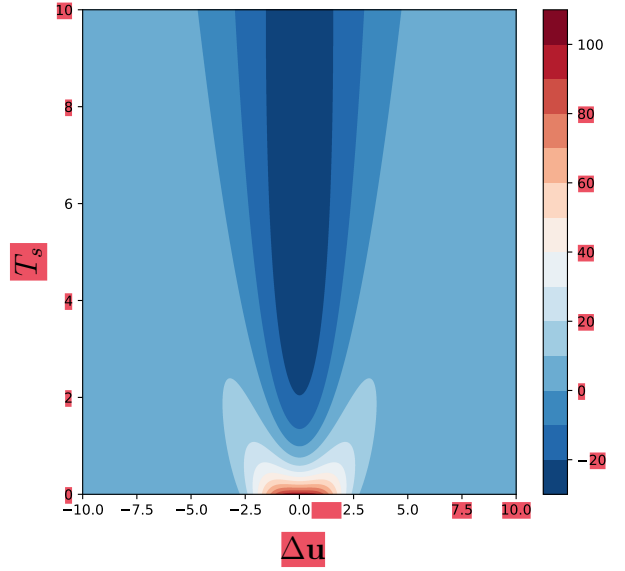
(d) $\delta \mathrm{E}_s/\delta t$ at $\kappa = 3$
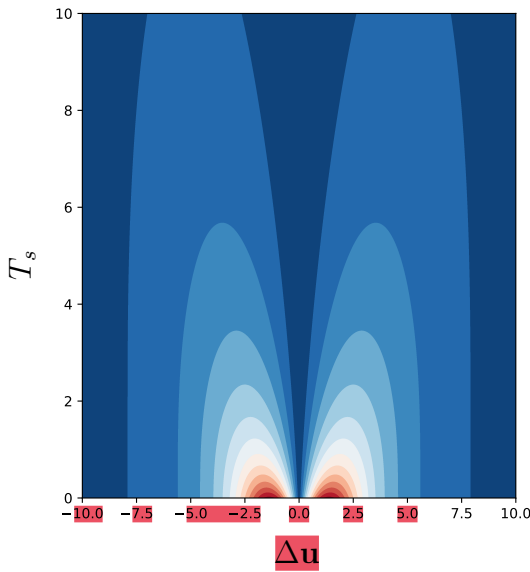
(e) $\delta \mathbf{M}_s/\delta t$ at $\kappa = 4$
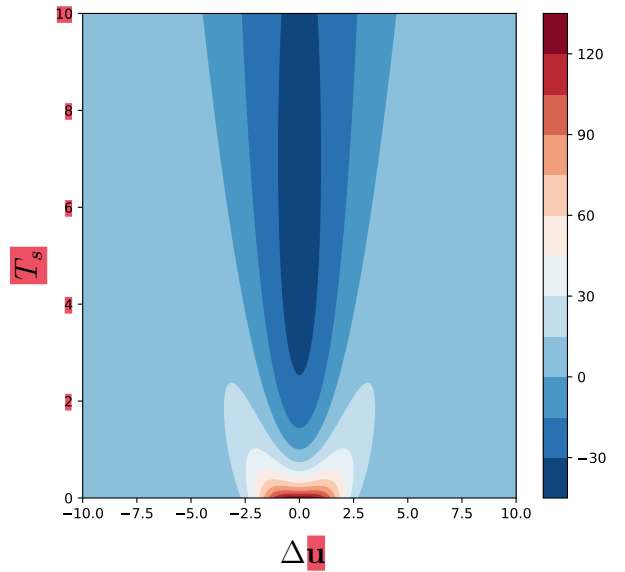
(f) $\delta \mathrm{E}_s/\delta t$ at $\kappa = 4$

Figure 3: The transport coefficients, momentum and energy for the Kappa velocity distribution function in the case of Coulomb collisions at different values of κ: 2, 3, and 4.
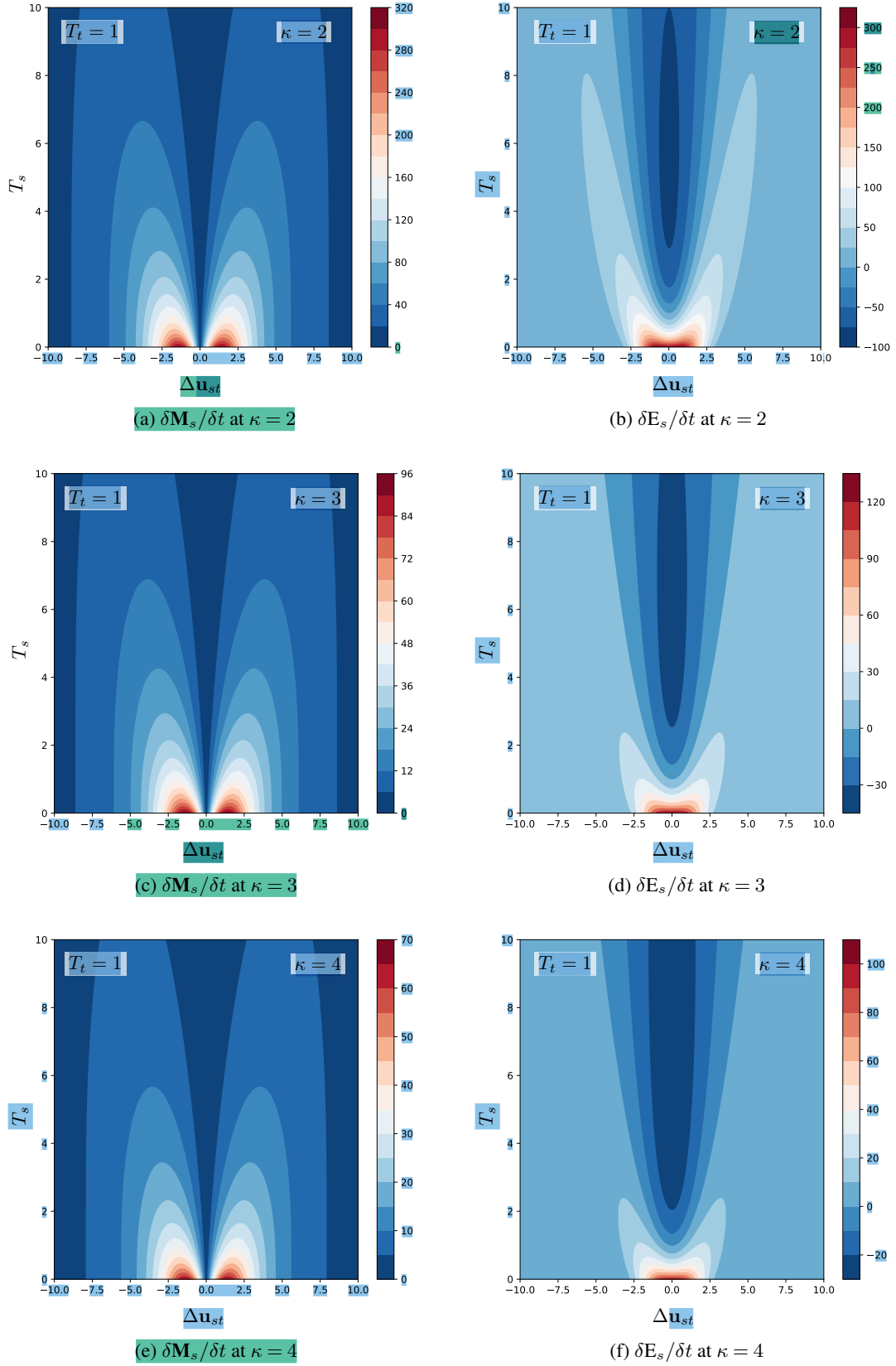
Figure 5. The momentum and energy collision terms for the modified Kappa velocity distribution function in the case of Coulomb collisions at different values of κ: 2, 3, and 4.
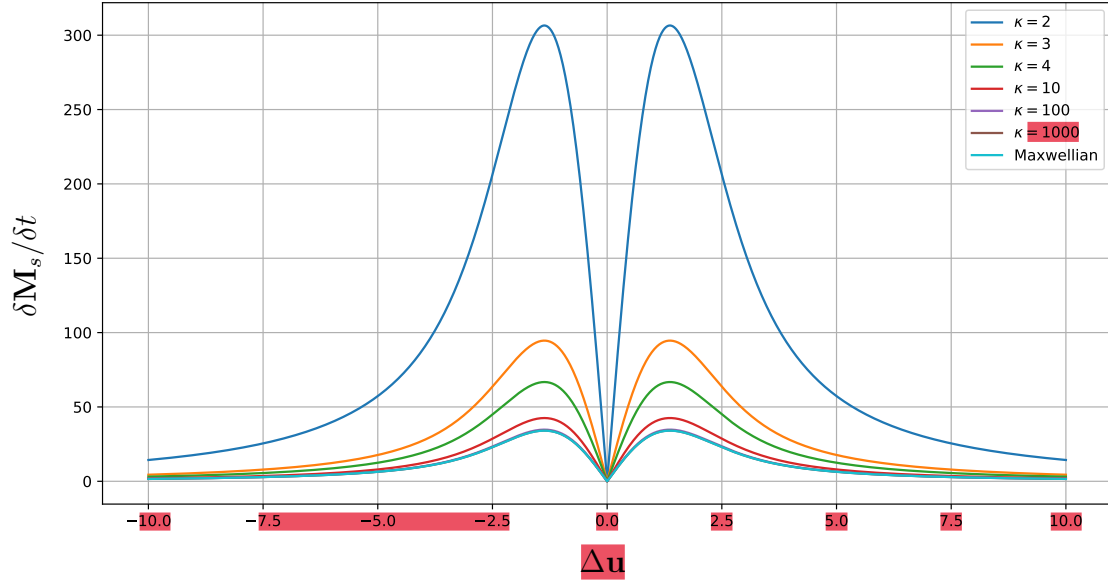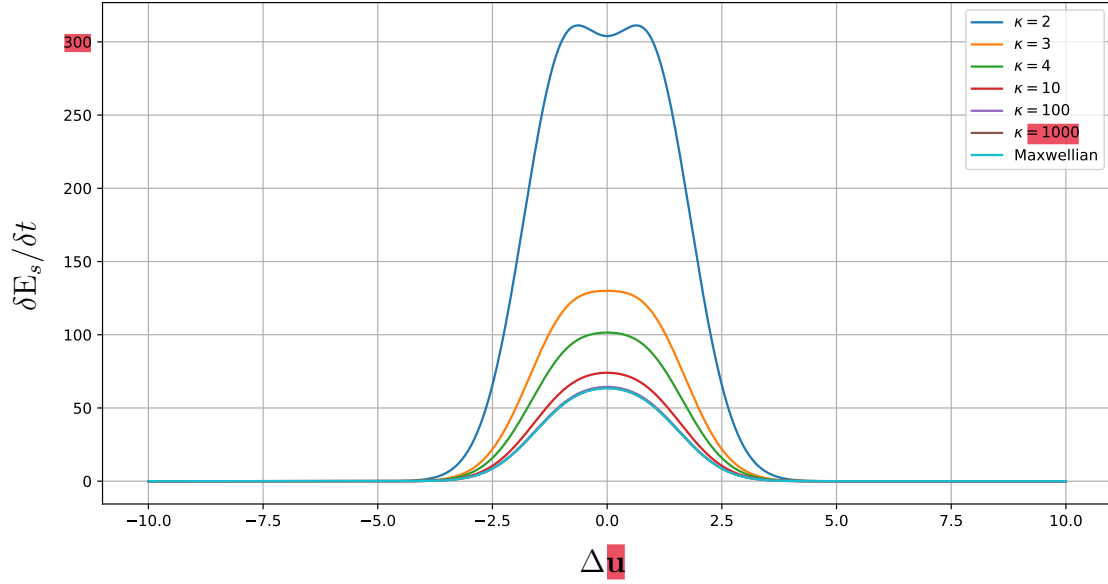
(a) $\delta \mathbf{M}_s / \delta t$ at $T_s = 0$

(b) $\delta \mathrm{E}_s / \delta t$ at $T_s = 0$

Figure 4: The cross-section of the transport coefficients, momentum and energy, for Kappa and Maxwell velocity distribution functions in the case of Coulomb collisions, at $T_s = 0$.

κ	$\mathrm{D}(\kappa, \kappa)$	$\mathrm{W}(\kappa, \kappa)$
2	9.0000	4.7873
3	2.7778	2.0474
4	1.9600	1.5986
10	1.2491	1.1661
100	1.0204	1.0140
1000	1.0020	1.0014

Table 1: $\mathrm{D}(\kappa, \kappa)$ and $\mathrm{W}(\kappa, \kappa)$ at different values of κ

The change in the energy comes from the potential energy, specifically the difference between the temperatures of the interacting particles. Figure (3d) shows the cross-section of the energy collision term for the case $\Delta\mathbf{u}_{st} = 0$. At $T_s = 0$, the energy exchange between particles is most significant, as particles s gain temperature from particles t. As T_s increases and approaches T_t, the energy transfer decreases and vanishes when the temperatures of the two species are equal. This occurs at $T_s = T_t = 1$ in Figure (3d), where $\Delta\mathrm{T}_{st} = 0$, leading to no energy transfer and the energy collision term becomes zero. As the temperature of particles s increases above the temperature of particles t, $T_s > T_t$, particles s lose temperature to particles t, and the energy collision term becomes negative and decreases until it reaches a minimum value, which in our case occurs at $T_s = 5$. Beyond this point, the increase in the temperature of particles s reduces the effective collision frequency, see equation (79). As a result, particles s keep their temperature without losing any of it to particles t. This explains the subsequent increase in the change of energy. Eventually, as the effective collision frequency tends to zero, no further collisions occur, and the temperature change vanishes, making the energy collision term approach zero as T_s goes to infinity. Back to Figure (3c), as the absolute value of the difference in drift velocity increases, the distance between particles also increases. This greater distance between particles makes collisions less likely, which in turn reduces energy exchange for species s. Consequently, the energy collision term approaches zero as the drift velocity difference, $\Delta\mathbf{u}_{st}$, tends to $\pm\infty$, similar to the behaviour of the momentum collision term when either $\mathbf{u}_s \gg \mathbf{u}_t$ or $\mathbf{u}_t \gg \mathbf{u}_s$.

Third case, the *temperature* of the t particles T_t. In Figure (4), we plot the isolines of the collision terms under the same conditions as in Figure (3), but for different values of T_t. As T_t increases, the collision terms exhibit the same overall behaviour, but their magnitude decreases. For example, $\delta\mathbf{M}_s/\delta t$ drops from 35 at $T_t = 1$ (Figure 3a) to 18 at $T_t = 2$ (Figure 4a), 7 at $T_t = 5$ (Figure 4c), and 3.5 at $T_t = 10$ (Figure 4e). A similar trend is observed for $\delta E_s/\delta t$, which drops from 60 to 48, then to 30, and finally to 21 (Figures 3c, 4b, 4d, and 4f). This reduction occurs because, as the temperature increases, the number of collisions decreases as mentioned before. Additionally, Figure (4) shows that the range of $\Delta\mathbf{u}_{st}$ contributing to the collision terms (red area along the horizontal axis) expands with T_t, since fewer collisions allow particles to accelerate more under external forces, increasing their drift velocities.

2.4.2 Modified Kappa distribution

The modified Kappa distribution affects the collision terms through two functions $\mathrm{D}(\kappa_s, \kappa_t)$ and $\mathrm{H}(\kappa_\alpha)$, $\alpha = s, t$, which appear in the effective collision frequency, the thermalisation rate and the relative temperature difference. Assuming equal kappa values for both species, s and t, $\kappa_s = \kappa_t = \kappa$, allows for a direct comparison with the Maxwellian case. To understand how modified Kappa distribution changes the collision terms, we plot the isolines of the momentum and energy collision terms as functions of $\Delta\mathbf{u}_{st}$ and T_s, as shown in Figure (5), with the same conditions as in Figure (3a), for various κ values. Cross-sections at $T_s = 0$ are shown in Figure 6. For the momentum collision term, the behavior is similar to the Maxwellian case, with $\mathrm{D}(\kappa, \kappa)$ scaling the effective collision frequency, as shown in Figures (5) and (6). At low κ, the effective collision frequency increases, as discussed in Section 2.3, leading to greater momentum transfer due to collisions at these values. For the energy collision term, the function $\mathrm{W}(\kappa, \kappa)$, defined as

$$\mathrm{W}(\kappa, \kappa) = \mathrm{D}(\kappa, \kappa)\,\mathrm{H}(\kappa), \tag{80}$$

appears in the first term of equation (42), while $\mathrm{D}(\kappa, \kappa)$ contributes to the second term. The general behavior of the energy coefficient is approximately the same as in the Maxwellian case, particularly at high κ values. However, at low kappa values, particularly $\kappa = 2$, $\mathrm{D}(\kappa, \kappa) > \mathrm{W}(\kappa, \kappa)$, as outlined in Table (1), making the kinetic term dominant and producing peaks near zero, as shown in Figure 6b. Overall, both collision terms decrease with increasing κ, converging toward the Maxwellian result, confirming the result of Subsubsection 2.2.2.

Table 1. $\mathrm{D}(\kappa, \kappa)$ and $\mathrm{W}(\kappa, \kappa)$ at different values of κ.

κ	$\mathrm{D}(\kappa, \kappa)$	$\mathrm{W}(\kappa, \kappa)$
2	9.0000	4.7873
3	2.7778	2.0474
4	1.9600	1.5986
10	1.2491	1.1661
100	1.0204	1.0140
1000	1.0020	1.0014

3 Transport coefficients

In this section, we derive and discuss the behavior of the transport coefficients—namely, the electrical conductivity σ_e, thermoelectric coefficient α_e, diffusion coefficient D_e, and mobility coefficient μ_e—for a Lorentz plasma using the modified Kappa distribution. A Lorentz plasma is a type of plasma in which the contribution of electron-electron collisions is negligible compared to electron-ion collisions. In this model, electrons are considered to move relative to nearly stationary ions because their much smaller mass allows them to move much faster (Du, 2013). The Lorentz plasma model is particularly useful for calculating transport coefficients, such as electrical conductivity, because electron-electron collisions do not contribute significantly to these properties.

(a) $\delta \mathbf{M}_s / \delta t$ at $T_s = 0$

(b) $\delta \mathrm{E}_s / \delta t$ at $T_s = 0$
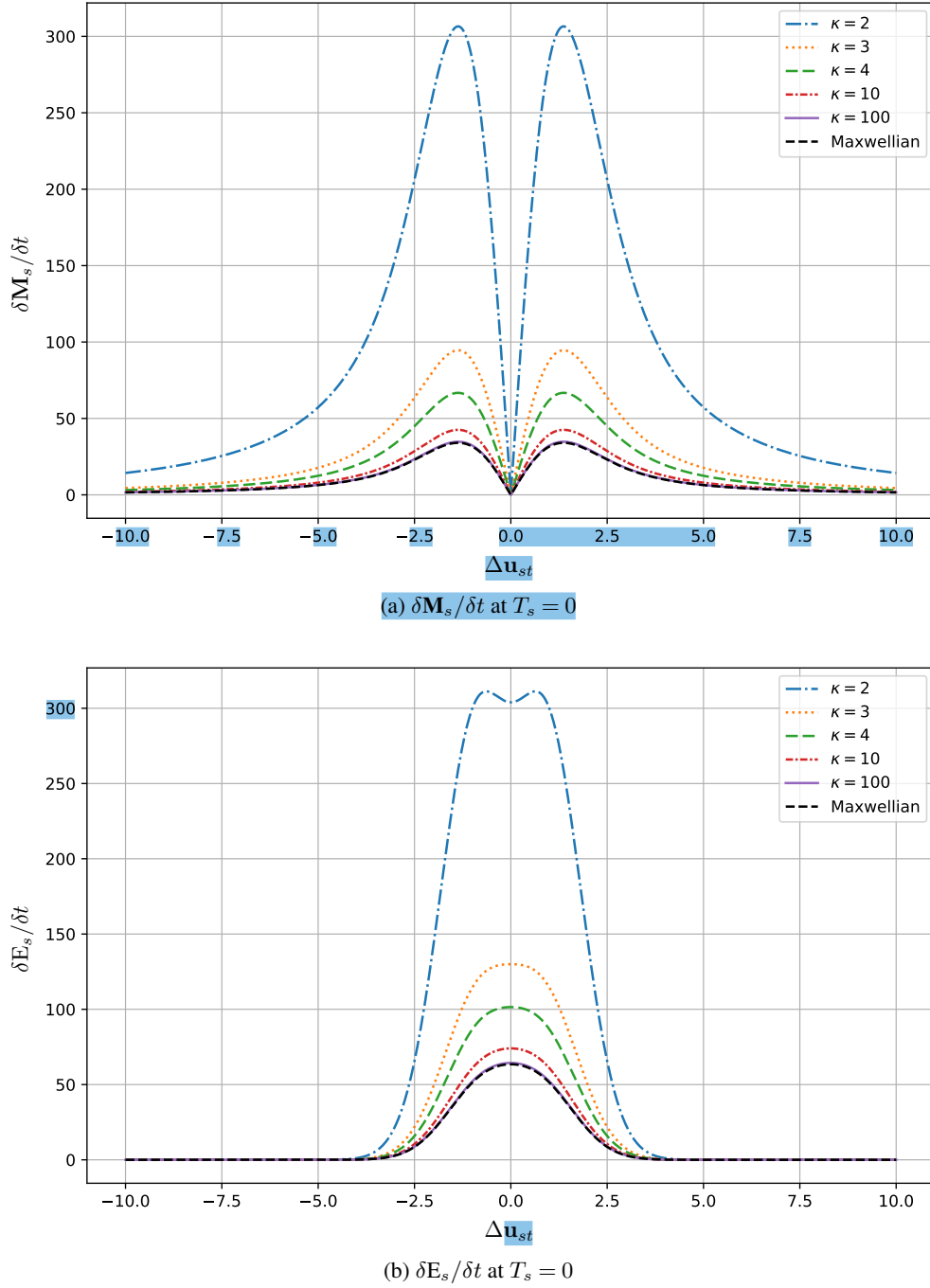
Figure 6. The cross-section of the momentum and energy collision terms for the modified Kappa and Maxwellian velocity distribution functions in the case of Coulomb collisions at $T_s = 0$.

The transport coefficients for Lorentz plasma without a magnetic field appear in the following macroscopic laws (Husidic et al., 2021),

$$\mathbf{E} = \frac{\mathbf{J}_e}{\sigma_e} + \alpha_e \nabla T_e, \tag{81}$$

$$\Gamma_e = -D_e \nabla n_e - \mu_e n_e \mathbf{E}. \tag{82}$$

Equation (81) represents generalizes Ohm's law, where $\mathbf{E}$ denotes the electric field and $\mathbf{J}_e$ is the current density, defined as (Schunk and Nagy, 2009),

$$\mathbf{J}_e = e n_e (\mathbf{u}_i - \mathbf{u}_e), \tag{83}$$

with e being the charge, n_e the electron density, and $\mathbf{u}_i, \mathbf{u}_e$ the ion and electron velocities, respectively. Similarly, Equa-

8 Conclusion

For isotropic plasmas, we have presented a closed system of transport equations. In these equations, the transport properties of a given species are defined with respect to the random velocity of that species, where the species velocity distribution function is expanded in an orthogonal polynomial series about a drifting Kappa weighting function. By taking the first term of the expansion, ignoring all higher moments of the velocity distribution, and showing that the drifting kappa has zero heat flux and zero stress pressure tensor, we obtain the five-moment approximation equation (25–27). We then obtained the transport coefficients for density, momentum and energy, as a result of collisions, based on a drifting Kappa velocity distribution function using the Boltzmann collision integral. We provide these coefficients for different types of collisions, including Coulomb collisions, hard-sphere interactions, and Maxwell molecules collisions in equation (97−99). Given the complexity of the terms involved in the transport coefficient, we have expressed the final results using hypergeometric functions in equations (111–116), to optimize and simplify the process for performing numerical calculations. Next, we investigate two special cases; The first case, when kappa index approaches infinity, which reproduces the result for the Maxwellian distribution case. In this limit, κ goes to infinity, the functions $D(\kappa, \kappa)$ and $W(\kappa, \kappa)$ approach 1. The second case involves taking the zeroth-order function to be a non-drifting Kappa distribution for the interacting particles by setting the drift velocity of the interacting particles to be zero. This case corresponds to an isolated system with no external force acting on the particles, and the collisions turns to be elastic. As a result, both total momentum and total kinetic energy are conserved, meaning the change in momentum is zero and the change in energy is affected by changes in the potential energy of the interacting particle. We concluded with a discussion on Coulomb collisions and how they affect the momentum and energy of the particles for both Maxwellian and Kappa velocity distributions, we found at low kappa index values, the number of collisions increased significantly, resulting in a greater changes in the momentum and energy of the particles, due to the increase in the number of particles with very high speeds. In general, as kappa index increases, the number of particles in the suprathermal tails decreases and the result become closer and closer to the Maxwellian distribution case.

Building on the foundation developed in this study, future efforts will focus on extending transport theory to more general plasma conditions. While the present work is limited to isotropic plasmas, a significant next step involves extending the model to account for anisotropic plasmas, where pressure and temperature vary with direction. Addressing anisotropy is particularly relevant for magnetized and space plasmas, where directional dependencies are essential for accurately describing transport processes. Another point of focus is providing a complete transport theory that covers the kappa velocity distribution case, as introduced by Schunk [1977], for the Maxwellian distribution function. This involves obtaining transport equations by expanding the species distribution function in a generalized orthogonal polynomial series with a kappa weighting function, resulting in various approximations, such as the eight-, ten-, thirteen-, and twenty-moment approximations. These advancements will allow for a more comprehensive understanding of collisional transport in a broader range of plasma environments.

A Appendix A

In this appendix, we want to calculate the following average values of the Kappa distribution function;

$$\langle A \rangle, \quad \langle \mathbf{c}_\alpha \rangle, \quad \langle c_\alpha^2 \rangle, \quad \langle \mathbf{c}_\alpha \mathbf{c}_\alpha \rangle, \quad \langle c_\alpha^2 \mathbf{c}_\alpha \rangle,$$

where A is constant, and $\mathbf{c}_\alpha$ is the random speed. The Kappa distribution,

$$f_\alpha^\kappa = \frac{n_\alpha \, \eta(\kappa)}{\pi^{3/2} \, w_\alpha^3} \left(1 + \frac{c_\alpha^2}{\kappa_0 \, w_\alpha^2} \right)^{-\kappa - 1}, \tag{131}$$

tion (82) extends Fick's law to account for electric field effects, with $\mathbf{\Gamma}_e$ denotes the particle flux density, defined as (Schunk and Nagy, 2009),

$$\mathbf{\Gamma}_e = n_s \mathbf{u}_e. \tag{84}$$

3.1 Derivation of transport coefficients

The transport coefficients can be obtained by deriving equations (81) and (82) using the five-moment approximation. For a simple electron-ion collision, using equation (41), the momentum equation with a drifting modified Kappa distribution, can be expressed as

$$\frac{\delta \mathbf{M}_e}{\delta t} = n_e m_e \frac{\mathrm{D}_e \mathbf{u}_e}{\mathrm{D}t} + \nabla p_e$$
$$- n_e m_e \mathbf{G} + n_e e \left(\mathbf{E} + \frac{\mathbf{u}_e \times \mathbf{B}}{c} \right), \tag{85}$$

with the momentum collision term is given by

$$\frac{\delta \mathbf{M}_e}{\delta t} = n_e m_e \nu_{ei}^{\mathrm{MK}} \Delta \mathbf{u}_{st}, \tag{86}$$

where ν_{ei}^{MK} is the effective collision frequency for the modified Kappa distribution, as defined in equation (47). In equation (85), the electron drift velocity is assumed negligible compared to the thermal velocity, which is equivalent to setting $\epsilon_{ei} = 0$ and therefore $\Phi(0) = 1$ in equation (41). To obtain the transport coefficients, we adopt the standard approximations. First, we assume a steady and low-inertia regime so that $n_e m_e D_e \mathbf{u}_e / Dt \approx 0$. Second, we neglect external gravity and magnetic fields, i.e., $\mathbf{G} = 0$ and $\mathbf{B} = 0$, which corresponds to unmagnetized scalar transport. For convenience, we also take the background ion flow to be $\mathbf{u}_i \approx 0$. Under these assumptions, the electron momentum equation reduces to

$$-n_e \mathbf{u}_e = \frac{k_B T_e}{m_e \nu_{ei}^{\mathrm{MK}}} \nabla n_e + \frac{n_e k_B}{m_e \nu_{ei}^{\mathrm{MK}}} \nabla T_e + \frac{n_e e}{m_e \nu_{ei}^{\mathrm{MK}}} \mathbf{E}, \tag{87}$$

since

$$\nabla p_e = k_B T_e \nabla n_e + n_e k_B \nabla T_e. \tag{88}$$

To derive the electrical conductivity and the thermoelectric coefficients, we begin by setting $\nabla n_e = 0$ and using the definition of the current density $\mathbf{J}_e$ with $\mathbf{u}_i \approx 0$, we write

$$\mathbf{J}_e = e n_e (\mathbf{u}_i - \mathbf{u}_e) = -e n_e \mathbf{u}_e. \tag{89}$$

Substituting this expression into the electron momentum equation (87), we obtain

$$\mathbf{J}_e = \frac{e n_e k_B}{m_e \nu_{ei}^{\mathrm{MK}}} \nabla T_e + \frac{n_e e^2}{m_e \nu_{ei}^{\mathrm{MK}}} \mathbf{E}. \tag{90}$$

Solving the equation for the electric filed gives

$$\mathbf{E} = \frac{m_e \nu_{ei}^{\mathrm{MK}}}{n_e e^2} \mathbf{J}_e - \frac{k_B}{e} \nabla T_e. \tag{91}$$

By comparing this result with the generalized Ohm's law, equation (81), we can identify the electrical conductivity and the thermoelectric coefficient as

$$\sigma_e = \frac{n_e e^2}{m_e \nu_{ei}^{\mathrm{MK}}}, \tag{92}$$

$$\alpha_e = -\frac{k_B}{e}. \tag{93}$$

Similar to how we derive the electrical conductivity and the thermoelectric coefficient, the diffusion and mobility coefficients can be obtained by setting $\nabla T_e = 0$ and using the definition of the particle flux density, $\mathbf{\Gamma}_e$, in equation (84), equation (87) gives

$$\mathbf{\Gamma}_e = -\frac{k_B T_e}{m_e \nu_{ei}^{\mathrm{MK}}} \nabla n_e - \frac{n_e e}{m_e \nu_{ei}^{\mathrm{MK}}} \mathbf{E}. \tag{94}$$

By comparing this to Fick's law, equation (82), the diffusion and mobility coefficients are identified as

$$D_e = \frac{k_B T_e}{m_e \nu_{ei}^{\mathrm{MK}}}, \tag{95}$$

$$\mu_e = \frac{e}{m_e \nu_{ei}^{\mathrm{MK}}}. \tag{96}$$

3.2 Discussion of transport coefficients

From the first look at the derived transport coefficients, we can see that they satisfy the familiar relation between the electric conductivity and the mobility coefficient

$$\sigma_e = n_e e \mu_e, \tag{97}$$

and Einstein relation

$$D_e = \frac{k_B T_e}{e} \mu_e. \tag{98}$$

The resulting transport coefficients show a different dependency on the kappa parameters. The thermoelectric coefficient α_e has no kappa term in it. On the other hand, the electrical conductivity, diffusion, and mobility coefficients all include the same kappa term, which appears through the effective collision frequency v_{ei}^{MK}. The transport coefficients-electrical conductivity, diffusion, and mobility-are inversely proportional to the effective collision frequency. As discussed earlier, when $\kappa = \kappa_s = \kappa_t$, the effective collision frequency for the modified Kappa distribution influences different types of collisions in distinct ways. Consequently, the impact of the modified Kappa distribution on the transport coefficients depends on the specific type of collision. For Maxwell molecules, the effective collision frequency remains identical to that of the Maxwellian distribution, implying that the modified Kappa distribution does not affect the transport coefficients in this kind of collision. However, for Coulomb collisions and hard-sphere interactions, the effective collision frequency increases as κ decreases, leading
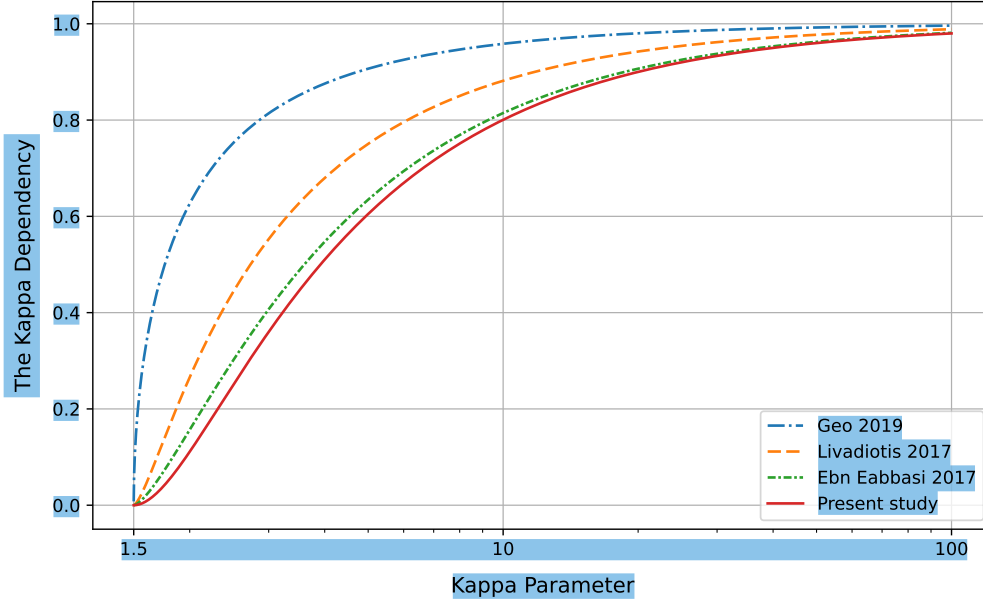
Figure 7. The kappa dependency for the electrical conductivity

to a decrease in the transport coefficients at low values of κ compared to the Maxwellian case, as shown in Figure 7, where we have plotted the kappa dependency for the electrical conductivity as functions of the kappa parameter. As κ approaches ∞, the effective collision frequency v_{ei}^{MK} reduces to the Maxwellian case v_{ei}, making the transport coefficients recover their Maxwellian limits. The obtained transport coefficients have both differences and similarities with other studies. One can compare this with a number of studies that predicted a similar trend in the transport coefficients. In Figure 7, we also show the dependence on the κ parameter of the electrical conductivity from different studies and compare it with the present work, by plotting the ratio σ_e/σ_e^M as a function of κ, where $\kappa = \kappa_t = \kappa_s$, and

$$\sigma_e^M = \frac{n_e e^2}{m_e \nu_{ei}}. \tag{99}$$

All studies show a different dependence on the κ parameter, but they still exhibit the same behavior: at low values of κ, the electrical conductivity becomes smaller compared to the Maxwellian case, and as κ increases, we approach the Maxwellian case but never exceed it. This confirms that plasmas with larger κ values are better conductors. Thus, deviations from the Maxwellian limit lead to a decrease in electrical conductivity. Figure 7 also shows that, the curves converge to the present work. This can be explained through the collision models used in the derivation of the transport coefficients. In each study, a more general collision term model was used. For example, Guo and Du (2019) used the Linearized Lorentz Collision Model with a relaxation-time approximation for electron-ion collisions. Livadiotis (2017)

used the Fokker–Planck collision operator with simplifications related to the direction of the electric field. Finally, the work of Ebne Abbasi et al. (2017) used the Fokker–Planck collision operator, where the derivation was generalized, and the only approximation occurred in the last step for the hypergeometric function. The work of Ebne Abbasi et al. (2017) is the closest to our present study, as can be seen clearly in the figure. The reason is that, in our study, we used the full Boltzmann collision integral, of which the Fokker–Planck operator can be considered an approximation.

4 Conclusions

For a Lorentz plasma described by a modified Kappa distribution, we have derived the transport coefficients: electrical conductivity, thermoelectric, diffusion, and mobility. The derivation begins with deriving a closed system of transport equations for isotropic plasmas within the five-moment approximation. In these equations, the transport properties of a given species are defined with respect to the random velocity of that species, where the species velocity distribution function is expanded in an orthogonal polynomial series about a drifting modified Kappa weighting function. By taking only the first term of the expansion and neglecting all higher order moments of the velocity distribution, we obtain the five-moment approximation. The corresponding momentum and energy collision terms were evaluated via the Boltzmann collision integral for several interaction types, including Coulomb collisions, hard-sphere interactions, and Maxwell molecule collisions. Given the complexity of the collision terms, the final expressions were represented us-

ing hypergeometric functions to simplify numerical calculations. Next, we investigated the limiting case in which the kappa index approaches infinity, where the collision terms reduce to Maxwellian form. Then we analyzed the influence of the kappa index on the effective collision frequency and thermalisation rate. It was observed that systems described by modified Kappa distribution exhibit distinct behaviour compared to those with Maxwellian distribution. The modified kappa distribution directly influences collision dynamics, where, for interactions in which collision frequency is velocity-independent, such as Maxwell molecule interaction, the distribution does not affect the effective collision frequency or thermalisation rate. In contrast, for velocity-dependent collisions, such as Coulomb and hard-sphere interactions, smaller κ values increase collision frequency and thermalization, and larger κ values approach the Maxwellian limit. We further examined the influence of the kappa index on the momentum and energy collision terms of the particles during Coulomb collisions. At low kappa parameter values, the number of collisions increases significantly, making both the effective collision frequency and the thermalisation rate produce greater changes in the momentum and energy of the particles, while larger κ values recover Maxwellian behavior. Starting from the momentum equation and applying suitable assumptions for an unmagnetized, steady-state plasma, explicit expressions for the electrical conductivity, thermoelectric coefficient, diffusion coefficient, and mobility coefficient were obtained for the modified Kappa distribution. The analysis reveals that while the thermoelectric coefficient is unaffected by the κ parameter, the electrical conductivity, diffusion, and mobility coefficients are all inversely proportional to the effective collision frequency, thereby reflecting its κ dependency. Furthermore, the results indicate that lower κ values lead to an increase in collision frequency and consequently a decrease in the transport coefficients. In the limit $(\kappa \to \infty)$, the coefficients naturally reduce to Maxwellian form, confirming the consistency of the approach.

While the current study provides an important step towards a comprehensive non-Maxwellian transport theory, the present work is limited in several ways. First, the approach was derived within the five-moment approximation of the transport equation, considering only the first term of the expansion and neglecting higher-order moments. This simplification represents a poor approximation, as the neglected terms could significantly affect the system's behavior. Second, the analysis assumes isotropic plasmas, which restricts its applicability to real space plasma environments. In reality, most space plasmas are magnetized and exhibit temperature and pressure anisotropies. Ignoring these effects may overlook important physical mechanisms that govern plasma dynamics. Third, the Coulomb collision cross-section was simplified using a constant Coulomb logarithm and large-velocity approximation, which may affect quantitative accuracy at low velocities (Fichtner et al., 1996). Finally, the model employs the modified Kappa distribution, whose applicability breaks down for $\kappa \le 3/2$, as lower values cause divergent moments and thermodynamic inconsistencies. In this regime, the functions $D(\kappa, \kappa)$ and $H(\kappa)$ diverge, making the effective collision frequency and the thermalisation rate become unphysical. Therefore, the derived collision terms and transport coefficients are valid only for $\kappa > 3/2$.

Future work should address the current model's limitations through several key extensions. First, developing a comprehensive transport theory that accounts for the modified Kappa velocity distribution, would significantly advance the framework beyond the standard Maxwellian assumption. This can be achieved by expanding the species distribution function in a generalized orthogonal polynomial series with a κ-weighting function, allowing for systematic derivation of various approximations (e.g. eight-, ten-, thirteen-, and twenty-moment models). Second, extending the theory to anisotropic plasmas—where pressure and temperature vary with direction—would enhance its realism and applicability, particularly in magnetized and space plasma environments. In addition, incorporating the exact velocity-dependent Coulomb cross-section would improve the accuracy of the collision transfer integrals. Furthermore, adopting the Regularized Kappa Distribution proposed by (Scherer et al., 2017, 2019), which preserves the core features of the κ-function while ensuring finite moments for all $\kappa > 0$ and maintaining thermodynamic consistency, would provide a more stable and physically meaningful representation.

Appendix A

This appendix presents the derivation of the collision terms for each type of collision for the drifting modified Kappa distribution introduced in Section 2.2.

A1 Coulomb collisions

The collision terms for Coulomb collisions can be obtained by substituting equation (37) into equations (32-34), leading to the following form

$$\frac{\delta n_s}{\delta t} = 0, \tag{A1}$$

$$\frac{\delta \mathbf{M}_s}{\delta t} = -\sum_t m_{st} Q_{Co} \int_{\mathbb{R}^3 \times \mathbb{R}^3} f_s^{MK} f_t^{MK} \frac{\mathbf{g}_{st}}{\mathbf{g}_{st}^3} \, d\mathbf{c}_t \, d\mathbf{c}_s, \tag{A2}$$

$$\frac{\delta E_s}{\delta t} = -\sum_t m_{st} Q_{Co} \int_{\mathbb{R}^3 \times \mathbb{R}^3} f_s^{MK} f_t^{MK} \frac{(\hat{\mathbf{V}}_c \cdot \mathbf{g}_{st})}{\mathbf{g}_{st}^3} \, d\mathbf{c}_t \, d\mathbf{c}_s. \tag{A3}$$

The Momentum Coefficient

The momentum coefficient for Coulomb collision is given in

is normalized to n_α, so by the definition of the average value,

$$\langle \xi_\alpha \rangle = \frac{1}{n_\alpha} \int \xi_\alpha \, f_\alpha^\kappa \, d\mathbf{c}_\alpha, \tag{132}$$

we have

$$\langle A \rangle = A. \tag{133}$$

The Kappa distribution is an even function in $\mathbf{c}_\alpha$, and its components $c_{\alpha x}$, $c_{\alpha y}$, and $c_{\alpha z}$ imply that these average values are zero,

$$\langle \mathbf{c}_\alpha \rangle = \langle c_\alpha^2 \, \mathbf{c}_\alpha \rangle = 0, \tag{134}$$

and

$$\langle c_{\alpha i} \rangle = \langle c_{\alpha i} \, c_{\alpha j} \rangle = 0, \quad i \neq j \quad i, j = x, y, z. \tag{135}$$

To evolute the expectation value of c_α^2, we substitute f_α^κ into equation (132), to get

$$\langle c_\alpha^2 \rangle = \frac{1}{n_\alpha} \int_{\mathbb{R}^3} c_\alpha^2 \, f_\alpha^\kappa \, d\mathbf{c}_\alpha = \frac{\eta(\kappa)}{\pi^{3/2} \, w_\alpha^3} \int_{\mathbb{R}^3} c_\alpha^2 \left(1 + \frac{c_\alpha^2}{\kappa_0 \, w_\alpha^2} \right)^{-\kappa-1} d\mathbf{c}_\alpha, \tag{136}$$

by transforming the integral to the spherical coordinates, we have

$$\langle c_\alpha^2 \rangle = \frac{3}{2} w_\alpha^2 = \frac{3 k_B T_\alpha}{m_\alpha}. \tag{137}$$

In the same way, the expectation value of $\mathbf{c}_\alpha \mathbf{c}_\alpha$ is

$$\langle \mathbf{c}_\alpha \mathbf{c}_\alpha \rangle = \frac{1}{n_\alpha} \int_{\mathbb{R}^3} \mathbf{c}_\alpha \mathbf{c}_\alpha \, f_\alpha^\kappa \, d\mathbf{c}_\alpha, \tag{138}$$

$\mathbf{c}_\alpha \mathbf{c}_\alpha$ is second rank tenser, so

$$\langle \mathbf{c}_\alpha \mathbf{c}_\alpha \rangle = \begin{bmatrix} \langle c_{\alpha x}^2 \rangle & \langle c_{\alpha x} \, c_{\alpha y} \rangle & \langle c_{\alpha x} c_{\alpha z} \rangle \\ \langle c_{\alpha y} \, c_{\alpha x} \rangle & \langle c_{\alpha y}^2 \rangle & \langle c_{\alpha y} \, c_{\alpha z} \rangle \\ \langle c_{\alpha z} \, c_{\alpha x} \rangle & \langle c_{\alpha z} \, c_{\alpha y} \rangle & \langle c_{\alpha z}^2 \rangle \end{bmatrix},$$

all the off-diagonal expectation values are zero, according to equation (135), and the expectation values on the diagonal are equal

$$\langle \mathbf{c}_\alpha \mathbf{c}_\alpha \rangle = \langle c_{\alpha x}^2 \rangle \, \mathbf{I}, \tag{139}$$

smilier to $\langle c_\alpha^2 \rangle$, the average value of $\langle c_{\alpha x}^2 \rangle$ is

$$\langle c_{\alpha x}^2 \rangle = \frac{w_\alpha^2}{2} = \frac{k_B T_\alpha}{m_\alpha}, \tag{140}$$

which makes equation (139) become

$$\langle \mathbf{c}_\alpha \mathbf{c}_\alpha \rangle = \langle c_{\alpha x}^2 \rangle \, \mathbf{I} = \frac{k_B T_\alpha}{m_\alpha} \, \mathbf{I}. \tag{141}$$

B   Appendix B

In the process of evaluating the transport coefficient, three kinds of integrals that takes the form

$$I_1^n = \int_{\mathbb{R}^3} g_{st}^n \, e^{-|\mathbf{g}_{st} + \Delta\mathbf{u}|^2/b^2} \, \mathbf{g}_{st} \, d\mathbf{g}_{st}, \tag{142}$$

$$I_2^n = \int_{\mathbb{R}^3} (g_{st}^{n+2} + g_{st}^n \, \Delta\mathbf{u} \cdot \mathbf{g}_{st}) \, e^{-|\mathbf{g}_{st} + \Delta\mathbf{u}|^2/b^2} \, d\mathbf{g}_{st}, \tag{143}$$

$$I_3^n = \int_{\mathbb{R}^3} g_{st}^n \, \Delta\mathbf{u} \cdot \mathbf{g}_{st} \, e^{-|\mathbf{g}_{st} + \Delta\mathbf{u}|^2/b^2} \, d\mathbf{g}_{st}, \tag{144}$$

equation (A2). Evaluating it requires computing the integral

$$I_M = \int_{\mathbb{R}^3 \times \mathbb{R}^3} f_s^{\text{MK}} f_t^{\text{MK}} \frac{\mathbf{g}_{st}}{\mathbf{g}_{st}^3} \, d\mathbf{c}_t \, d\mathbf{c}_s, \tag{A4}$$

to do this, we begin by rewriting the distribution function of the interacting species s and t in an integral representation, instead of writing them in the form of equation (20), as

$$f_s^{\text{MK}} = \frac{n_s \eta(\kappa_s)}{\pi^{3/2} w_s^3} \frac{1}{\Gamma(\kappa_s + 1)} \int_0^\infty \xi_1^{\kappa_s} e^{-\xi_1} \exp\left[-\frac{\xi_1 c_s^2}{\kappa_{0_s} w_s^2} \right] d\xi_1, \tag{A5}$$

$$f_t^{\text{MK}} = \frac{n_t \eta(\kappa_t)}{\pi^{3/2} w_t^3} \frac{1}{\Gamma(\kappa_t + 1)} \int_0^\infty \xi_2^{\kappa_t} e^{-\xi_2} \exp\left[-\frac{\xi_2 c_t^2}{\kappa_{0_t} w_t^2} \right] d\xi_2. \tag{A6}$$

Substituting the distributions given in equations (A5) and (A6) in the integral, equation (A4), gives

$$I_M = \frac{n_s n_t}{\pi^3 w_s^3 w_t^3} \frac{\eta(\kappa_s)\eta(\kappa_t)}{\Gamma(\kappa_s+1)\Gamma(\kappa_t+1)} \int_0^\infty\int_0^\infty \xi_1^{\kappa_s} \xi_2^{\kappa_t} e^{-\xi_1-\xi_2}$$

$$\left(\int_{\mathbb{R}^3}\int_{\mathbb{R}^3} \exp\left[-\frac{\xi_1 c_s^2}{\kappa_{0_s} w_s^2} - \frac{\xi_2 c_t^2}{\kappa_{0_t} w_t^2} \right] \frac{\mathbf{g}_{st}}{\mathbf{g}_{st}^3} \, d\mathbf{c}_s d\mathbf{c}_t \right) d\xi_1 \, d\xi_2. \tag{A7}$$

To solve the integral in equation (A7), we introduce the following transformation

$$\mathbf{c}_s = \left(\frac{\kappa_{0_s}}{\xi_1} \right)^{1/2} \left(\mathbf{c}_* - \mathbf{A}\,\mathbf{g}_* \right), \tag{A8}$$

$$\mathbf{c}_t = \left(\frac{\kappa_{0_t}}{\xi_2} \right)^{1/2} \left(\mathbf{c}_* + \mathbf{B}\,\mathbf{g}_* \right). \tag{A9}$$

The constant A and B are defined by:

$$A = \frac{m_t T_s}{m_t T_s + m_s T_t}, \qquad B = \frac{m_s T_t}{m_t T_s + m_s T_t}. \tag{A10}$$

Here $\mathbf{c}_*$ and $\mathbf{g}_*$ are expressed as:

$$\mathbf{c}_* = \mathbf{V}_c - \mathbf{u}_c + \xi \Delta\mathbf{u}_{st} + \xi \mathbf{g}_{st}, \tag{A11}$$

$$\mathbf{g}_* = -\mathbf{g}_{st} - \Delta\mathbf{u}_{st}, \tag{A12}$$

with

$$\mathbf{u}_c = \frac{m_s \mathbf{u}_s + m_t \mathbf{u}_t}{m_s + m_t}, \qquad \xi = \frac{m_{st}}{m_s + m_t} \frac{T_t - T_s}{T_{st}}. \tag{A13}$$

Calculating the determinant of the Jacobian matrix $\mathbf{J}$ for the transformation described in equations (A8-A10) gives

$$d\mathbf{c}_s d\mathbf{c}_t = \det(\mathbf{J})\, d\mathbf{c}_* d\mathbf{g}_* = \left[\frac{\kappa_{0_s}\kappa_{0_t}}{\xi_1\xi_2} \right]^{1/2} d\mathbf{c}_* d\mathbf{g}_*. \tag{A14}$$

Applying the transformation make the integrals in equation (A7) independent of each other, so by evaluating the integrals with respect to $\mathbf{c}_*$, ξ_1 and ξ_2 , and rewriting the $\mathbf{g}_*$ integral, we have

$$I_M = \frac{n_s n_t}{\pi^{3/2} b^3} D(\kappa_s, \kappa_t) \int_{\mathbb{R}^3} e^{-|\mathbf{g}_{st} + \Delta\mathbf{u}_{st}|^2/w_{st}^2} \frac{\mathbf{g}_{st}}{\mathbf{g}_{st}^3} \, d\mathbf{g}_{st}. \tag{A15}$$

where $D(\kappa_s, \kappa_t)$ is defined in equation (52). The integral on $\mathbf{g}_{st}$ can be solved by setting z-axis in the direction of vector $\Delta\mathbf{u}_{st}$, so that the angle between $\mathbf{g}_{st}$ and $\Delta\mathbf{u}_{st}$ corresponds to the polar angle in spherical coordinates. We then transform the integrals into spherical coordinates and perform the integration, to get

$$I_M = -\frac{4}{3} \frac{n_s n_t}{\pi^{1/2} w_{st}^3} D(\kappa_s, \kappa_t)\, \Phi_{\text{Co}}(\varepsilon_{st})\, \Delta\mathbf{u}_{st}. \tag{A16}$$

Substituting equation (A16) into equation (A2), we can write the momentum coefficient for Coulomb collision as

$$\frac{\delta \mathbf{M}_s}{\delta t} = \sum_t n_s m_s \nu_{st}^{\text{Co}} D(\kappa_s, \kappa_t)\Phi_{\text{Co}}(\varepsilon_{st})\, \Delta\mathbf{u}_{st}, \tag{A17}$$

where ν_{st}^{Co} and Φ_{Co} are defined in equations (49) and (50).

The Energy Coefficient

The energy coefficient for Coulomb collisions is given in equation (A3). Substituting the dot product from equation (35) into the integral

$$I_E = \int_{\mathbb{R}^3 \times \mathbb{R}^3} f_s^{\text{MK}} f_t^{\text{MK}} \frac{(\hat{\mathbf{V}}_c \cdot \mathbf{g}_{st})}{\mathbf{g}_{st}^3} \, d\mathbf{c}_t \, d\mathbf{c}_s, \tag{A18}$$

produces three integrals, which can be evaluated by following the same steps as the integral in equation (A4), where we substitute the distributions given in equations (A5) and (A6) into the integrals, and apply the transformation mentioned in equations (A8-A10). This results in two integrals that depend on $\mathbf{g}_{st}$, which can be evaluated using the same steps used for the integral in equation (A15). Combining all integrals, we obtain:

$$I_E = -\frac{4}{3} \frac{1}{m_s + m_t} \frac{n_s n_t}{\pi^{1/2} w_{st}^3} \left[3k_B D(\kappa_s, \kappa_t)\, \Psi_{\text{Co}}(\varepsilon_{st})\, \Delta\text{T}_{st}^{\text{MK}} \right.$$

$$\left. + m_t D(\kappa_s, \kappa_t)\, \Phi_{\text{Co}}(\varepsilon_{st}) \left| \Delta\mathbf{u}_{st} \right|^2 \right], \tag{A19}$$

Substituting equation (A19) into equation (A3), we can write the energy coefficient for Coulomb collision as

$$\frac{\delta E_s}{\delta t} = \sum_t \frac{n_s m_s \nu_{st}^{\text{Co}}}{m_s + m_t} \left[3k_B\, D(\kappa_s, \kappa_t)\, \Psi_{\text{Co}}(\varepsilon_{st}) \Delta\text{T}_{st}^{\text{MK}} \right.$$

$$\left. + m_t D(\kappa_s, \kappa_t)\, \Phi_{\text{Co}}(\varepsilon_{st}) \left| \Delta\mathbf{u}_{st} \right|^2 \right], \tag{A20}$$

where $\Delta\text{T}_{st}^{\text{MK}}$ and Ψ_{Co} are defined as in equations (44) and (51), respectively.

appears, with n equal -3 or 1. The evaluation of these integrals follows the same steps, where the first step is to use the vector property,

$$|\mathbf{g}_{st} + \Delta\mathbf{u}|^2 = \mathrm{g}_{st}^2 + |\Delta\mathbf{u}|^2 + 2\,\mathbf{g}_{st} \cdot \Delta\mathbf{u}, \tag{145}$$

By setting z-axis in the direction of vector $\Delta\mathbf{u}$, the dot product of the vectors $\mathbf{g}_{st}$ and $\Delta\mathbf{u}$ is

$$\mathbf{g}_{st} \cdot \Delta\mathbf{u} = \mathrm{g}_{st}\,|\Delta\mathbf{u}|\,\cos\theta, \tag{146}$$

where here θ is the angle between vectors $\mathbf{g}_{st}$ and $\Delta\mathbf{u}$ in the same time its the polar angle in the spherical coordinates, because vector $\Delta\mathbf{u}$ is in the direction of the z-axis. After using the expressions in equations (145) and (146), the second step is to transform the integrals to the spherical coordinates, and preform the integrals in the cases we are interested in, $n = -3$ and $n = 1$, to get

$$I_1^{-3} = -\frac{4}{3}\pi\,\Delta\mathbf{u}\,\Phi_{\mathrm{Co}}(\varepsilon_{st}), \tag{147}$$

$$I_1^1 = -\frac{8}{3}\pi\,b^4\,\Delta\mathbf{u}\,\Phi_{\mathrm{HS}}(\varepsilon_{st}), \tag{148}$$

$$I_2^{-3} = 2\pi b^2\,\Psi_{\mathrm{Co}}(\varepsilon_{st}), \tag{149}$$

$$I_2^1 = 4\pi b^6\,\Psi_{\mathrm{HS}}(\varepsilon_{st}), \tag{150}$$

$$I_2^{-3} = -\frac{4}{3}\pi\,|\Delta\mathbf{u}|^2\,\Phi_{\mathrm{Co}}(\varepsilon_{st}), \tag{151}$$

$$I_2^1 = -\frac{8}{3}\pi\,b^4\,|\Delta\mathbf{u}|^2\,\Phi_{\mathrm{HS}}(\varepsilon_{st}). \tag{152}$$

where

$$\Phi_{\mathrm{Co}}(\varepsilon_{st}) = \frac{3\sqrt{\pi}}{4}\frac{\mathrm{erf}(\varepsilon_{st})}{\varepsilon_{st}^3} - \frac{3\,e^{-\varepsilon_{st}^2}}{2\,\varepsilon_{st}^2}, \tag{153}$$

$$\Phi_{\mathrm{HS}}(\varepsilon_{st}) = \frac{3\sqrt{\pi}}{8}\left(\varepsilon_{st} + \frac{1}{\varepsilon_{st}} - \frac{1}{4\varepsilon_{st}^3}\right)\mathrm{erf}(\varepsilon_{st}) + \frac{3}{8}\left(1 + \frac{1}{2\varepsilon_{st}^2}\right)e^{-\varepsilon_{st}^2}, \tag{154}$$

$$\Psi_{\mathrm{Co}}(\varepsilon_{st}) = e^{-\varepsilon_{st}^2}, \tag{155}$$

$$\Psi_{\mathrm{HS}}(\varepsilon_{st}) = \frac{\sqrt{\pi}}{2}\left(\varepsilon_{st} + \frac{1}{2\varepsilon_{st}}\right)\mathrm{erf}(\varepsilon_{st}) + \frac{1}{2}e^{-\varepsilon_{st}^2}. \tag{156}$$

References

J.A. Bittencourt. *Fundamentals of Plasma Physics*. Springer New York, 2004.

J.M. Burgers. Flow equations for composite gases. Technical report, 1969.

Sydney Chapman and TG Cowling. *The Mathematical Theory of non-uniform*. University Press, 1970.

Geoffrey F Chew, Marvin L Goldberger, and FE Low. The boltzmann equation an d the one-fluid hydromagnetic equations in the absence of particle collisions. *Proceedings of the Royal Society of London. Series A. Mathematical and Physical Sciences*, 236(1204):112–118, 1956.

Michael R Collier, DC Hamilton, G Gloeckler, P Bochsler, and RB Sheldon. Neon-20, oxygen-16, and helium-4 densities, temperatures, and suprathermal tails in the solar wind determined with wind/mass. *Geophysical research letters*, 23(10):1191–1194, 1996.

Sergio Davis, Gonzalo Avaria, Biswajit Bora, Jalaj Jain, José Moreno, Cristian Pavez, and Leopoldo Soto. Kappa distribution from particle correlations in nonequilibrium, steady-state plasmas. *Physical Review E*, 108(6):065207, 2023.

Howard G Demars and Robert W Schunk. Transport equations for multispecies plasmas based on individual bi-maxwellian distributions. *Journal of Physics D: Applied Physics*, 12(7):1051, 1979.

J.P. Freidberg. *Plasma Physics and Fusion Energy*. Cambridge University Press, 2008. ISBN 9781139462150.

Harold Grad. On the kinetic theory of rarefied gases. *Communications on pure and applied mathematics*, 2(4):331–407, 1949.

Petr Hellinger and Pavel M Trávníček. On coulomb collisions in bi-maxwellian plasmas. *Physics of Plasmas*, 16(5), 2009.

Walaa'Najeeb Jubeh and Imad Ahmad Barghouthi. Hypergeometric function representation of transport coefficients for drifting bi-maxwellian plasmas. *Physics of Plasmas*, 24(12), 2017.

Walaa'Najeeb Jubeh and Imad Ahmad Barghouthi. Transport coefficients for drifting maxwellian plasmas: The effect of coulomb collisions. *AIP Advances*, 8(1), 2018.

George Livadiotis. Kappa distributions: Thermodynamic origin and generation in space plasmas. In *Journal of Physics: Conference Series*, volume 1100, page 012017. IOP Publishing, 2018.

Nicole Meyer-Vernet, Michel Moncuquet, and Sang Hoang. Temperature inversion in the io plasma torus. *Icarus*, 116(1):202–213, 1995.

David Mintzer. Generalized orthogonal polynomial solutions of the boltzmann equation. *The Physics of Fluids*, 8(6):1076–1090, 1965.

V Pierrard and M Lazar. Kappa distributions: Theory and applications in space plasmas. *Solar physics*, 267:153–174, 2010.

Kurt D Retherford, HW Moos, and DF Strobel. Io's auroral limb glow: Hubble space telescope fuv observations. *Journal of Geophysical Research: Space Physics*, 108(A8), 2003.

R. Schunk and A. Nagy. *Ionospheres: Physics, Plasma Physics, and Chemistry*. Cambridge Atmospheric and Space Science Series. Cambridge University Press, 2009.

RW Schunk. Mathematical structure of transport equations for multispecies flows. *Reviews of Geophysics*, 15(4):429–445, 1977.

Andrew J Steffl, Fran Bagenal, and A Ian F Stewart. Cassini uvis observations of the io plasma torus: Ii. radial variations. *Icarus*, 172(1):91–103, 2004.

B.S. Tanenbaum. *Plasma Physics*. McGraw-Hill physical and quantum electronics series. McGraw-Hill, 1967.

A2 Hard-sphere interactions

The collision terms for hard-sphere interactions can be obtained by substituting equation (38) into equations (32-34), leading to the following form

$$\frac{\delta n_s}{\delta t} = 0, \tag{A21}$$

$$\frac{\delta \mathbf{M}_s}{\delta t} = -\sum_t m_{st}\, Q_{HS} \int_{\mathbb{R}^3 \times \mathbb{R}^3} f_s^{MK} f_t^{MK} \mathbf{g}_{st}\, g_{st}\, d\mathbf{c}_t\, d\mathbf{c}_s, \tag{A22}$$

$$\frac{\delta E_s}{\delta t} = -\sum_t m_{st}\, Q_{HS} \int_{\mathbb{R}^3 \times \mathbb{R}^3} f_s^{MK} f_t^{MK} \mathbf{g}_{st} \left(\hat{\mathbf{V}}_c \cdot \mathbf{g}_{st} \right) d\mathbf{c}_t\, d\mathbf{c}_s. \tag{A23}$$

Calculating the collision terms for hard-sphere interactions follows the same steps as those applied previously for the Coulomb collision. The main difference between the integrals in equations (A21−A23) and (A1−A3) is that g_{st} has a power of 1 rather than -3. This difference affects only the final integrals. Using the same technique, we obtain the momentum coefficient for hard-sphere interactions,

$$\frac{\delta \mathbf{M}_s}{\delta t} = \sum_t n_s m_s \nu_{st}^{HS}\, D(\kappa_s, \kappa_t)\, \Phi_{HS}(\varepsilon_{st})\, \Delta\mathbf{u}_{st}, \tag{A24}$$

and the energy coefficient for hard-sphere interactions,

$$\frac{\delta E_s}{\delta t} = \sum_t \frac{n_s m_s \nu_{st}^{HS}}{m_s + m_t} \Big[3k_B\, D(\kappa_s, \kappa_t)\, \Psi_{HS}(\varepsilon_{st})\, \Delta T_{st}^{MK}$$

$$+ m_t\, D(\kappa_s, \kappa_t)\, \Phi_{HS}(\varepsilon_{st})\, |\Delta\mathbf{u}_{st}|^2 \Big], \tag{A25}$$

where ν_{st}^{HS}, Φ_{HS}, and Ψ_{HS} are defined in equations (54-56).

A3 Maxwell molecule collisions

The collision terms for Maxwell molecule collisions can be obtained by substituting equation (39) into equations (32-34), leading to the following form

$$\frac{\delta n_s}{\delta t} = 0, \tag{A26}$$

$$\frac{\delta \mathbf{M}_s}{\delta t} = -\sum_t m_{st}\, Q_{MC} \int_{\mathbb{R}^3 \times \mathbb{R}^3} f_s^{MK} f_t^{MK} \mathbf{g}_{st}\, d\mathbf{c}_t\, d\mathbf{c}_s, \tag{A27}$$

$$\frac{\delta E_s}{\delta t} = -\sum_t m_{st}\, Q_{MC} \int_{\mathbb{R}^3 \times \mathbb{R}^3} f_s^{MK} f_t^{MK} \left(\hat{\mathbf{V}}_c \cdot \mathbf{g}_{st} \right) d\mathbf{c}_t\, d\mathbf{c}_s. \tag{A28}$$

There's no integration technique required to evaluate equations (A26−A28), since after rewriting the relative velocity in equation (4) and the dot product in equation (35) in terms of the random velocities $\mathbf{c}_s$ and $\mathbf{c}_t$, allows us to use the following expectation values for the modified Kappa distribution,

$$\langle c_\alpha^2 \rangle = \frac{3k_B T_\alpha}{m_\alpha}, \quad \langle \mathbf{c}_\alpha \rangle = 0, \quad \langle A \rangle = A, \tag{A29}$$

where A is constant and α denotes the species type s or t, to obtain the momentum coefficient for Maxwell molecule collisions

$$\frac{\delta \mathbf{M}_s}{\delta t} = \sum_t n_s m_s \nu_{st}^{MC}\, \Delta\mathbf{u}_{st}, \tag{A30}$$

and the energy coefficient for Maxwell molecule collisions

$$\frac{\delta E_s}{\delta t} = \sum_t \frac{n_s m_s \nu_{st}^{MC}}{m_s + m_t} \Big[3k_B\, \Delta T_{st} + m_t\, |\Delta\mathbf{u}_{st}|^2 \Big], \tag{A31}$$

where ν_{st}^{MC} is defined in equation (57).

Author contributions. Mahmood Jwailes carried out the theoretical work, derived the framework used to obtain the figures and results, wrote the initial manuscript, and led the discussion of the findings. Imad Barghouthi proposed the research idea, supervised the study, verified the validity of the results, and assisted in scientific editing of the manuscript. Qusay Atawnah contributed to the final revisions of the manuscript.

Competing interests. The authors declare that they have no competing interests.

Disclaimer. The views expressed in this article are solely those of the authors and do not necessarily represent the views of their affiliated institutions.

Acknowledgements. The authors thank the reviewers, Dr. Horst Fichtner and Prof. Marina Stepanova, for their critical reading of the manuscript and for their constructive suggestions, which significantly improved the quality of this work.

References

Barakat, A. R. and Schunk, R. W.: Momentum and energy exchange collision terms for interpenetrating bi-Maxwellian gases, Journal of Physics D: Applied Physics, 14, 421, https://doi.org/10.1088/0022-3727/14/3/013, 1981.

Barakat, A. R. and Schunk, R. W.: Transport equations for multi-component anisotropic space plasmas: a review, Plasma Physics, 24, 389, https://doi.org/10.1088/0032-1028/24/4/004, 1982.

Bittencourt, J.: Fundamentals of Plasma Physics, Springer New York, 3rd ed edn., 2004.

Burgers, J.: Flow Equations For Composite Gases, Applied Mathematics And Mechanics, Academic Press, 1969.

Chapman, S. and Cowling, T.: The Mathematical Theory of Non-uniform Gases: An Account of the Kinetic Theory of Viscosity, Thermal Conduction and Diffusion in Gases, Cambridge Mathematical Library, Cambridge University Press, 1990.

Collier, M. R. and Hamilton, D. C.: The relationship between kappa and temperature in energetic ion spectra at Jupiter, Geophysical Research Letters, 22, 303–306, https://doi.org/10.1029/94GL02997, 1995.

Davis, S., Avaria, G., Bora, B., Jain, J., Moreno, J., Pavez, C., and Soto, L.: Kappa distribution from particle correlations in nonequilibrium, steady-state plasmas, Physical Review E, 108, 065 207, https://doi.org/10.1103/PhysRevE.108.065207, 2023.

Demars, H. G. and Schunk, R. W.: Transport equations for multispecies plasmas based on individual bi-Maxwellian distributions, Journal of Physics D: Applied Physics, 12, 1051, https://doi.org/10.1088/0022-3727/12/7/011, 1979.

Du, J.: Transport coefficients in Lorentz plasmas with the power-law kappa-distribution, Physics of Plasmas, 20, 092 901, https://doi.org/10.1063/1.4820799, 2013.

Ebne Abbasi, Z. and Esfandyari-Kalejahi, A.: Transport coefficients of a weakly ionized plasma with nonextensive particles, Physics of Plasmas, 26, 012 301, https://doi.org/10.1063/1.5051585, 2019.

Ebne Abbasi, Z., Esfandyari-Kalejahi, A., and Khaledi, P.: The collision times and transport coefficients of a fully ionized plasma with superthermal particles, Astrophysics and Space Science, 362, 103, https://doi.org/10.1007/s10509-017-3081-4, 2017.

Fichtner, H., Sreenivasn, S. R., and Vormbrock, N.: Transfer integrals for fully ionized gases, Journal of Plasma Physics, 55, 95–120, https://doi.org/10.1017/S0022377800018699, 1996.

Formisano, V., Moreno, G., Palmiotto, F., and Hedgecock, P. C.: Solar Wind Interaction with the Earth's Magnetic Field 1. Magnetosheath, Journal of Geophysical Research (1896-1977), 78, 3714–3730, https://doi.org/10.1029/JA078i019p03714, 1973.

Grad, H.: On the kinetic theory of rarefied gases, Communications on Pure and Applied Mathematics, 2, 331–407, https://doi.org/10.1002/cpa.3160020403, 1949.

Guo, R. and Du, J.: Transport coefficients of the fully ionized plasma with kappa-distribution and in strong magnetic field, Physica A: Statistical Mechanics and its Applications, 523, 156–171, https://doi.org/10.1016/j.physa.2019.02.011, 2019.

Hellinger, P. and Trávníček, P. M.: On Coulomb collisions in bi-Maxwellian plasmas, Physics of Plasmas, 16, 054 501, https://doi.org/10.1063/1.3139253, 2009.

Husidic, E., Lazar, M., Fichtner, H., Scherer, K., and Poedts, S.: Transport coefficients enhanced by suprathermal particles in nonequilibrium heliospheric plasmas, Astronomy & Astrophysics, 654, A99, https://doi.org/10.1051/0004-6361/202141760, 2021.

Jubeh, W. N. and Barghouthi, I. A.: Hypergeometric function representation of transport coefficients for drifting bi-Maxwellian plasmas, Physics of Plasmas, 24, 122 104, https://doi.org/10.1063/1.5000937, 2017.

LeBlanc, F. and Hubert, D.: A Generalized Model for the Proton Expansion in Astrophysical Winds. I. The Velocity Distribution Function Representation, The Astrophysical Journal, 483, 464, https://doi.org/https://doi.org/10.1086/304232, 1997.

Leblanc, F. and Hubert, D.: A Generalized Model for the Proton Expansion in Astrophysical Winds. II. The Associated Set of Transport Equations, The Astrophysical Journal, 501, 375, https://doi.org/https://doi.org/10.1086/305789, 1998.

Leblanc, F., Hubert, D., and Blelly, P.-L.: A Generalized Model for the Proton Expansion in Astrophysical Winds. III. The Collisional Transfers and Their Properties, The Astrophysical Journal, 530, 478, https://doi.org/10.1086/308335, 2000.

Livadiotis, G.: Kappa distributions: Theory and applications in plasmas, Elsevier, 2017.

Livadiotis, G.: Kappa distributions: Thermodynamic origin and Generation in space plasmas, 1100, 012 017, https://doi.org/10.1088/1742-6596/1100/1/012017, 2018.

Livadiotis, G.: Collision frequency and mean free path for plasmas described by kappa distributions, AIP Advances, 9, 105 307, https://doi.org/10.1063/1.5125714, 2019.

Maksimovic, M., Pierrard, V., and Riley, P.: Ulysses electron distributions fitted with Kappa functions, Geophysical Research Letters, 24, 1151–1154, https://doi.org/10.1029/97GL00992, 1997.

Marsch, E.: Kinetic Physics of the Solar Corona and Solar Wind, Living Reviews in Solar Physics, 3, https://doi.org/10.12942/lrsp-2006-1, 2006.

Mintzer, D.: Generalized Orthogonal Polynomial Solutions of the Boltzmann Equation, The Physics of Fluids, 8, 1076–1090, https://doi.org/10.1063/1.1761357, 1965.

Olbert, S.: Summary of Experimental Results from M.I.T. Detector on IMP-1, in: Physics of the Magnetosphere, edited by Carovillano, R. L., McClay, J. F., and Radoski, H. R., pp. 641–659, Springer Netherlands, Dordrecht, ISBN 978-94-010-3467-8, https://doi.org/10.1007/978-94-010-3467-8_23, 1968.

Pierrard, V. and Lazar, M.: Kappa Distributions: Theory and Applications in Space Plasmas, Solar Physics, 267, 153–174, https://doi.org/10.1007/s11207-010-9640-2, 2010.

Pierrard, V., Maksimovic, M., and Lemaire, J.: Core, Halo and Strahl Electrons in the Solar Wind, Astrophysics and Space Science, 277, 195–200, https://doi.org/10.1023/A:1012218600882, 2001.

Qureshi, M. N. S., Pallocchia, G., Bruno, R., Cattaneo, M. B., Formisano, V., Reme, H., Bosqued, J. M., Dandouras, I., Sauvaud, J. A., Kistler, L. M., Möbius, E., Klecker, B., Carlson, C. W., McFadden, J. P., Parks, G. K., McCarthy, M., Korth, A., Lundin, R., Balogh, A., and Shah, H. A.: Solar Wind Particle Distribution Function Fitted via the Generalized Kappa Distribution Function: Cluster Observations, AIP Conference Proceedings, 679, 489–492, https://doi.org/10.1063/1.1618641, 2003.

Scherer, K., Fichtner, H., and Lazar, M.: Regularized κ-distributions with non-diverging moments, Europhysics Letters, 120, 50 002, https://doi.org/10.1209/0295-5075/120/50002, 2017.

Scherer, K., Lazar, M., Husidic, E., and Fichtner, H.: Moments of the Anisotropic Regularized κ-distributions, The Astrophysical Journal, 880, 118, https://doi.org/10.3847/1538-4357/ab1ea1, 2019.

Schunk, R. and Nagy, A.: Ionospheres: Physics, Plasma Physics, and Chemistry, Cambridge Atmospheric and Space Science Series, Cambridge University Press, 2009.

Schunk, R. W.: Mathematical structure of transport equations for multispecies flows, Reviews of Geophysics, 15, 429–445, https://doi.org/10.1029/RG015i004p00429, 1977.

Shizgal, B. D.: Suprathermal particle distributions in space physics: Kappa distributions and entropy, Astrophysics and Space Sci-

ence, 312, 227–237, https://doi.org/10.1007/s10509-007-9679-1, 2007.

Tanenbaum, B.: Plasma Physics, McGraw-Hill Physical and Quantum Electronics Series, McGraw-Hill, 1967.

5 Vasyliunas, V. M.: A Survey of Low-Energy Electrons in the Evening Sector of the Magnetosphere with OGO 1 and OGO 3, Journal of Geophysical Research (1896-1977), 73, 2839–2884, https://doi.org/10.1029/JA073i009p02839, 1968.

Wang, L. and Du, J.: The diffusion of charged parti-
10 cles in the weakly ionized plasma with power-law kappa-distributions, Physics of Plasmas, 24, 102 305, https://doi.org/10.1063/1.4996775, 2017.